

# STROJNIŠKI

## VESTNIK 1

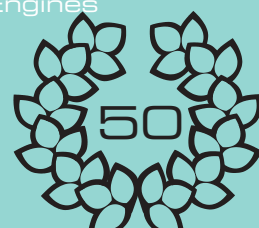
JOURNAL OF MECHANICAL ENGINEERING

strani - pages 1 - 70

ISSN 0039-2480 . Stroj V . STJVAX

cena 800 SIT

- 1.** Analiza visokotlačnega in nizkotlačnega vračanja izpušnih plinov v tlačno polnjenem dizelskem motorju  
An Analysis of the Application of High- and Low-Pressure Exhaust-Gas Recirculation to a Turbocharged Diesel Engine
- 2.** Obravnavo motorja z notranjim zgorevanjem in vbrizgavanjem plinskega goriva  
A Rapid-Compression-Machine Study of Gaseous Fuel Injection and Combustion
- 3.** Možne vrste cenenih motorjev s prostornino 50 kubičnih centimetrov z majhno emisijo  
Possible Solutions for EURO 2 "Low-Emission Low-Cost" 50cc Engines
- 4.** Numerične analize preoblikovanja cevi z visokim notranjim tlakom  
Numerical Analyses of Tube Hydroforming by High Internal Pressure
- 5.** Obravnavanje curka plinskega olja in nadomestnih goriv  
A Spray Analysis of Petrol and Alternative Fuels
- 6.** Metode za oblikovanje elementov sesalnega zbiralnika batnega motorja z notranjim zgorevanjem  
Design Methods for the Intake-Manifold Elements of Reciprocating Internal Combustion Engines



## Vsebina

### Contents

Strojniški vestnik - Journal of Mechanical Engineering  
letnik - volume 50, (2004), številka - number 1

#### Uvodnik

Alujevič, A.: Petdeseti letnik Strojniškega  
vestnika

#### Razprave

- Hribenik, A., Bombek, G.: Analiza visokotlačnega  
in nizkotlačnega vračanja izpušnih plinov v  
tlačno polnjenem dizelskem motorju  
Klimkiewicz, D., Leżański, T., Jarnicki, R., Rychter,  
T.J.: Obravnava motorja z notranjim  
zgorevanjem in vbrizgavanjem plinskega goriva  
Kirchberger, R., Koller, G.: Možne vrste cenениh  
motorjev s prostornino 50 kubičnih  
centimetrov z majhno emisijo  
Pepelnjak, T.: Numerične analize preoblikovanja cevi  
z visokim notranjim tlakom  
Volmajer, M., Kegl, B.: Obravnavanje curka  
plinskega olja in nadomestnih goriv  
Kozarac, D., Mahalec, I., Lulić, Z.: Metode za  
oblikovanje elementov sesalnega zbiralnika  
batnega motorja z notranjim zgorevanjem

#### Editorial

- 2 Alujevič, A.: The 50th Volume of Journal of Me-  
chanical Engineering

#### Papers

- 3 Hribenik, A., Bombek, G.: An Analysis of the Application  
of High- and Low-Pressure Exhaust-Gas  
Recirculation to a Turbocharged Diesel Engine  
15 Klimkiewicz, D., Leżański, T., Jarnicki, R., Rychter,  
T.J.: A Rapid-Compression-Machine Study of  
Gaseous Fuel Injection and Combustion  
15 Kirchberger, R., Koller, G.: Possible Solutions for  
EURO 2 "Low-Emission Low-Cost" 50cc  
22 Engines  
22 Pepelnjak, T.: Numerical Analyses of Tube  
31 Hydroforming by High Internal Pressure  
31 Volmajer, M., Kegl, B.: A Spray Analysis of Petrol  
44 and Alternative Fuels  
44 Kozarac, D., Mahalec, I., Lulić, Z.: Design Methods  
55 for the Intake-Manifold Elements of  
55 Reciprocating Internal Combustion Engines

#### 66 Professional Literature

#### 68 Personal Events

#### 69 Instructions for Authors

#### Strokovna literatura

#### Osebne vesti

#### Navodila avtorjem

## Uvodnik Editorial

### Petdeseti letnik Strojniškega vestnika

Minilo je že skoraj petdeset let, kar je začel izhajati Strojniški vestnik, torej vstopa sedaj v svoje jubilejno petdeseto leto. Proslava v marcu 2005 se bliža s hitrimi koraki. Zato je sedaj čas, da se spomnimo, kaj vse se je zgodilo v preteklem obdobju. Od 1993 izhajamo v dveh jezikih (znanstveni prispevki), uvrščeni smo tudi v mednarodno bazo "Institute for Scientific Information", pri kateri imamo količnik citiranosti 0,05. V letu 2003 smo izdali 10 enojnih in eno dvojno številko. V teh 11 zvezkih smo nabrali 45 člankov, od tega 37 znanstvenih (izvirni ali pregledni znanstveni ter kratki znanstveni prispevki oz. predhodne objave) in 8 strokovnih člankov. Za vse izvirne znanstvene članke smo pridobili tudi recenzije priznanih strokovnjakov iz tujine, ki potrjujejo kakovost objavljenih prispevkov. Redno smo objavljali tudi rubriki Strokovna literatura in Osebne vesti ter občasno Poročila. Kot novost naj omenim, da bomo odslej izvirne znanstvene članke tujih avtorjev objavljali samo v angleščini (s slovenskim povzetkom).

V letošnjem 50. letniku nameravamo izdati nekaj tematskih zvezkov, pozornost pa bomo posvetili tudi več pomembnim obletnicam. Mineva namreč 250. obletnica rojstva slavnega kanonirja Jurija pl. Vege, ki je poleg svojih logaritmovnikov in balističnih znanj prispeval kar nekaj strojev in naprav, še prej pa se je pet let ukvarjal tudi z rečno plovbo. Na tem področju se je uveljavil tudi le tri dni mlajši ljubljanski hidrotehnik Jožef Schemmerel pl. Leytembach, ki je pod vplivom Gabriela Gruberja (graditelj Cesarskega grabna med Ljubljanskim gradom in Golovcem) načrtoval plovno pot med Dunajem in Jadranom, kar pa je padlo v pozabovo zaradi gradnje južne železnice. V letošnjem letu se bomo spomnili tudi našega termodinamika prof.dr. Zorana Ranta (rojen je bil 14.9.1904), znanega predvsem po pojmu eksbergija. Bil je tudi v prvem uredniškem odboru SV.

Glavni in odgovorni urednik SV  
prof.dr.Andro Alujevič

The image shows the front cover of the first issue of the journal from 1955. The title 'STROJNISKI VESTNIK' is prominently displayed at the top. Below it, the subtitle 'GLASILO DRUŠTVA STROJNIH INŽENIRJEV IN TEHNIKOV LJUDSKE REPUBLIKE SLOVENIJE' and 'GLASILO ODELKA ZA STROJNISTVO TEHNIŠKE FAKULTETE, INSTITUTA ZA TURBO STROJEV IN TITOVIH ZAVODOV LITOSTROJA V LJUBLJANI TER TOVARNE AVTOМОБИЛОВ V MARIBORU' are visible. A small logo consisting of three circles with letters 'T', 'A', and 'M' is located above the title. The main photograph on the cover depicts a vintage bus driving on a snowy road. To the right of the bus is a large, multi-story industrial building. The year '1955 - 1' is printed in the bottom left corner of the cover.

# Analiza visokotlačnega in nizkotlačnega vračanja izpušnih plinov v tlačno polnjenem dizelskem motorju

An Analysis of the Application of High- and Low-Pressure Exhaust-Gas Recirculation to a Turbocharged Diesel Engine

Aleš Hribenik - Gorazd Bombek

Vračanje izpušnih plinov je učinkovita metoda za zmanjšanje emisije dušikovih oksidov (NOx). Dva različna postopka vračanja izpušnih plinov se lahko uporabita za tlačno polnjene dizelske motorje. Pri nizkotlačnem postopku vodimo del izpušnih plinov, ki izteka iz turbine, na polnilno stran motorja, kjer se pomešajo s svežim zrakom. Alternativna pot je visokotlačni postopek. Pri tem postopku odvzemamo del izpušnih plinov že pred turbino in jih pri nadtlaku tlačimo v polnilni zbiralnik za kompresorjem. Z enorazsežno metodo smo simulirali tokovne in termodinamične procese v štirivaljnem motorju z vračanjem izpušnih plinov po obeh postopkih. Raziskali smo možnost doseganja želene stopnje vračanja z obema postopkoma in njun vpliv na obratovalne karakteristike motorja in turbokompressorja. Rezultati so prikazani v prispevku.

© 2004 Strojniški vestnik. Vse pravice pridržane.

(Ključne besede: motor z notranjim zgorevanjem, recirkulacija izpušnih plinov, emisije NOx, meritve, simuliranje)

Exhaust-gas recirculation (EGR) is an effective way of reducing NOx emissions. Two different strategies can be applied when using EGR in a turbocharged diesel engine. The first one is known as low-pressure EGR, where a passage is provided enabling exhaust gasses from below the turbine to pass to the fresh-air side of the engine. Its alternative is high-pressure EGR. In this EGR configuration the exhaust gas is withdrawn from the exhaust manifold above the turbine and fed to the intake manifold below the compressor. The applications of both strategies to a four-cylinder diesel engine were studied by means of a one-dimensional simulation. The possible range of EGR applications for both concepts and their effects on the engine and turbocharger operations were examined and are discussed in this paper.

© 2004 Journal of Mechanical Engineering. All rights reserved.

(Keywords: internal combustion engines, exhaust gas recirculation, NOx emissions, measurements, simulations)

## 0 UVOD

Vračanje izpušnih plinov je uveljavljen postopek za zmanjšanje emisij dušikovih oksidov NOx v motorjih s prisilnim vžigom in se vse bolj uveljavlja tudi v manjših dizelskih motorjih. Z vračanjem izpušnih plinov zmanjšamo NOx pri vseh obratovalnih pogojih motorja. Še posebej pomembno pa je zmanjšanje NOx pri visokih obremenitvah motorja, saj v teh razmerah nastaja največ NOx [1].

Med razlogi za zmanjšanje NOx zaradi vračanja izpušnih plinov se najpogosteje omenja znižanje najvišjih temperatur v valju motorja zaradi zmanjšanja koncentracije kisika in povečanja toplotne kapacitete zmesi v valju. Ker je visoka temperatura v valju najpomembnejši dejavnik pri nastanku NOx, je uporaba vračanja izpušnih plinov izredno učinkovit postopek za njegovo zmanjševanje [2]. Z raziskavami

## 0 INTRODUCTION

Exhaust-gas recirculation (EGR) is a well-established approach for NOx-emission reduction in spark-ignition engines, and is now used extensively in small diesel engines. EGR is effective for reducing NOx under all load conditions. High-load NOx reduction in diesel engines is especially important because most of the NOx is produced under high loads [1].

Several explanations have been proposed for the reduction in NOx emissions using EGR. These explanations focus on EGR's reduction of the peak cylinder temperature due to the reduced oxygen concentration and the increased heat capacity of in-cylinder gases. EGR is an effective means of controlling NOx formation, because the peak cylinder temperature is the most influential variable affecting NOx pro-

je ugotovljeno, da je mogoče zmanjšati koncentracijo NOx v izpušnih plinih za 30 do 75 % pri uporabi 5 do 25 % stopnje vračanja izpušnih plinov ([1] in [3]).

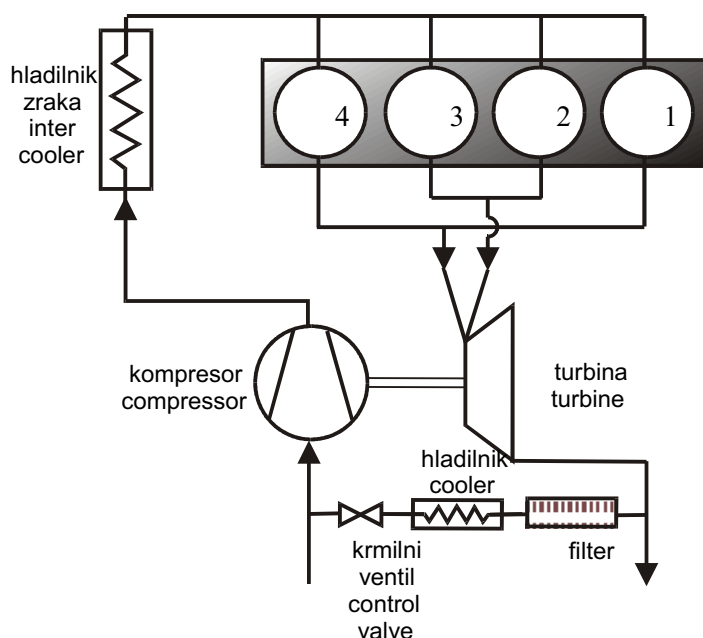
Žal se pojavljajo pri uporabi vračanja izpušnih plinov tudi neželeni stranski učinki. Poveča se obraba motornih delov, potreben je višji polnilni tlak in povečajo se emisije nezgorelih ogljikovodikov (HC) in saj. Povečana obraba je predvsem posledica abrazije, ki jo povzročajo delčki (saje) v polnilnem zraku in žveplene kislina v recirkuliranih izpušnih plinih, in povzroča razgradnjo mazalnega olja [1]. Povečan tlak polnjenja je potreben zato, ker izpušni plini nadomestijo del zraka v polnilnem zbirjalniku in je potrebna večja skupna masa polnjenja valjev motorja, da lahko zgori enaka količina goriva in ostane gostota moči motorja nespremenjena [1]. Povečanje emisije delčkov (saj) je opaziti predvsem pri velikih obremenitvah. Predpostavlja se, da je posledica znižanja temperature zgrevanja, kar zmanjša hitrost oksidacije saj [4].

Vračanje izpušnih plinov v tlačno polnjenem dizelskem motorju lahko izvedemo z dvema postopkoma. Tako imenovani nizkotlačni postopek prikazuje slika 1. Del izpušnih plinov, ki izteka iz turbine, vodimo na polnilno stran motorja in jih mešamo s svežim zrakom. Pozitivna tlačna razlika med izpušno in sesalno stranjo motorja omogoča preprosto vodenje s krmilnim ventilom in veliko stopnjo vračanja v širokem delovnem področju motorja. Potrebna je uporaba filtra za saje, da se izognemo obrabi kompresorskih lopatic in zamašitvi hladilnika polnilnega zraka [5]. Alternativa nizkotlačni je visokotlačno vračanje izpušnih plinov, ki izkorišča tlačne valove v izpušnem sistemu pred turbino.

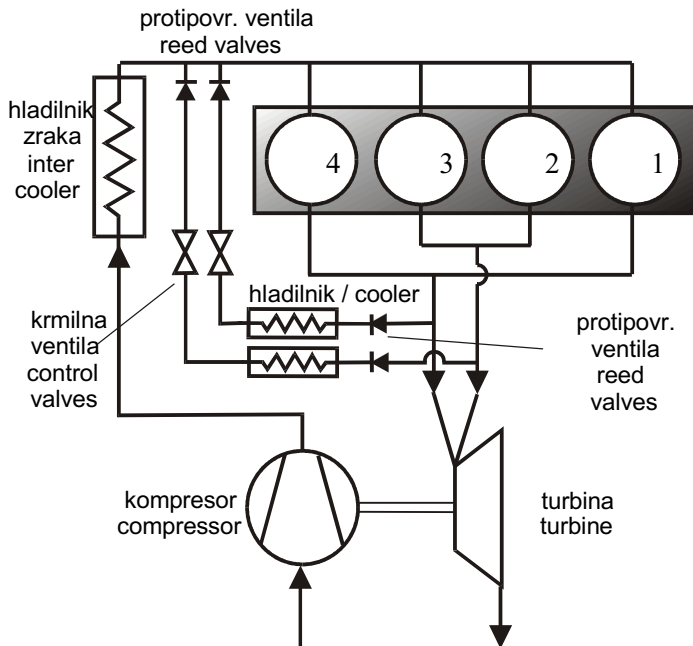
duction [2]. Researchers observed 30 % to 75 % reductions in NOx when using 5 % to 25 % EGR rates ([1] and [3]).

Unfortunately, EGR also has undesirable side-effects, these include: increased engine wear, higher required boost pressure, and higher HC and particulate emissions. The increased engine wear is due to abrasion by the particulates present in the intake air, and from the sulphuric acid present in the recirculating exhaust gas, which tends to break-down the lubricating oil [1]. Higher boost pressures are required because the exhaust is replacing some of the oxygen in the intake manifold. The increased total mass must, therefore, be forced into the cylinder to burn the same quantity of fuel and retain the original power density [1]. The increase in particulate emissions occurs mainly under high loads, and is believed to be due to the reduced combustion temperatures resulting from reduced soot-oxidation rates [4].

Two different strategies can be applied to EGR in a turbocharged diesel engine. The first one is known as the low-pressure EGR concept (Fig. 1). A passage is provided for the exhaust gases from below the turbine to pass to the fresh-air side of the engine. The positive pressure difference across the appropriate EGR valve makes EGR possible over a wide range of engine operating conditions. Increased wear on the compressor blades, and charge air cooler contamination may occur, however, if no diesel particulate filter is used [5]. The alternative is high-pressure EGR, which makes use of the dynamic pressure above the turbine. In this EGR configuration (Fig. 2) the exhaust gas is withdrawn from the ex-



Sl. 1. Nizko-tlačni postopek vračanja  
Fig. 1. Low-pressure EGR concept



Sl. 2. Visoko-tlačni postopek vračanja  
Fig. 2. High-pressure EGR concept

Postopek je prikazan na sliki 2. Del izpušnih plinov se že pred turbino odcepi in vteka v polnilni zbiralnik za kompresorjem. Vrnjeni izpušni plini zato ne potujejo skozi kompresor in hladilnik polnilnega zraka. S tem se izognemo problemom, značilnim za nizkotlačni postopek vračanja izpušnih plinov.

Raziskave in primerjava obeh postopkov vračanja na 6-valjnem tlačno polnjenem dizelskem so že bile opravljene, tako z eksperimentalnim postopkom [5] kakor tudi z uporabo simulacijskih metod [6]. Namens predstavljene študije pa je bil preučiti uporabo obeh postopkov na 4-valjnem motorju. Dela smo se lotili tako, da smo najprej z meritvami ugotovljali vpliv stopnje vračanja na znižanje NO<sub>x</sub> in na spremembo preostalih emisijskih komponent v izpušnih plinih. S tem smo poskušali določiti najprimernejšo stopnjo vračanja izpušnih plinov za obravnavan motor. Nato pa smo z uporabo enorazsežne metode simulirali tokovne in termodinamične procese v štirivaljnem motorju z vračanjem izpušnih plinov po obeh postopkih. Raziskali smo možnost doseganja želene stopnje vračanja z obema postopkoma in vpliv vračanja na obratovalne karakteristike motorja in turbokompressorja.

#### 1 RAZISKAVE VPLIVA STOPNJE VRAČANJA IZPUŠNIH PLINOV NA EMISIJO ŠKODLJIVIH KOMPONENT V IZPUŠNIH PLINIH

Raziskave smo izvedli s prototipnim motorjem TAM BF4L515. Osnovne karakteristike motorja so zbrane v preglednici 1. Uporabili smo nizkotlačni postopek vračanja (slika 1). Vrnjene izpušne pline smo najprej vodili skozi filter za saje. Nato smo jih ohladili v prenosniku toplotne voda –

haust manifold above the turbine and fed to the intake manifold below the compressor. The recirculated exhaust gas, therefore, does not pass through the compressor and intercooler and the problems encountered using the low-pressure EGR strategy do not occur.

The application of both strategies for a six-cylinder engine have already been studied by means of both experiment [5] and simulation [6]. The purpose of this presented study was to examine the application of both concepts for a four-cylinder engine. First, the effect of EGR on NO<sub>x</sub> reduction and emissions formation was studied using a set of measurements performed on the test engine, and the results were used to predict the optimal EGR rate. Then a one-dimensional simulation was used to simulate flow and thermodynamic processes within the four-cylinder engine with both EGR concepts applied in order to establish the possibility of achieving the optimum experimentally obtained EGR rate for each individual concept, and to study the effects of EGR on the engine and turbocharger operation.

#### 1 INVESTIGATION OF THE INFLUENCE OF EGR RATE ON THE ENGINE EMISSIONS

Investigations were performed on the TAM BF4L515 diesel engine. The characteristics of this engine are summarised in Table 1. The low-pressure EGR concept (Fig. 1) was applied. A passage was provided for the exhaust gases from below the turbine to pass to the fresh-air side of the engine through

Preglednica 1. Podatki o testnem motorju

Table 1. Test engine specifications

Motor Engine	tlačno poljeni, 4-taktni dizelski z neposrednim vbrizgom goriva turbocharged, 4-stroke direct injected diesel engine
Dobava goriva Fueling	tlačilka BOSCH BOSCH in-line pump
Število valjev Number of cylinders	4
Premer x gib bata Bore x stroke	125 mm x 145 mm
Gibna prostornina Total displacement	7117 cm <sup>3</sup>
Tlačno razmerje Compression ratio	15,8
Turbokompressor Turbocharger	HOLSET H1E8264AX/GA26*11

plin na temperaturo 25 °C in jih prek krmilnega ventila vodili v sesalno cev motorja. Stopnjo vračanja smo spreminjali z nastavitevijo krmilnega ventila in jo določili kot razmerje masnega toka vrnjenih izpušnih plinov in celotnega masnega pretoka skozi motor.

Meritve smo izvajali pri nespremenljivi vrtilni frekvenci in stalnem srednjem dejanskem tlaku motorja. Merili smo osnovne obratovalne parametre motorja, to so: vrtilna frekvenca motorja in turbokompressorja, vrtilni moment motorja, pretok svežega zraka, pretok vrnjenih izpušnih plinov, poraba goriva, tlak in temperatura polnilnega zraka in izpušnih plinov v značilnih točkah, temperatura glave in valjev motorja. Hkrati smo merili tudi koncentracijo plinskih komponent v izpušnih plinih. Koncentracijo NOx smo izmerili s kemoluminiscenčno metodo, koncentracijo nezgorelih ogljikovodikov HC s plamenško ionizacijskim detektorjem, stopnjo sajavosti z Boschevo metodo, koncentracijo CO z metodo apsorbicije nerazsejane infrardeče svetlobe in koncentracijo O<sub>2</sub> z elektrolitsko metodo. Na sliki 3 je prikazana značilna sprememb koncentracije plinskih komponent v odvisnosti od povečevanja stopnje recirkulacije. Koncentracija NOx se močno zmanjša že pri 8-odstotni stopnji vračanja in je pri 21-odstotni stopnji vračanja manjša za 65 odstotkov. Vračanje ne vpliva pomembno na povečanje koncentracije HC, pač pa vpliva predvsem na povečanje sajavosti in povečanje koncentracije CO; v obeh primerih za dobrih 300 odstotkov pri 21-odstotni stopnji vračanja. Ugotovimo lahko, da je za prikazan primer najprimernejša 14-odstotna stopnja vračanja, pri kateri je osnovna koncentracija NOx več ko razpolovljena, medtem ko se sajavost in koncentracija CO niti ne podvojita.

## 2 RAČUNALNIŠKA SIMULACIJA TLAČNO POLNJENEGA MOTORJA

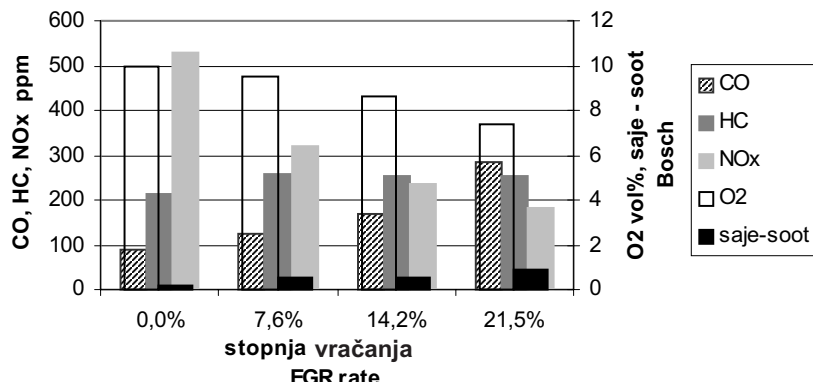
Uporabili smo enorazsežno metodo za simulacijo tokovnih in termodinamičnih postopkov v

a diesel particulate filter. The recirculated gas was externally cooled by water to gas heat exchanger, and the gas temperature was maintained at 25 °C. The EGR rate was defined as the ratio of the recirculated mass flow and the total mass flow through the engine, and it was controlled by the EGR valve.

Measurements were performed at a constant engine speed and a constant mean effective pressure. All the basic engine operational parameters, such as engine speed and turbocharger (rpm), engine torque, fresh-air flow rate, recirculated-gas flow rate, fuel consumption, pressures and temperatures at the intake and exhaust side of the engine, were measured. The exhaust-gas emissions were measured simultaneously. The NOx concentration was measured by a chemiluminescence analyser; a flame ionisation detector was used for the unburned hydro-carbon measurement, particulates were monitored with the AVL 450 smoke meter, the carbon monoxide concentration was measured with a nondispersive infrared analyser, and a ZrO<sub>2</sub> electrolytic method was used for the oxygen concentration measurement. A typical effect of EGR on the exhaust-gas emissions of the investigated engine is shown in Fig. 3. NOx was already drastically reduced with 8 % EGR. It was reduced by more than 65 % with 21 % EGR. Almost no EGR effect on the emissions of the unburned hydrocarbons (HCs) was observed. However, the emissions of carbon monoxide and particulates tripled with 21 % EGR. In this particular case it can be seen that 14 % EGR was the optimum, NOx emissions were reduced by more than 50 %, while CO and particulate emissions were still satisfactory.

## 2 COMPUTER SIMULATION OF TURBOCHARGED ENGINE

A one-dimensional method was used to simulate the flow and thermodynamic processes



Sl. 3. Vpliv stopnje vračanja izpušnih plinov na spremembo koncentracije škodljivih komponent v izpušnih plinih ( $n = 1600 \text{ min}^{-1}$ ,  $p_e = 9 \text{ bar}$ )

Fig. 3. Effect of EGR rate on engine emissions ( $n = 1600 \text{ min}^{-1}$ ,  $p_e = 9 \text{ bar}$ )

motorju z notranjim zgorevanjem. Metodo smo večkrat uspešno uporabili za obravnavani tlačno polnjeni motor, jo testirali s primerjavo računskih in eksperimentalnih rezultatov in podrobno predstavili v [7].

Uporabili smo dva simulacijska modela. Oba smo razvili iz osnovnega modela motorja in uporabili nekaj manjših sprememb polnilnega in izpušnega cevnega sistema potrebnih za izvedbo vračanja izpušnih plinov po sistemu nizkega oz. visokega tlaka. Omejili smo se le na simulacijo obratovanja pri nizkih vrtljnih frekvencah motorja (1100 in 1300  $\text{min}^{-1}$ ) pri treh obremenitvah ( $p_e = 10 \text{ bar}$ ,  $p_e = 12 \text{ bar}$  in  $p_e = 14 \text{ bar}$ ). V teh obratovalnih razmerah je presežek zraka v tlačno polnjem motorju najmanjši in potrebna je skrbna izbira stopnje recirkulacije izpušnih plinov, da se razmerje zrak – gorivo ne zmanjša pod kritično mejo (meja sajenja motorja) in koncentracija saj ne zveča čez vse meje. Povečanje tlaka v polnilnem zbiralniku za kompresorjem in tem povečan pretok skozi motor je najučinkovitejši ukrep, da se temu izognemo. Zagotovimo ga lahko z uporabo turbine s spremenljivo geometrijsko obliko. Z nekoliko manjšo uspešnostjo (nižje stopnje vračanja) pa lahko uporabimo kar turbino z manjšim okrovom in sistemom obtekanja turbine, ki prek posebnega ventila prepušča del izpušnih plinov mimo turbine in preprečuje pojav dušenega toka v turbini pri velikih vrtljnih frekvencah motorja. Odločili smo se, da preizkusimo oba postopka. Zato smo stopnjo vračanja omejili na 10% pri polni obremenitvi ( $p_e = 14 \text{ bar}$ ) in jo nato stopnjevali do 20% pri 70-odstotni obremenitvi ( $p_e = 10 \text{ bar}$ ). Kakor so pokazale raziskave (slika 3), lahko pri teh stopnjah vračanja izpušnih plinov pričakujemo več ko 50-odstotno zmanjšanje koncentracije NOx.

## 2.1 Nizkotlačno vračanje izpušnih plinov

Tok vrnjenih izpušnih plinov poteka od izpušne cevi za turbino, prek filtra za saje, hladilnika izpušnih plinov in krmilnega ventila v sesalno cev motorja, kjer se pomeša s svežim zrakom (sl. 1). Delovanje krmilnega ventila smo simulirali z modelom lokalne spremembe tlaka [8]. Uporaba tega robnega

within the internal combustion engine. The method was successfully used for simulations of the investigated turbocharged diesel engine and it was tested against the experimental data. The method is presented in detail in [7].

Two simulation models were used. These models were based on the original engine model with some minor modifications necessary for setting up the EGR system. EGR concepts were simulated for three different EGR rates, at two engine speeds and three loads. The engine operation was studied only at low engine speeds (1100 and 1300 rpm, both at  $p_e = 10 \text{ bar}$ ,  $p_e = 12 \text{ bar}$  and  $p_e = 14 \text{ bar}$ ). Fresh-air excess is the lowest at these speeds, EGR can reduce the equivalent air-to-fuel ratio under the soot limit and the soot emission can increase dramatically. EGR rates, therefore, have to be chosen carefully. This problem can be avoided by the application of a variable geometry turbine (VGT). However, an appropriate size of turbine housing using the waste gate system can also do the job when the low-pressure EGR concept is applied and the EGR rate is kept small at high engine loads. It was decided, therefore, to graduate the rate of EGR from 10 % at full engine load ( $p_e = 14 \text{ bar}$ ) to 20 % at 70% of full engine load ( $p_e = 10 \text{ bar}$ ). These EGR rates normally ensure up to 50 % NOx-emission reductions according to the experimental results presented in Fig. 3.

## 2.1 Low-pressure EGR

The low-pressure EGR system recirculates exhaust gas from below the turbine and EGR cooler (Fig. 1). The exhaust gas is supplied to the fresh-air side of the engine via a flow-control valve. Operation of the flow-control valve was simulated by the so-called “local pressure drop” boundary [8]. Using this

pogoja na stiku dveh cevi namreč omogoča spreminjanje stopnje vračanja izpušnih plinov. Model hladilnika vrnjenih izpušnih plinov smo poenostavili in ga obravnavali kot nadzorno prostornino z okrepljenim prestopom topote v okolico. Pri tem smo s primerno izbranim koeficientom prenosa topote dosegli želeno temperaturo izpušnih plinov na izstopu.

Povečanje vrtilne frekvence turbokompressorja in s tem tlaka v polnilnem zbiralniku za kompresorjem smo dosegli z uporabo manjšega okrova turbine (GA19\*11), katerega vstopni prerez je 27 % manjši od vstopnega prereza izvirne turbine (GA26\*11) in je opremljen z obtočnim ventilom. Tako je bilo mogoče pri vseh obravnavanih režimih doseči predpisano stopnjo vračanja izpušnih plinov, ne da bi ob tem primerjalni razmernik zrak – gorivo padel pod mejno vrednost 1,4 (meja sajenja za obravnavani motor), kakor prikazuje slika 4.

## 2.2 Visokotlačno vračanje izpušnih plinov

Za visokotlačno vračanje smo uporabili dvovejni povratni sistem z dvema hladilnikoma izpušnih plinov. Izpušni plini izpred levega ali desnega vtoka v turbino lahko prek prenosnika topote, krmilnega ventila in protipovratnega ventila tečejo v polnilno cev za kompresorjem in hladilnikom polnilnega zraka (sl. 2). Prav uporaba protipovratnih peresnih ventilov, ki jih pogosto srečamo pri dvotaktnih motorjih [9], omogoča izrabo tlačnih valov v izpušnem sistemu za stiskanje izpušnih plinov v polnilni sistemu tudi pri negativni povprečni tlačni razliki ( $p_3/p_2 < 1$ ). Ker vstopajo izpušni plini v polnilni sistem za kompresorjem in hladilnikom polnilnega zraka, odpadejo problemi zaradi povečane obrabe kompresorja in mašenja pretočnih kanalov prenosnika topote.

Pravilno delovanje protipovratnih peresnih ventilov odločilno vpliva na uspešnost visokotlačnega vračanja. Za popis delovanja protipovratnih ventilov smo uporabili model pretoka skozi polnilni ventil motorja [8]. Značilni enosmerni pretok skozi smo dosegli z nizkimi

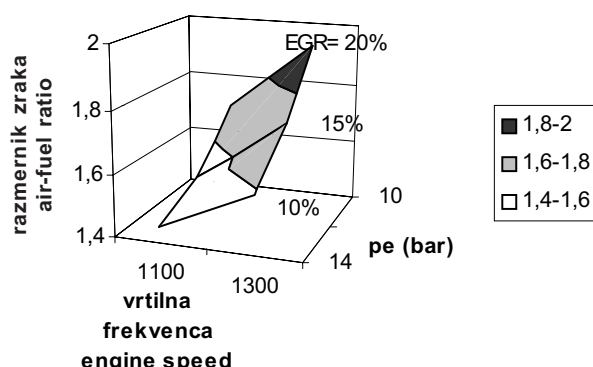
type of boundary it was possible to achieve different EGR rates. The EGR cooler model was simplified, and simulated as a single control volume with an increased convection heat transfer. The rate of convection heat transfer within the EGR cooler was intensified to a degree at which the recirculated exhaust gas left the water-cooled EGR heat exchanger at the desired temperature.

The turbocharger speed and, consequently, the boost pressure were increased by the application of a smaller turbine housing (GA19\*11) equipped with a “Waste-Gate” valve. The inflow cross section of this turbine housing is 27 % smaller than the inflow cross-section of the original one (turbine housing GA26\*11). This measure ensured the equivalent air-fuel ratio remained above 1.4 (soot limit) during all engine-operation regimes and with the desired EGR rate (Fig. 4).

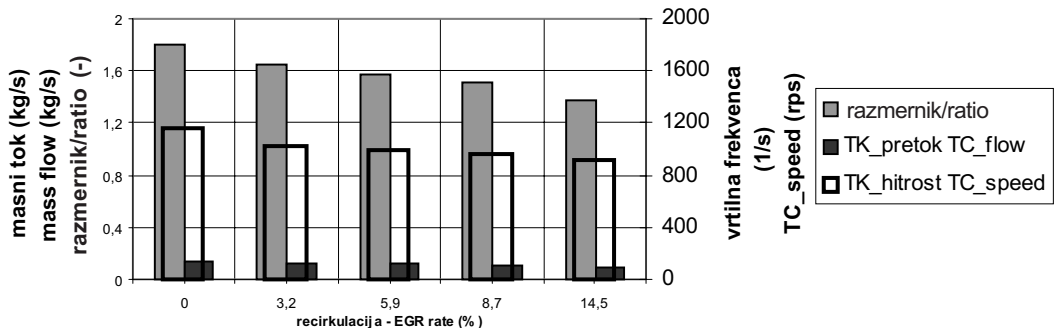
## 2.2 High-pressure EGR

In this EGR configuration of a four-cylinder engine, a dual duct, cooled exhaust recirculation system was applied. The exhaust gas was withdrawn from either duct of the exhaust pipe above the turbine and fed to a reed valve (commonly used by two-stroke engines [9]) via a flow-control valve and an exhaust cooler (Fig. 2). The dual-duct configuration, which employs individual control valves, coolers and reed valves, makes use of the dynamic exhaust pressure. In this way, sufficiently high EGR rates were sustained even under negative mean differential pressures ( $p_3/p_2 < 1$ ). The recirculated exhaust gas entered the charge air line downstream of the charge air cooler. This preserves the compressor and inter-cooler from increased wear and contamination.

The correct operation of the reed valves was crucial for this EGR concept. An adapted cylinder-valve boundary-condition model [8] was used for this simulation. The one-way operation of this valve was achieved by the application of a very low dis-



Sl. 4. Izračunani primerjalni razmernik zrak gorivo v sistemu z nizko-tlačnim vračanjem  
Fig. 4. Predicted equivalent air-fuel ratio with low-pressure EGR



Sl. 5. Vpliv visoko-tlačnega vračanja na ekvivalentni razmernik zrak-gorivo ter na masni pretok in vrtilno frekvenco turbokompressorja ( $n=1300 \text{ min}^{-1}$ ,  $p_e=12\text{bar}$ )

Fig. 5. Effects of application of high-pressure EGR on equivalent air-fuel ratio, mass flow rate and turbocharger speed ( $n=1300 \text{ min}^{-1}$ ,  $p_e=12\text{bar}$ )

pretočnimi števili, ki smo jih predpisali za povratni tok. Tako smo dopustili majhno netesnost, kar ustreza dejanskim razmeram [9]. Preizkusili smo različne lege protipovratnega ventila v povratni veji in različne kombinacije ventilov. Ugotovili smo, da je najprimernejša uporaba dveh protipovratnih ventilov, ki sta nameščena na začetek in konec vsakega povratnega sistema. V takšni razporeditvi deluje prenosnik toplote kot nekakšen akumulator visokega tlaka. Prenos snovi v postopku vračanja izpušnih plinov je zato precej bolj ustaljen in ne vpliva negativno na delovanje kompresorja.

Ponovno smo skušali doseči višji tlak polnjenja kar z uporabo manjšega okrova turbine. Simulacije delovanja motorja z manjšim okrovom turbine GA19\*11 in pri različnih stopnjah vračanja smo izvedli pri vrtilni frekvenci  $1300 \text{ min}^{-1}$  in 85-odstotni obremenitvi motorja ( $p_e=12\text{bar}$ ). Vpliv stopnje visokotlačnega vračanja izpušnih plinov na izračunan masni pretok, vrtilno frekvenco turbokompressorja in ekvivalentni razmernik zrak – gorivo prikazuje slika 5. Visokotlačno vračanje izpušnih plinov močno vpliva na delovanje turbokompressorja. Zaradi zmanjšanega pretoka skozi turbino se zmanjša moč turbine z njo pa vrtilna frekvanca turbokompressorja in tlak polnjenja (stopnja kompresije). Ustaljeno delovanje sistema motor – turbokompressor se zaradi tega vzpostavi pri precej nižjih obratovalnih parametrih (masni pretok, vrtilna frekvencia turbokompressorja, presežek zraka itn.). Zato želene 15-odstotne stopnje vračanja ne moremo doseči s primerjalnim razmernikom zrak – gorivo, ki bi bil višji od meje sajenja, saj je že pri 14.5-odstotni stopnji vračanja ekvivalentni razmernik le še 1,38 (sl. 5).

Potreben povečanje tlaka polnjenja lahko torej dosežemo le z uporabo turbine s spremenljivo geometrijsko obliko. Delovanje turbine s spremenljivo geometrijsko obliko smo simulirali z modelom, ki izhaja iz modela dvonatočne turbine [10]. Tega sestavljajo trije pod-modeli: spiralni vodilnik, vmesni prostor in goniščnik. Model vmesnega prostora smo nadomestili z modelom obroča vodilnih lopatic [10]. Tako smo s spremenjanjem kota nagiba lopatic simulirali delovanje turbine s spremenljivo geometrijsko obliko ter pri enakih

charge coefficient for the reverse-flow operation, allowing very little leakage characteristic for the reed-valve operation [9]. The different positions and combinations of the reed valves were examined, and it was discovered that the application of the reed valve was optimum on each side of the EGR cooler. In this combination, the EGR cooler operated as a high-pressure accumulator, thus the mass transfer was smooth, without any extreme exhaust pressure pulses, which might have travelled through the EGR coolers into the intake system and interfered with the proper operation of the compressor, causing it to surge.

Firstly, any possibility of application for the turbocharger with a smaller turbine housing (GA19\*11) was examined. Simulations of the engine operation using different EGR rates were performed at 1300 rpm and 85 % load ( $p_e=12\text{bar}$ ). As shown in Fig. 5, high-pressure EGR dramatically affected the turbocharger's operation, because reducing the flow through the turbine decreased the turbine output. The turbocharger speed and boost pressure, therefore, decreased as well. The steady-state operation of the turbocharger-engine system was reached at significantly lower engine-operation parameters (mass flow, turbocharger speed, equivalent air to fuel ratio, etc.), and the desired EGR rate (15% at this load) could not be obtained when the air-to-fuel ratio was above the stoichiometric limit (lambda is 1.38 at 14.5 % EGR rate – Fig. 5).

This problem can be solved by the application of a variable-geometry turbine. The simulation of the variable-geometry turbine operation was performed by a turbine model adapted from a twin-turbine model [10]. This model consists of three submodels: the spiral volute, the interspace and the turbine rotor. In the adapted model the model of interspace between the volute and rotor was supplemented, however, by guide vanes [10]. The angle of the guide vanes was varied during simulations, and the flow-control valve was adjusted simultaneously in order to achieve the same boost pressure and the

stopnjah vračanja z visokotlačnim postopkom dosegli enake tlake polnjenja kakor pri nizkotlačnem vračanju izpušnih plinov. Na sliki 6 je prikazan kot nagiba vodilnih lopatic, ki je potreben, da so stopnja vračanja, tlak polnjenja in preostali parametri obratovanja motorja enaki kakor pri nizkotlačnem postopku. Potrebno je bilo precejšnje pripiranje turbine, saj so koti nagiba vodilnih lopatic do 40% manjši od srednjega kota iztekanja ( $\alpha_s = 20^\circ$ ) iz izvirnega turbinskega okrova GA19\*11, ki je brez obroča vodilnih lopatic.

### 3 PRIMERJAVA NIZKO- IN VISOKOTLAČNEGA POSTOPKA VRAČANJA

Rezultati računalniških simulacij so pokazali, da je mogoče tako z nizko- kakor z visokotlačnim sistemom dosegati enake stopnje vračanja izpušnih plinov. Predpostavimo torej lahko, da sta oba postopka enako učinkovita z vidika zmanjševanja emisije NOx. Delovanje turbokompresorja v obeh sistemih pa se precej razlikuje. Masni pretok skozi kompresor in turbino je pri visokotlačnem postopku manjši kakor pri nizkotlačnem. Relativna razlika znaša prav toliko, kolikor je stopnja vračanja. Zmanjšan masni pretok lahko ogrozi stabilno delovanje kompresorja, saj se delovne točke pomaknejo bliže k meji črpanja, kakor to prikazuje slika 7. Delovne točke kompresorja v sistemu z nizko-tlačnim postopkom vračanja so tik ob delovnih točkah kompresorja testnega motorja brez regeneracije. V sistemu z visokotlačnim postopkom so se delovne točke precej bolj približale meji črpanja. Kadar se takemu premiku pridružijo še tlačni valovi, ki se prek visokotlačnega recirkulacijskega sistema razširijo v polnilno cev, lahko postane delovanje kompresorja nestabilno.

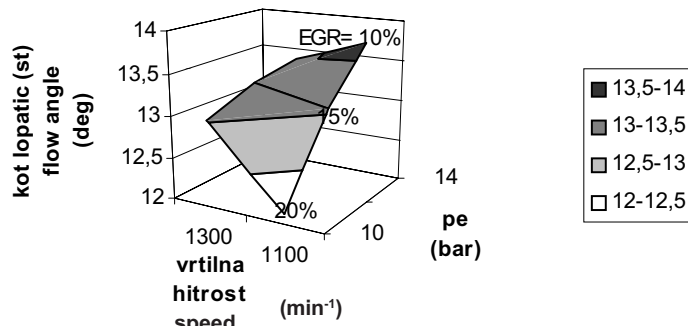
Potovanje tlačnih valov skozi visokotlačni povratni sistem lahko preprečimo z uporabo dveh protipovratnih ventilov. Pri tem je prvi postavljen na vstopu drugi pa na izstopu iz sistema. Pri tem deluje hladilnik izpušnih plinov kot visokotlačni akumulator. To podaljša obdobje polnjenja polnilne cevi z izpušnimi plini in zmanjša intenzivnost pretoka. Kakor

same EGR rates as with the low-pressure EGR concept. A diagram of the guide-vanes angle used in the simulations of the high-pressure EGR concept using the VG turbine is shown in Fig. 6. The mean volute outflow angle of the original turbine without guide vanes was  $\alpha_s=20^\circ$ . As can be seen from Fig. 6, an almost 40 % reduction of the flow angle was necessary for the operation of high-pressure EGR with the same engine system performance as low-pressure EGR in terms of the operational parameters.

### 3 COMPARISON OF LOW- AND HIGH-PRESSURE EGR

The computations showed that similar EGR rates can be generated in both high- and low-pressure EGR configurations. Since the charge-mixture temperatures did not differ significantly, it can be assumed that the NOx-emission reduction is also similar for both concepts. The operation of the turbocharger, however, differed significantly with both EGR systems. In contrast to low-pressure EGR, the total air mass flow through the compressor and through the turbine decreased when using high-pressure EGR. This mass flow reduction is equal to the EGR rate, and may cause the compressor operation to be near, or even within, the non-stable surge region. Figure 7 shows the effects of EGR on the positions of the compressor's operational points on the compressor map. The compressor operational points using low-pressure EGR were located close to the compressor operational line of the original test engine, while the compressor operational points using high-pressure EGR shifted towards the surge line. When this shift is accompanied by pressure pulses passing through the high-pressure EGR system, compressor surge might occur.

The application of the reed valve on both sides of the EGR cooler hinders the pressure pulses when travelling through the EGR cooler. Moreover, in this configuration the EGR cooler operated as a high-pressure accumulator and distributed the recirculated exhaust gas into the intake system for an interval that was much longer than the filling period of the EGR cooler. The velocity and



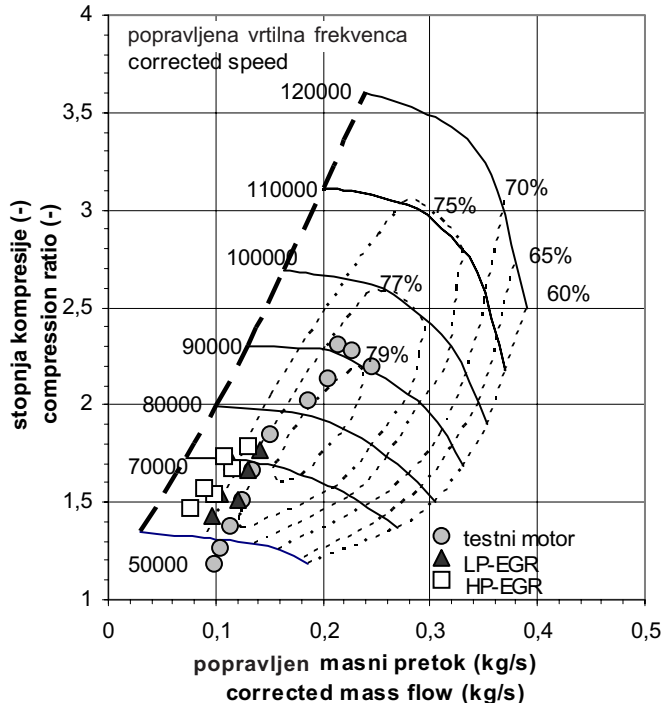
Sl. 6. Spremeba kota naklona vodilnih lopatic turbine – visoko-tlačni sistem vračanja  
Fig. 6. Map of guide vane angles for VG turbine in combination with high-pressure EGR

prikazuje slika 8, se največja hitrost plinov od vstopa v sistem do izstopa iz njega zmanjša od 140 m/s na 25 m/s, tlačna amplituda pa se zmanjša z 0,4 bar na 0,05 bar.

Kljub temu, da je masni pretok skozi valje motorja enak, pa obstajajo pomembne razlike med postopkom izmenjave delovne snovi v obeh sistemih. Primerjavo potekov tlaka v valju prikazuje slika 9. Med izpuhom se tlak v valju pri sistemu z visokotlačnim vračanjem znižuje precej hitreje kakor pri sistemu z nizkotlačnim vračanjem, saj izpušni

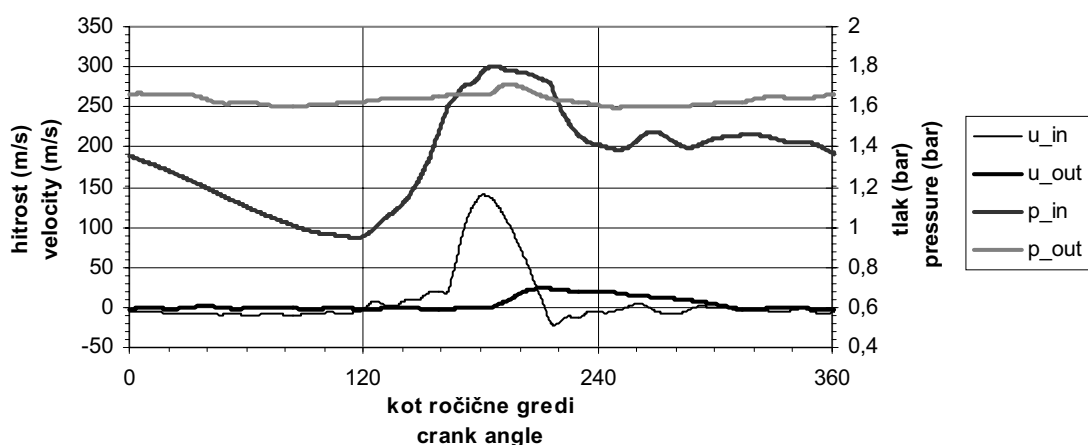
pressure pulses transferred into the intake system, therefore, were low (Fig. 8), and did not interfere with the compressor's operation. The maximum exhaust-gas velocity was reduced from 140 m/s at the EGR system's inflow side to 25 m/s at the outflow side, and similarly the pressure amplitude was reduced from 0.4 bar to 0.05 bar.

Although the mass flow through the engine cylinders and the boost pressure were similar in the cases of both EGR configurations, there were some evident differences during the gas-exchange process. In-cylinder pressure-time histories are compared in Fig. 9. During the



Sl. 7. Delovne točke kompresorja za motor brez vračanja, motor z nizko-tlačnim vračanjem (LP-EGR) in motor z visoko-tlačnim vračanjem (HP-EGR)

Fig. 7. The original test engine, the low-pressure EGR concept (LP-EGR) and the high pressure EGR concept (HP-EGR) compressor operational points



Sl. 8. Potek tlaka in hitrosti pred ( $p_{in}$ ,  $u_{in}$ ) in za hladilnikom izp. plinov ( $p_{out}$ ,  $u_{out}$ ) – visoko-tlačno vračanje

Fig. 8. Pressure- and velocity- time histories at the EGR cooler entry ( $p_{in}$ ,  $u_{in}$ ), and at the EGR cooler exit ( $p_{out}$ ,  $u_{out}$ ) - high-pressure EGR

Preglednica 2. Primerjava relativnega indiciranega dela izmenjave delovne snovi za sistem z nizkotlačnim (LP) in visokotlačnim (HP) vračanjem

Table 2. Comparison of relative indicated pumping work with low-pressure (LP) and high-pressure (HP) EGR configuration

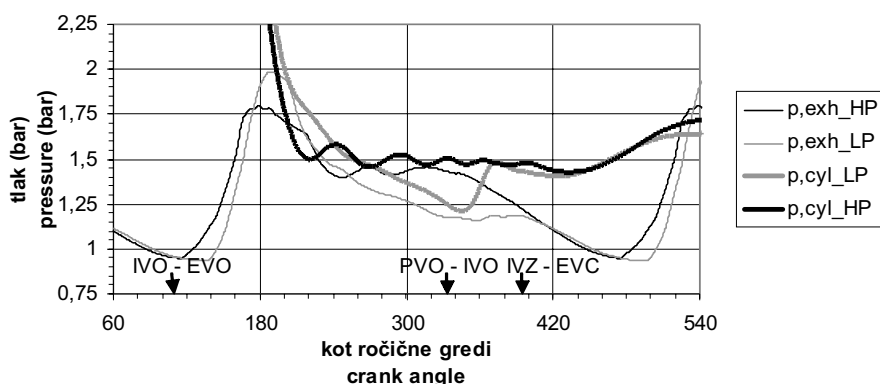
	$p_e=14$ bar, EGR=10% LP	$p_e=14$ bar, EGR=20% HP	$p_e=12$ bar, EGR=15% LP	$p_e=12$ bar, EGR=15% HP	$p_e=14$ bar, EGR=20% LP	$p_e=14$ bar, EGR=20% HP
1100 min <sup>-1</sup>	0,75%	0,54%	0,54%	0,35%	0,39%	0,18%
1300 min <sup>-1</sup>	0,12%	-0,17%	0,00%	-0,13%	-0,24%	-0,35%

plini hkrati ekspandirajo skozi turbino in v hladilnik izpušnih plinov. V trenutku, ko se na vstopnem protipovratnem ventilu vzpostavi negativno tlačno razmerje, se tlačni valovi odbijejo od njega nazaj v izpušni sistem. Tlak v izpušnem sistemu se zato zviša, z njim pa tudi tlak v valju. Ta sekundarni tlačni val vpliva na postopek izmenjave delovne snovi na dva načina. Močno se poveča masa zaostalih izpušnih plinov in poveča se delo, potrebno za izmenjavo delovne snovi. Povečanje mase zaostalih plinov (do 15 %) lahko štejemo za pozitiven učinek, saj poveča stopnjo vračanja, medtem ko pa je povečanje dela potrebnega za izmenjavo delovne snovi, nezaželeno.

V preglednici 2 je prikazano indicirano delo, potrebno za izmenjavo delovne snovi, ki smo ga določili z numerično integracijo izračunanega tlaka v valju motorja. Rezultati so podani v obliki relativnih deležev srednjega dejanskega dela. Delo izmenjave delovne snovi je pri vrtilni frekvenci motorja 1100 min<sup>-1</sup> pozitivno v vseh primerih, pri 1300 min<sup>-1</sup> pa je pozitivno le v sistemu z nizkotlačnim vračanjem. V povprečju je relativno delo izmenjave delovne snovi v sistemu z nizkotlačnim vračanjem za 0,1 do 0,3-odstotne točke manjše. Zato lahko sklepamo, da je dejanski izkoristek motorja z nizkotlačnim vračanjem v enaki meri (0,1 do 0,3-odstotne točke) večji.

exhaust period using high-pressure EGR the in-cylinder pressure decreased much faster, because the exhaust gases expanded into the EGR cooler and through the turbine at the same time. Once the pressure difference at the EGR cooler entry became negative, however, the pressure pulses were reflected from the reed valve back to the exhaust system, and both the exhaust system and the in-cylinder pressures increased. This secondary pressure pulse deteriorated the gas-exchange process in two ways. The residual gas mass fraction increased, and the pumping work, necessary for gas exchange, also increased. Up to 15 % higher residual mass fraction was observed using high-pressure EGR. Since this helped to increase the EGR rate the effect was regarded as positive. The increased pumping work reduced the overall engine efficiency and had a negative effect.

The indicated pumping work calculated from the computed in-cylinder pressure traces for both EGR configurations is presented in Table 2 and expressed as a percentage of the total effective work. The positive values relate to 1100 rpm, and the negative values to a 1300-rpm high-pressure EGR operating regime. The low-pressure EGR relative pumping work shows between 0.1 and 0.3 percentage points higher than its relative value for high-pressure EGR. It may, therefore, be assumed that the same difference (between 0.1 and 0.3 percentage points) also exists between the overall engine efficiencies.



Sl. 9. Potek tlaka v valju in v kanalu izpušnega ventila za motor z nizko-tlačnim ( $p_{cyl\_LP}$ ,  $p_{exh\_LP}$ ) in visoko-tlačnim vračanjem ( $p_{cyl\_HP}$ ,  $p_{exh\_HP}$ )

Fig. 9. Comparison of pressure-time histories within the cylinder and exhaust manifold with low-pressure EGR ( $p_{cyl\_LP}$ ,  $p_{exh\_LP}$ ) and high-pressure EGR ( $p_{cyl\_HP}$ ,  $p_{exh\_HP}$ )

## 4 SKLEP

V prispevku smo prikazali rezultate meritev vpliva vračanja izpušnih plinov na emisijo škodljivih komponent v izpušnih plinih. Ugotovili smo, da že 10-odstotna stopnja vračanja prepolovi emisijo NO<sub>x</sub>, pri čemer se emisija preostalih škodljivih komponent ne poveča pomembno. Šele pri 20-odstotni stopnji vračanja se močno zvečajo koncentracije CO in saj. Te ugotovitve smo upoštevali v nadaljevanju, ko smo z uporabo enorazsežne numerične simulacije ovrednotili dva postopka recirkulacije izpušnih plinov v 4-valjnem tlačno polnjenem dizelskem motorju. Na podlagi računskih rezultatov lahko podamo naslednje ugotovitve:

- Z obema postopkoma nizko- in visokotlačnim je mogoče doseči stopnje vračanja med 10 in 20 %, ki zagotavljajo občutno znižanje NO<sub>x</sub>.
- V sistemu z nizkotlačnim postopkom za povečanje tlaka polnjenja in ohranitev zadostnega presezka zraka zadošča manjši okrov turbine z obtočnim ventilom.
- V sistemu z visokotlačnim postopkom se turbina z manjšim okrovom ne obnese. Potrebna je turbina s spremenljivo geometrijsko obliko, da hkrati povečamo učinek turbo-kompresorja in stopnjo vračanja.
- Nizkotlačni postopek vračanja ne vpliva na postopek izmenjave delovne snovi. Prostorninski izkoristek, koeficient zaostalih plinov in delo izmenjave delovne snovi ostanejo enaki kakor v primeru motorja brez regeneracije.
- Z visokotlačnim postopkom se poveča poraba dela za izmenjavo delovne snovi. Pripomniti pa velja, da smo obdržali nespremenjene krmilne čase ventilov in da bi se lahko z njihovim optimiranjem razmere izboljšale.

## 4 CONCLUSIONS

The influence of exhaust-gas recirculation on engine emissions was experimentally investigated. It was found that a 10 % EGR rate halved the NO<sub>x</sub> emissions and did not increase the emissions of other pollutants significantly. A drastic increase in CO and soot emissions was observed at 20 % EGR. These stating were considered in the continuation where the applications of two different EGR configurations on a four-cylinder, turbocharged diesel engine were studied by means of a one-dimensional simulation. Based on the computational results the following conclusions can be reached:

- for both the configurations investigated it was possible to achieve EGR rates in a range between 10 % and 20 %, which reduce NO<sub>x</sub> emissions significantly.
- the application of a smaller turbine housing was successful for increasing the boost pressure and maintaining the air-to-fuel ratio above the soot limit when the low-pressure EGR concept was applied.
- the smaller turbine housing did not work for the high-pressure EGR concept, and the application of a variable-geometry turbine was necessary in order to simultaneously increase the turbocharger performance and the EGR rate.
- the low-pressure EGR configuration did not interfere significantly with the gas-exchange process. The pumping work, volumetric efficiency, and residual gas fraction remained the same as in the case of the original engine scheme.
- a deterioration in the gas-exchange process parameters was noticed using the high-pressure EGR configuration. Optimisation of the valve timing, however, which might have improved the effective engine data was not taken into consideration.

## 5 LITERATURA

### 5 REFERENCES

- [1] Needham, J.R., D.M. Doyle, A.J. Nicol (1991) The low NO<sub>x</sub> truck engine, SAE Paper 910731.
- [2] Heywood, J.B. (1988) Internal combustion engine fundamentals, McGrawHill, New York.
- [3] Ached, N., U.D.T. Sat, H. Sugar (1993) *Combined effects of EGR and supercharging on diesel combustion and emissions*, SAE Paper 930601.
- [4] Odaka, M., N. Koike, Y. Tsukamoto, K. Narusawa (1992) Optimizing control of NO<sub>x</sub> and smoke emissions from DI engine with EGR and methanol fumigation, SAE Paper 920468.
- [5] Kohketsu, S., K. Mori, K., Sakai, T. Hakozaki (1997) EGR technologies for a turbocharged and intercooled heavy-duty diesel engine, SAE Paper 970340.
- [6] Schmitt, F., A. Lingens (2001) The potential of different exhaust gas recirculation systems, *AutoTechnology* 2/2001, 70–73.
- [7] Hribenik, A. (1995) Primerjava brez- in enodimensionalnih metod za simuliranje procesov v tlačno polnjenem dizelskem motorju, *Strojniški vestnik*, let. 41, št. 7-8, 229-238.
- [8] Benson, R.S. (1982) The thermodynamic and gas dynamics of internal-combustion engines, Vol. I, Clarendon Press, Oxford.
- [9] Hinds, E.T., G.P. Blair, Unsteady gas flow through reed valve iduction system, SAE Paper 780766
- [10] Hribenik, A. (1994) Modeliraje robnih pogojev dvonatočne turbine turbokompresorja vozilskega dizel motorja, doktorska disertacija, Maribor.

Naslov avtorjev: doc. dr. Aleš Hribernik  
mag. Gorazd Bombek  
Fakulteta za strojništvo  
Univerza v Mariboru  
Smetanova 17  
SI-2000 Maribor  
[ales.hribernik@uni-mb.si](mailto:ales.hribernik@uni-mb.si)  
[gorazd.bombek@uni-mb.si](mailto:gorazd.bombek@uni-mb.si)

Author's Address: Doc. Dr. Aleš Hribernik  
Mag. Gorazd Bombek  
Faculty of Mechanical Eng.  
University of Maribor  
Smetanova 17  
SI-2000 Maribor, Slovenia  
[ales.hribernik@uni-mb.si](mailto:ales.hribernik@uni-mb.si)  
[gorazd.bombek@uni-mb.si](mailto:gorazd.bombek@uni-mb.si)

Prejeto: 22.10.2003  
Received: 22.10.2003

Sprejeto: 12.2.2004  
Accepted: 12.2.2004

Odperto za diskusijo: 1 leto  
Open for discussion: 1 year

# Obravnavo motorja z notranjim zgorevanjem in vbrizgavanjem plinskega goriva

A Rapid-Compression-Machine Study of Gaseous Fuel Injection and Combustion

Dariusz Klimkiewicz · Tomasz Leżański · Rafał Jarnicki ·  
Tadeusz J. Rychter

V prispevku so predstavljene analize sistema za dovajanje goriva pri motorjih z notranjem zgorevanjem in neposrednim vbrizgavanjem plinskega goriva. Kratki primerni časi za vbrizgavanje plinskega goriva ter slabo prodiranje goriva in mešanje le-tega z okoliškim zrakom pomenijo velike probleme pri pravilnem vžigu in nadzorovanem zgorevanju mešanice. Ena izmed rešitev za olajšanje vžiga je uporaba manjše vžigalne predkomore. Vžig mešanice se tako začne že v predkomori, vroči in kemično dejavni zgorevalni plini pa nato pripomorejo k razbitju curka goriva v glavnem zgorevalnem komori, kjer poteka nadaljnje zgorevanje. Predstavljeni so rezultati raziskav vpliva oblike zgorevalnih komor pri uporabi neposrednega vbrizgavanja plinskega goriva na učinkovitost in ponovljivost vžiga. Raziskave so podprte z rezultati numeričnih simulacij postopka vbrizgavanja in mešanja plinskega goriva. Prikazano je, da lahko s predlaganim sistemom obidemo težave pri doseganju ponovljivega vžiga pri motorjih z neposrednim vbrizgavanjam plinskega goriva.

© 2004 Strojniški vestnik. Vse pravice pridržane.

(Ključne besede: motorji z notranjim zgorevanjem, vbrizgavanje goriva, goriva plinska, zgorevanje)

Rapid-compression-machine studies of an engine's combustion system with the direct injection of gaseous fuel were made. The very short time available for the injection, combined with the poor penetration and mixing of the gas jet with the surrounding air, caused the serious problems with combustion initiation. One of the solutions to facilitate the ignition seems to be the use of a small ignition prechamber. The ignition takes place within the prechamber and the hot, chemically active combustion gases saturate the gaseous fuel jet that enters the main chamber where the mixing and combustion processes are continued. The results of the investigations aimed at obtaining an efficient and repetitive ignition of the gaseous fuel jet are presented. Various versions of the combustion chamber were investigated. The investigations were supported by the results of numerical calculations of the injection and mixing processes. We concluded that this type of combustion system has the potential to overcome the difficulties in achieving the repetitive ignition of the gaseous fuel jet.

© 2004 Journal of Mechanical Engineering. All rights reserved.

(Keywords: internal combustion engines, fuel injection, gaseous fuels, combustion)

## 0 INTRODUCTION

The use of natural gas as a fuel for internal combustion piston engines has a number of advantages, which are well known to engine designers and researchers. There are many production engines where gasoline has been substituted by natural gas without major changes to the engine's operating mode but with a change in the fuel feeding system. In all such gas engines the gaseous fuel is delivered through the induction tube, and this means that the gas occupies a certain volume of the entire charge, decreasing the amount of air that is delivered to the engine cylinder during each engine cycle. This, in

turn, tends to decrease the volumetric efficiency of the engine. To improve that efficiency, engine research centers try to find another solution, e.g., to develop the idea of injecting the gaseous fuel directly into the engine's combustion chamber. There are two ways to do this: to start the injection at an early stage of the compression stroke of the piston or to initiate the injection at the end of compression stroke. The former solution has already been applied to some production engines and it did not create major difficulties. The latter solution, however, still creates a lot of problems. The time available for the mixing of the injected gas with the air is very short, and the gaseous jet penetration in the combustion-chamber

Opomba uredništva: Znanstveni članki tujih avtorjev so lahko odslej samo v angleščini.

volume and its mixing with the air is weak. Compression-ignition of natural gas is practically impossible within the range of reasonable compression ratios; therefore, any type of forced ignition has to be used. If the mentioned problems were solved the combustion system with the late direct injection of natural gas would take advantage of the high compression ratio (on a diesel level) and still remain a spark-ignition system because of the necessary stabilizing role of the forced combustion initiation. The advantage of this type of combustion system is the reason that engine research centers try to remove the difficulties associated with the mixing and repeated ignition of the charge. It is appropriate to mention that practically all the problems with natural gas storage, its supply to injectors and the action of the injector itself have already been solved. However, the in-cylinder processes in this type of combustion system still wait for the right organization.

## 1 THE GENERAL IDEA OF THE INVESTIGATED SYSTEM

To ensure the repeated ignition of the charge and, at the same time, to increase the mixing rate of the injected gaseous fuel with air and the combustion rate, the use of an ignition prechamber was proposed (Fig. 1). This prechamber is connected to the main chamber by an orifice. The orifice diameter is carefully designed to be a little bigger than the dimension of the gas jet's cross-section. During injection the main volume of the injection stream passes undisturbed to the main chamber and only a small external part of the jet is scrubbed off by the orifice edges. This portion of the injected gas remains in the prechamber, is mixed with the air and creates the portion of the charge that is ignited by the conventional spark plug. Since the shape of the gas jet remains basically unchanged the stoichiometry of the mixture in the prechamber should also be, relatively speaking, the same during each consecutive engine cycle. Therefore, there is a chance for repeatable and reliable ignition. Moreover, the charge in the prechamber is

ignited when the injection is still in progress. The injected gas is then saturated with the combustion gases generated in the prechamber, which are then convected to the main chamber. The hot combustion gases containing chemically active free radicals create so-called multi-point ignition in the main chamber.

## 2 EXPERIMENTAL SETUP

The objective of this paper is to present the results of the preliminary investigations of the combustion system described above. The investigations were performed with the use of the rapid compression machine, described elsewhere, which makes it possible to visualize the in-cylinder phenomena [1]. The results of the experiments were compared with the results of calculations performed with the use of the KIVA3V computer code reduced to planar geometry [2]. The schematics of the experimental setup and combustion-chamber geometry are shown in Figures 2 and 3. The compression ratio was 10.8 and the piston velocity corresponded to an actual engine speed of 1600 rpm.

A Mitsubishi GDI injector was used for the gas injection. The injection pressure of the methane was 25 bar. The beginning of the injection, its duration and the ignition timing were adjusted and automatically controlled with an accuracy of 1 CA deg (crank angle degree). The reactions of the system investigated on the changes to following parameters were: beginning of the injection – (20–165 deg BTDC); injection duration – (15–50 CA deg); ignition timing – (10–30 deg BTDC).

Two prechamber geometries were investigated: without (Version I) and with the bypass channels (Version II).

## 3 RESULTS

As a result of the experimental investigations a number of pressure profiles and the corresponding series of framed pictures of the combustion processes was obtained. First, the development of the injected gaseous fuel jet was visualised to

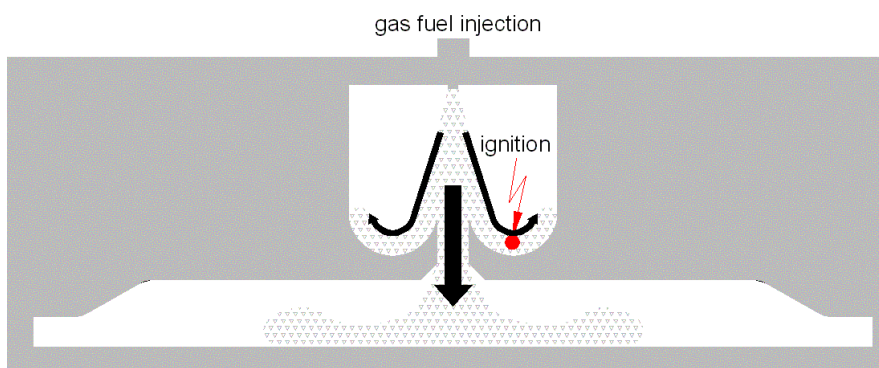


Fig. 1. Schematic of the general idea

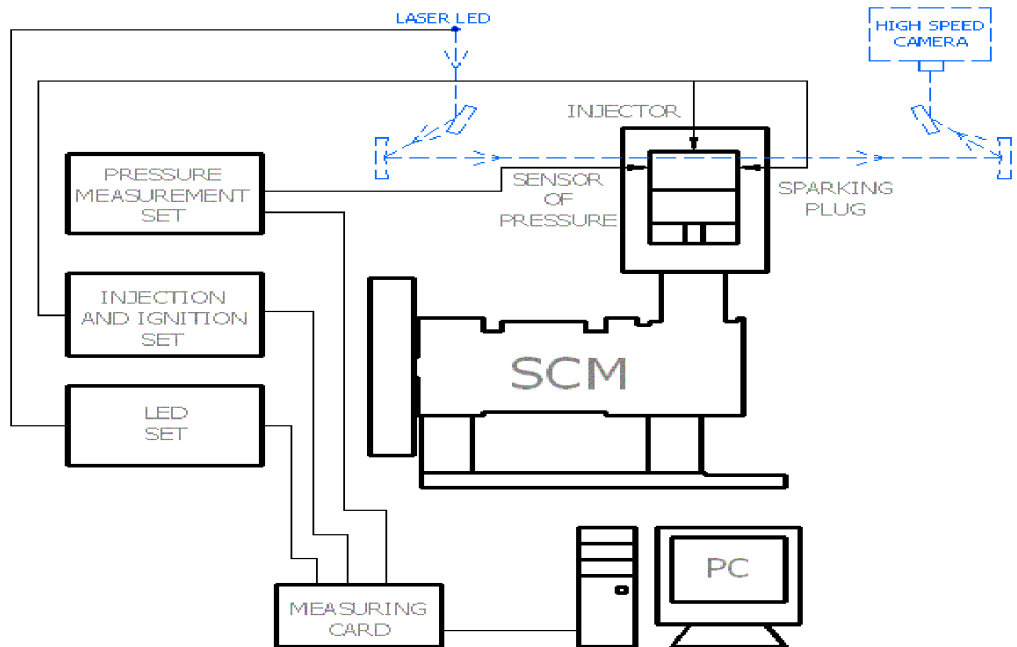


Fig. 2. Schematics of the experimental setup

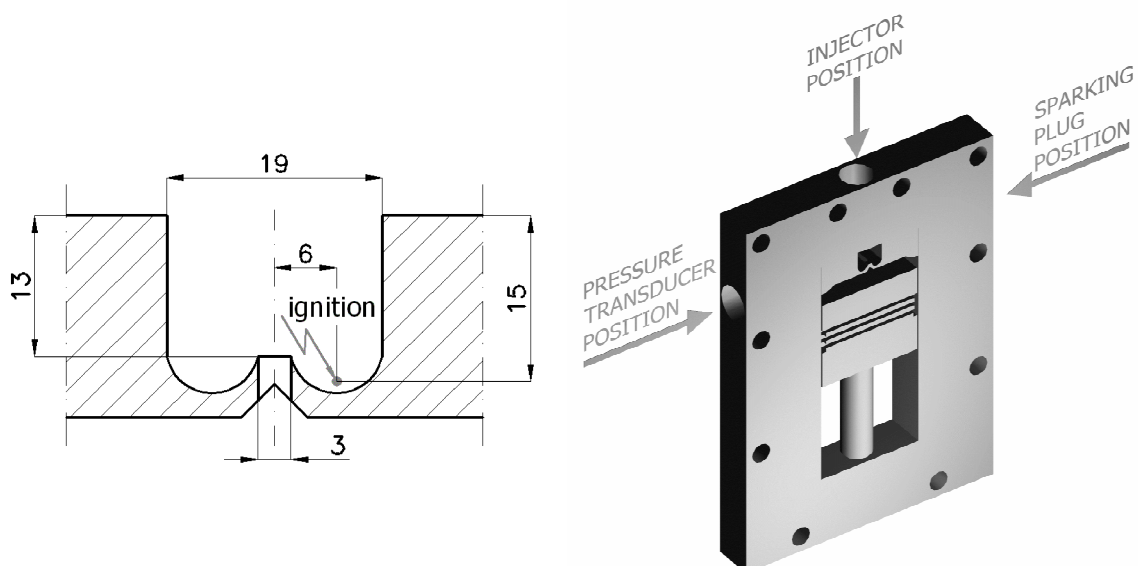


Fig. 3. Combustion-chamber geometry

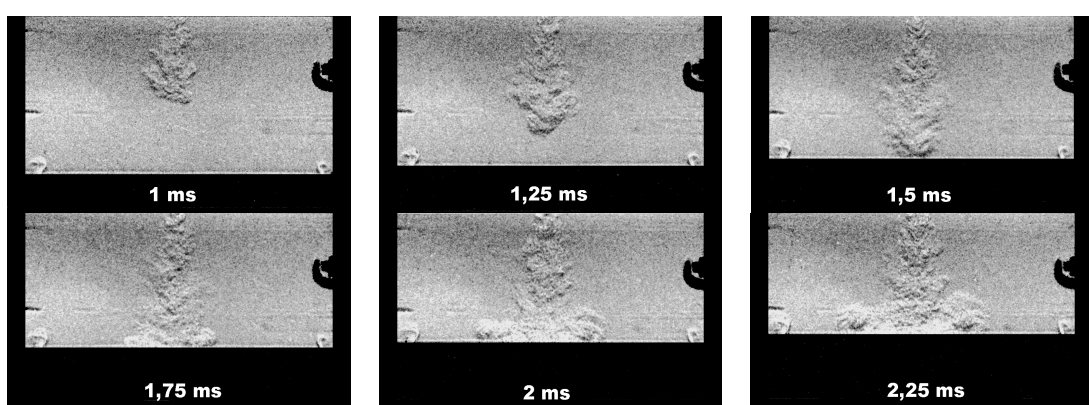


Fig. 4. Visualisation of methane injection

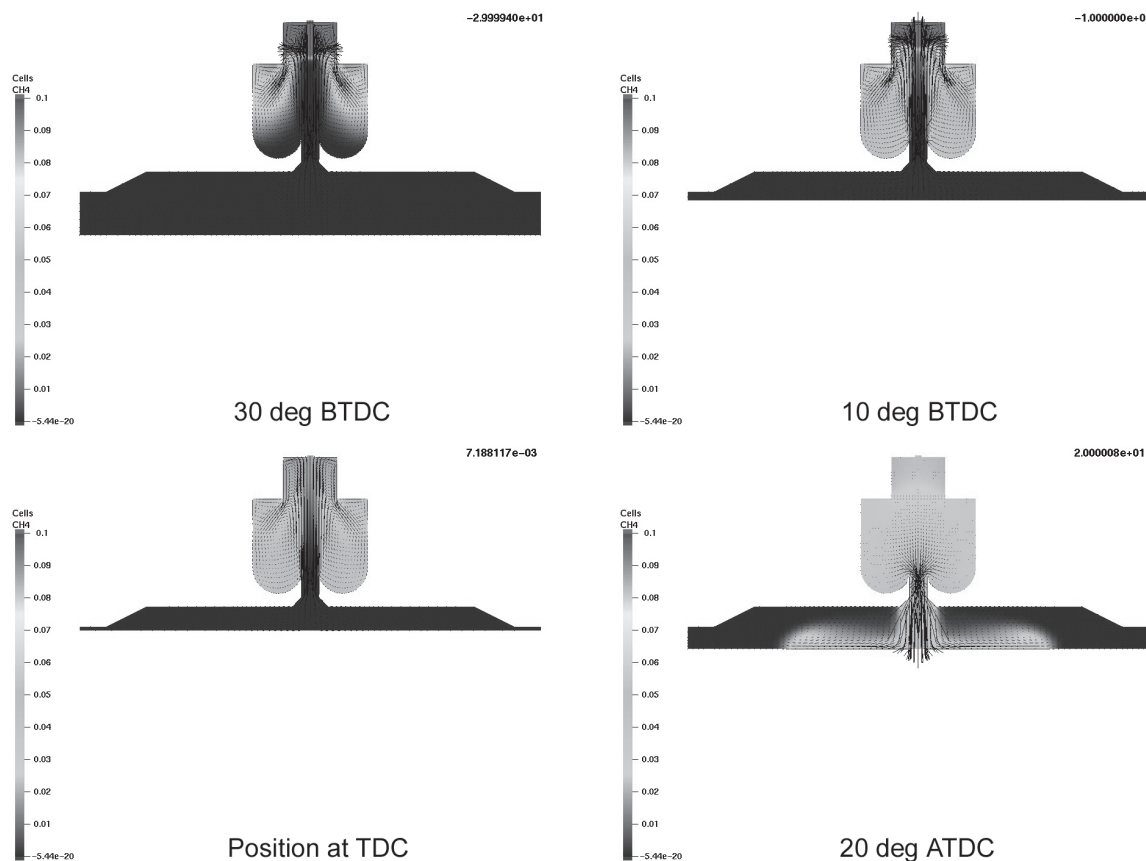


Fig. 5. Velocity and methane-concentration distribution (prechamber geometry - version I)

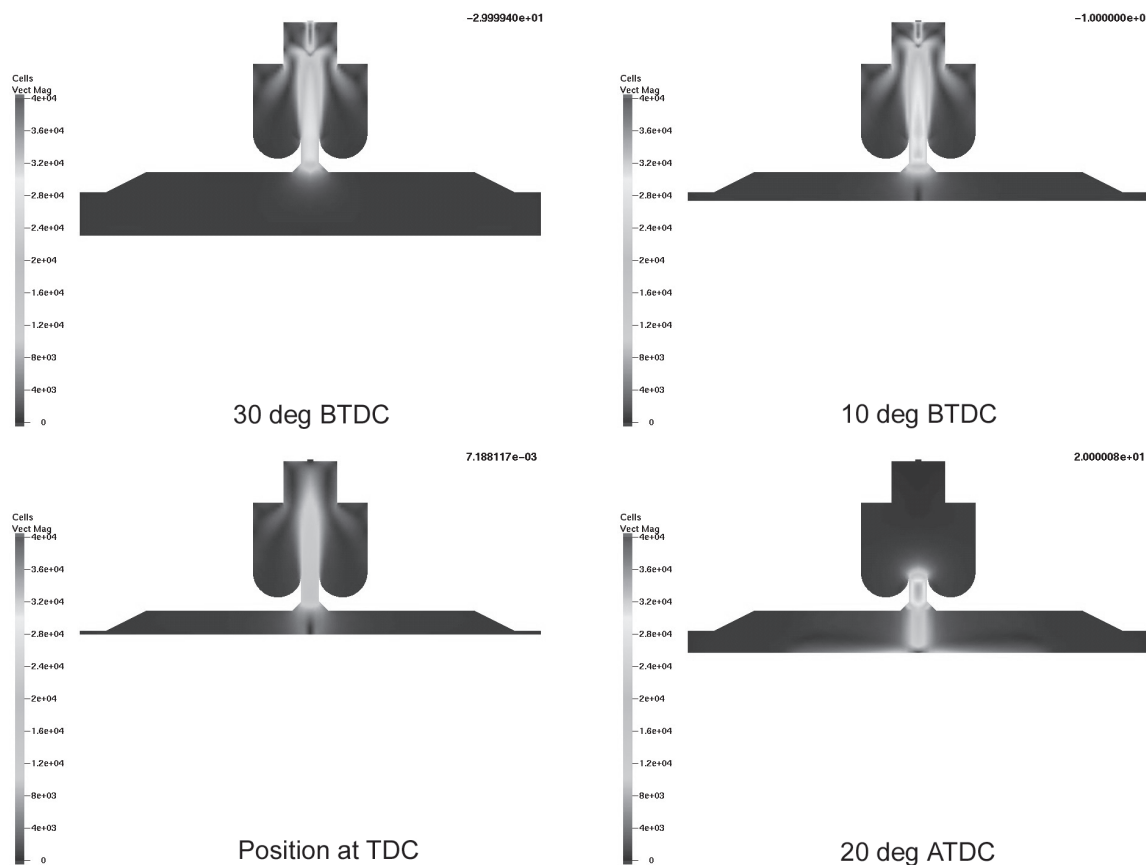


Fig. 6. Velocity field (prechamber geometry - version I)

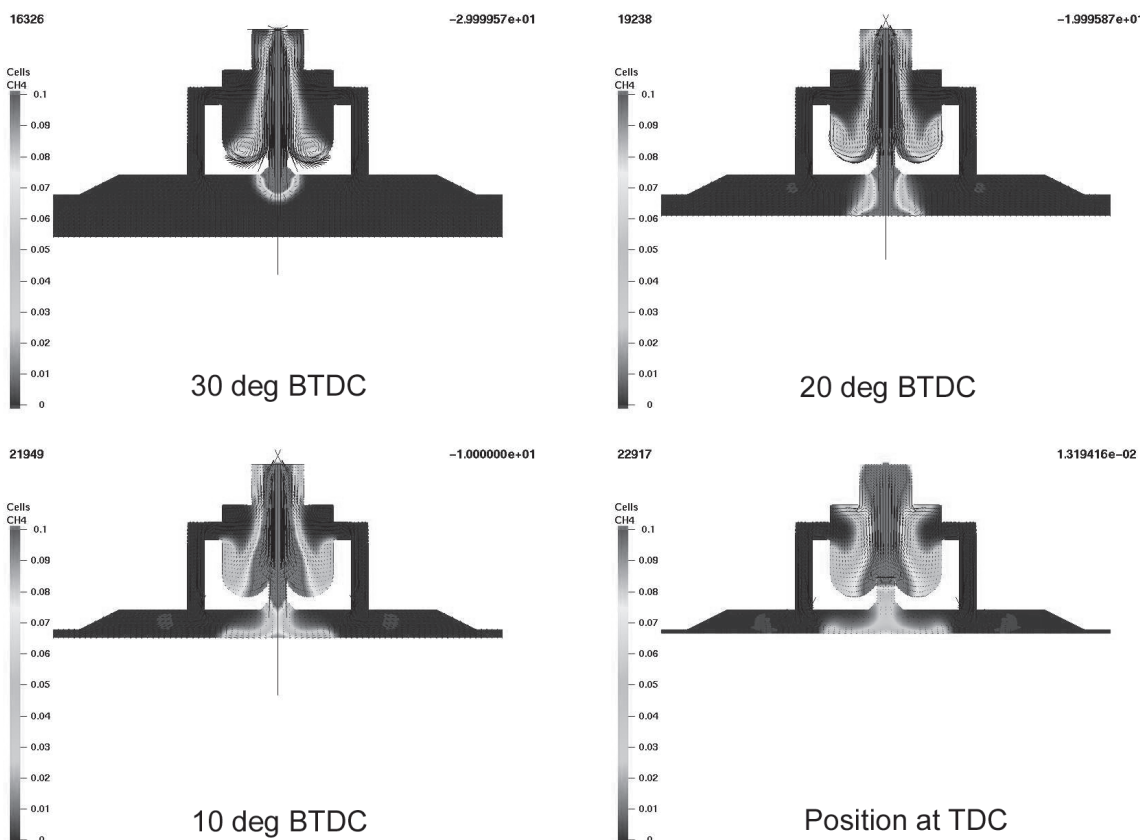


Fig. 7. Velocity and methane-concentration distribution ( prechamber geometry – version II )

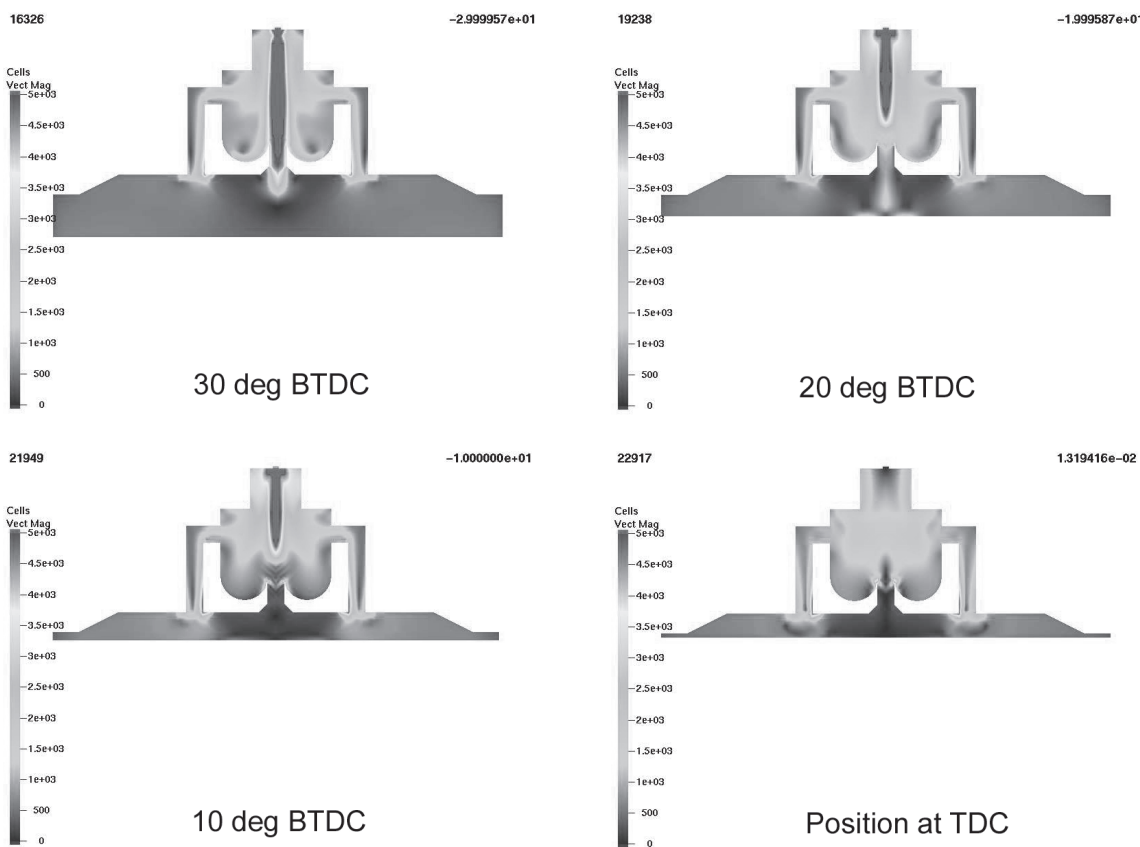


Fig. 8. Velocity field ( prechamber geometry – version II )

determine its geometry and its ability to mix with the air. The framed pictures (obtained with the use of a schlieren technique) of the injection process are presented in Figure 4. The generation of the fuel jet was also carefully tested and the full characteristics of the jet (jet dimensions, fuel dose etc.) were determined.

**Version I.** Preliminary investigations of the combustion process in the chamber geometry presented in Figure 3 have shown that it is impossible to achieve the ignition of the charge under any set of system parameters. To find the reason for that the numerical analysis of the injection process was performed. The resulting gas-velocity distribution and the methane concentration in the prechamber allowed for the determination of the cause of the lack of ignition. The simple reason for this was that the injection took place during the end of compression stroke when the intensive flow of the air from the main chamber to the prechamber occurred in the orifice. The upstream velocity, of the air in the orifice was much greater than fuel jet velocity and therefore whole amount of the fuel injected remained in the prechamber. The mixture in the prechamber was much too rich side. The demonstration of the velocity and methane-concentration distribution for this case is introduced in Figures 5 and 6.

**Version II.** To decrease the air velocity in the orifice generated by the compression it was necessary to increase the overall area of the channels connecting both chambers. The main orifice remained unchanged but two additional discharging channels were made. This drastically reduced the upstream air velocity in the orifice and the injected gaseous fuel was passing to the main chamber without difficulties. The motion of the gas in the chamber and the methane-concentration distribution in this case are presented in Figures 7 and 8. This change in the combustion-chamber geometry allowed for the repeatable ignition of the charge.

The framed pictures of the combustion process obtained from the experiments with the use of the rapid compression machine in the same combustion-chamber geometry are presented in Figure 9. First, the injected stream of fuel passes through the prechamber and its main portion enters the main chamber. The fuel gas scrubbed off the external part of the jet is mixed with the air in the prechamber where the flammable mixture is created. Then the charge in the prechamber is ignited and the combustion gases are intensively discharged to the main chamber due to the prechamber pressure rise and the action of the still injected gaseous fuel. Although it was observed that the overall pressure

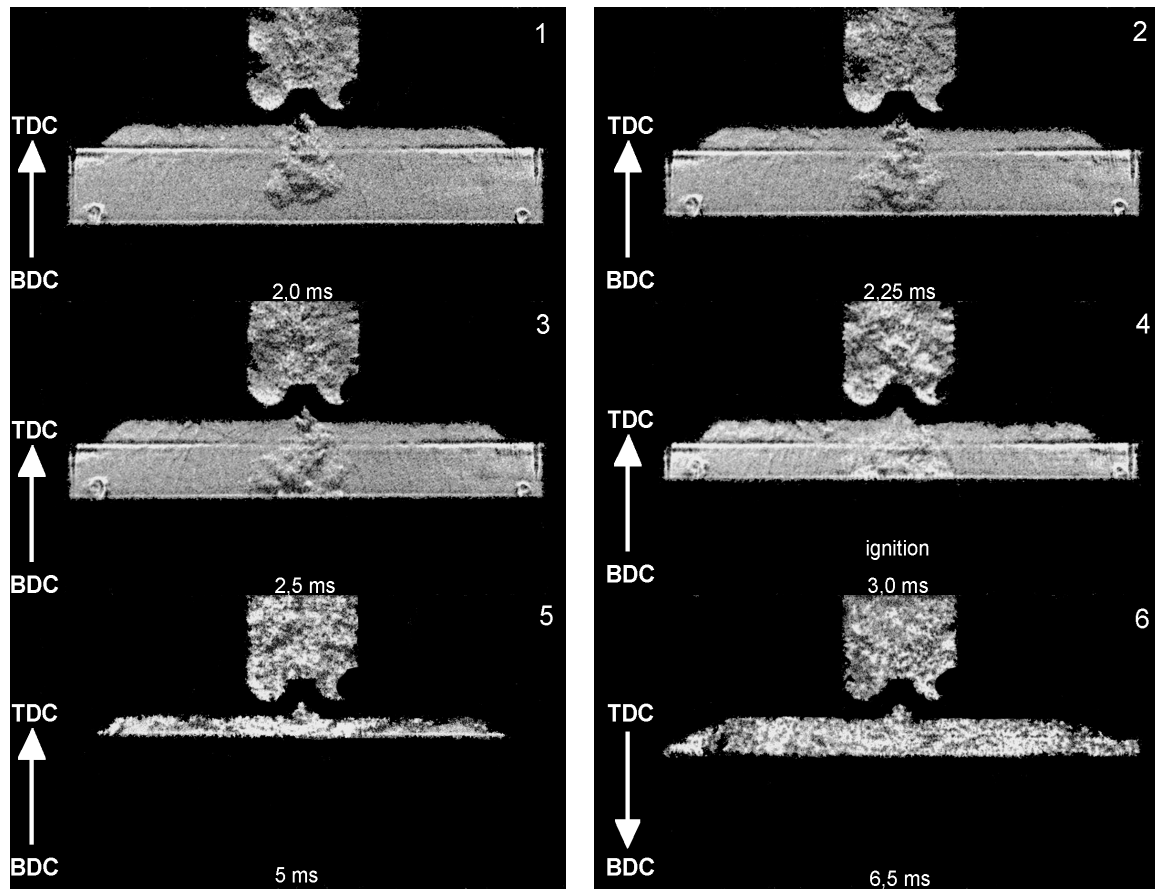


Fig. 9. Visualization of the methane-combustion process (prechamber geometry – ver. II)

rise rate in the combustion chamber is still not satisfactory, the difficulties with the ignition were removed.

The first frame in Figure 9 presents the methane jet 2 ms after the beginning of the injection. The methane jet enters the main chamber and the turbulence is generated in the prechamber. Frames 2 and 3 show the subsequent stages of methane injection. The ignition takes place during methane injection and this moment is presented in the fourth frame. Unfortunately, the high level of the turbulence in the prechamber is the reason why the combustion zone is hardly visible in the schlieren pictures. Moreover, the hot combustion gases generated in the prechamber are also ejected in the main chamber through the by-pass channels. The next frame was made just before TDC and shows the flame propagation process. The combustion has already been transferred in the main chamber but methane injection continues. The last frame taken after TDC presents the final stage of flame propagation, right after the end of the methane injection.

It is important to stress that the combustion-chamber geometry and dimensions were only designed for the rapid compression machine experiments and the aim of the presented

investigations was to check whether of not the assumed idea of the system operation has been right. For the actual engine experiments the shape and proportions of the combustion chamber must be completely redesigned.

It is worth mentioning that the attempts to decrease the volume of the prechamber or to change the size of the orifice between chambers were not successful and they again caused serious problems with ignition.

#### 4 SUMMARY

The major result of the investigation is that the proposed idea of a combustion system for engines with direct fuel-gas injection might be reasonable. The observed sensitivity of the system to its geometry and dimensions indicates that its application to the actual engine would require thorough optimization.

#### Acknowledgement

The presented investigations were supported by the State Committee for Scientific Research under the grant No. 9T12D 018 19.

#### 5 REFERENCES

- [1] Rychter, T.J., T. Leżański (2003) Inertia-driven single compression machine for combustion study, The Archive of Mechanical Engineering.
- [2] Amsden, A.A. (1997) KIVA-3V: A Block-structured KIVA Program for Engines with Vertical or Canted Valves, LA-13313-MS.

Authors' Address: Mag. Dariusz Klimkiewicz  
Mag. Tomasz Leżański  
Dr. Rafal Jarnicki  
Prof.Dr. Tadeusz J. Rychter  
Institute of Heat Engineering  
Warsaw Univ. of Technology  
Nowowiejska 21/25  
00-665 Warsaw, Poland  
[dklim@itc.pw.edu.pl](mailto:dklim@itc.pw.edu.pl)  
[lezanski@itc.pw.edu.pl](mailto:lezanski@itc.pw.edu.pl)  
[rjarn@wp.pl](mailto:rjarn@wp.pl)  
[rychter@itc.pw.edu.pl](mailto:rychter@itc.pw.edu.pl)

## Možne vrste cenih motorjev s prostornino 50 kubičnih centimetrov z majhno emisijo

Possible Solutions for EURO 2 "Low-Emission Low-Cost" 50cc Engines

Roland Kirchberger - Gernot Koller

*Predpis EURO 2, ki je stopil v veljavo junija 2002, postavlja velik izziv proizvajalcem majhnih dvotaktnih motorjev za pogon koles z motorjem. Če primerjamo razpoložljive tehnologije glede na stroške, tehnologijo izdelave in zmogljivost motorja, najdemo možnosti za uspešno rešitev omenjenega izizza.*

*Prispevek bo pokazal, da uporaba sistema za vbrizgavanje goriva ni nujno potrebna za doseg predpisov EURO 2 o izpušnih emisijah.*

*Pri proizvodnji dvotaktnih motorjev za pogon koles z motorji so stroški izdelave zelo pomembni. Ta prispevek opisuje metodo za doseganje predpisanih mej izpušnih emisij brez velikih stroškov, ki jih zahteva vrhunska tehnologija.*

*Opazno zmanjšanje škodljivih emisij in hkratno povečanje moči in navora motorja je mogoče doseči brez uporabe dodatnih delov, zgorj z optimiranjem termodinamike in mehanike motorja, kar kaže raziskava osnov delovanja motorja in proučevanje prototipa.*

*Preskusi različnih serijskih agregatov kažejo uporabnost predlagane izboljšave za serijsko izdelavo ob hkratnem izpolnjevanju zahtev po EURO 2.*

© 2004 Strojniški vestnik. Vse pravice pridržane.

**(Ključne besede: motorji dvotaktni, emisije majhne, stroški majhni)**

*The EURO 2 emission regulation, which has been in force since June 2002, is a challenge to the industry that produces small two-wheeler two-stroke vehicles. A summary and comparison of the available technologies, concerning costs, production technologies and aspects of performance will give a survey of the state of the art and will show possible ways of coping with this challenge.*

*It should be classified in advance if the use of an injection system is necessary in order to meet the EURO 2 exhaust-emission regulations.*

*Production costs are of special interest when dealing with the topic two-wheeler engines. This paper describes a method for achieving the required exhaust-emission limits without having to resort to "high-tech & high-cost" technologies. Without using any additional parts, only by optimising the given engine thermodynamics and mechanics, basic research and studies of prototypes will show how to achieve significant reductions in emissions and increases in the engine power and torque output.*

*Various vehicle tests will show the suitability for mass production, taking into account the required modifications necessary for fulfilling the EURO 2 exhaust-emission regulations.*

© 2004 Journal of Mechanical Engineering. All rights reserved.

**(Keywords: two-stroke engines, low emission, low costs)**

### 0 INTRODUCTION

It is a fact that an increase in the economic wealth of a society is matched by a growth in the amount of traffic.

Fig. 1 shows that there is a coherence between the per-capita gross national product and the number of vehicles in use. Therefore, an increase in the number of vehicles worldwide will, in all

probability, occur for the foreseeable future. Estimations for the next 10 years show that the global number of vehicles will increase by 45%. A disproportionate growth rate, of approximately 60%, will occur in the sector known as "two-wheeled vehicles".

This above-average growth in the two-wheeler sector is caused by the higher demand of the Asian markets. Legal regulations in most Asian

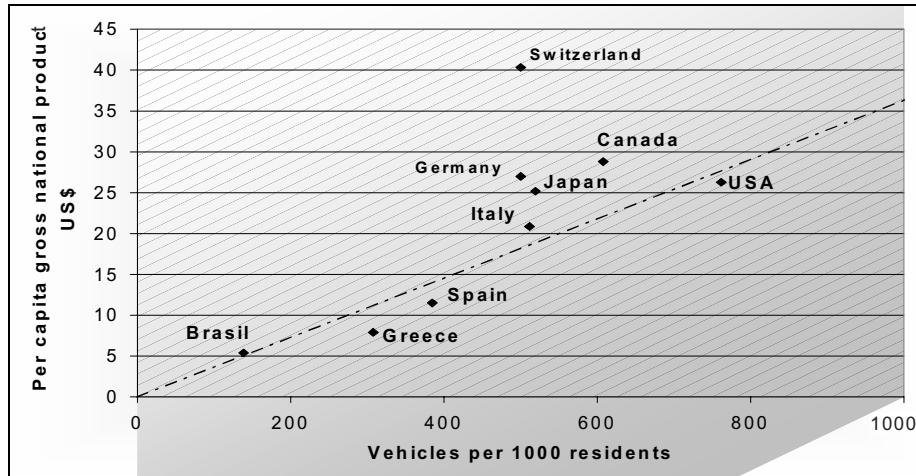


Fig. 1. Per-capita gross national product versus vehicles per residents [1]

countries take European regulations as a model. Taiwan, for example, has already established emission limits that are even stricter than those of the European Union. For this reason, two wheelers complying with the EUROMOPED Euro 2 exhaust-emission regulation, which came into force on the 1<sup>st</sup> of June 2002, are of global interest.

Most of the Euro 2 mopeds on the market today make use of high-tech and high-cost technologies in order to fulfill the legal requirements. This paper will show that Euro 2 can also be achieved with existing Euro 1 technologies, simply by optimizing the engine's thermodynamics.

## 1 REQUIREMENTS AND DEVELOPMENT TARGETS FOR SMALL TWO-WHEELER ENGINES

The first essential development target for all engine-development projects is to fulfil the corresponding legal regulations concerning maximum

power and torque, anti-tampering, as well as exhaust and noise emissions.

An additional requirement, especially for the small engines used in scooters and mopeds, are the production costs. The acceptance of additional costs for technologies necessary to fulfil legal limits is rather low. This means that the additional costs caused by the implementation of new technologies must be kept to the minimum. For this reason, lean production and the use of standard technologies are required for these engines.

Further development targets are weight optimisation, low fuel consumption, low maintenance and service costs as well as good performance characteristics and driveability.

### 1.1 EUROMOPED EURO 2 exhaust-emission regulation

Fig. 2 shows the large reduction in the exhaust-emission limits from the Euro 1 to the Euro 2

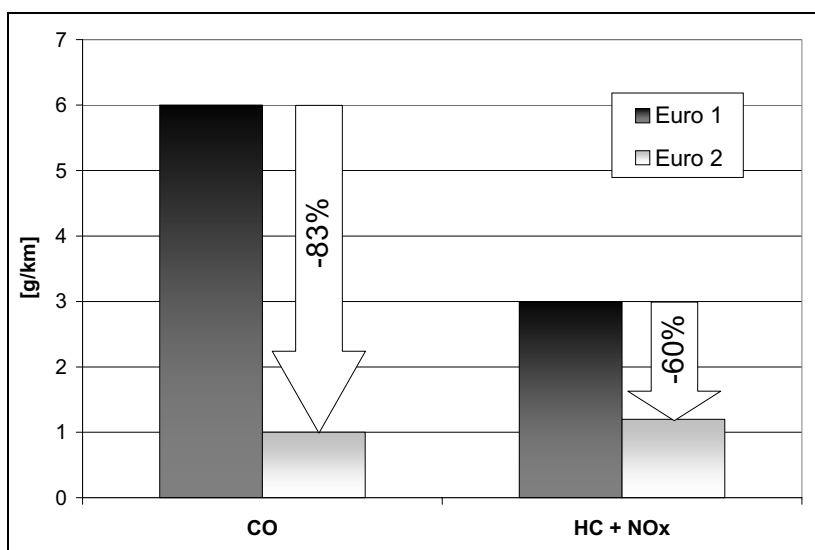


Fig. 2. Comparison between the Euro 1 and Euro 2 exhaust-emission limits [2]

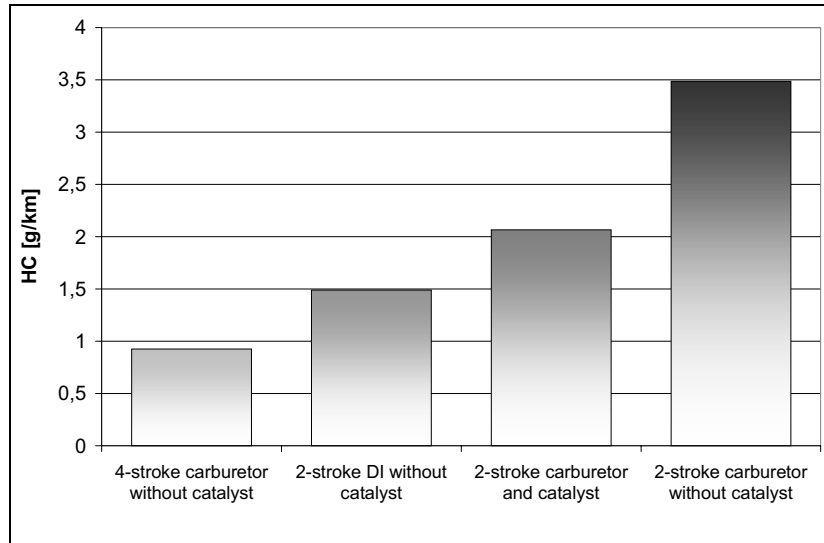


Fig. 3. Comparison between four-stroke and two-stroke HC exhaust emissions

regulation. This dramatic decrease in the tolerated level of exhaust emissions is a challenge for the small two-wheeler industry. The following is a short description of the different possible strategies to cope with this challenge.

#### 1.1.1 Four-stroke engine

Fig. 3 shows the hydro-carbon exhaust emissions in g/km in the ECE R 47 test-cycle for various 50cc engine configurations.

The comparison between the standard two-stroke and standard four-stroke engines, both with carburetor and without catalyst, shows a big advantage for the four-stroke concept. Not even the two-stroke direct-gasoline-injection technology can completely eliminate the disadvantage of the two-stroke concept with respect to HC emissions. This disadvantage is the result of the short circuiting of the fresh mixture to the exhaust port(s) during the two-stroke scavenging process. Because of the higher development, production and maintenance costs,

combined with the lower power output, hardly any four-stroke 50cc vehicles are available on the market at present.

#### 1.1.2 Two-stroke engine

Standard two-stroke engines for two-wheeler applications utilize the loop-scavenging process and a carburetor. By lean engine tuning and the application of an oxidation catalyst it was possible, until the commencement of the Euro 2 exhaust-emission limits, to comply with the exhaust emission limits. However, the upcoming stricter emission regulations are forcing two-wheeler manufacturers to apply new technologies to two-stroke engines in order to fulfill the legal requirements.

Fig. 4 gives a schematic overview of the different injection strategies for two-stroke engines. Figure A shows a possible solution for a high-pressure fuel-injection system. Figure B is a low-pressure injection system, and figure C shows a possible layout for an air-assisted fuel-injection system.

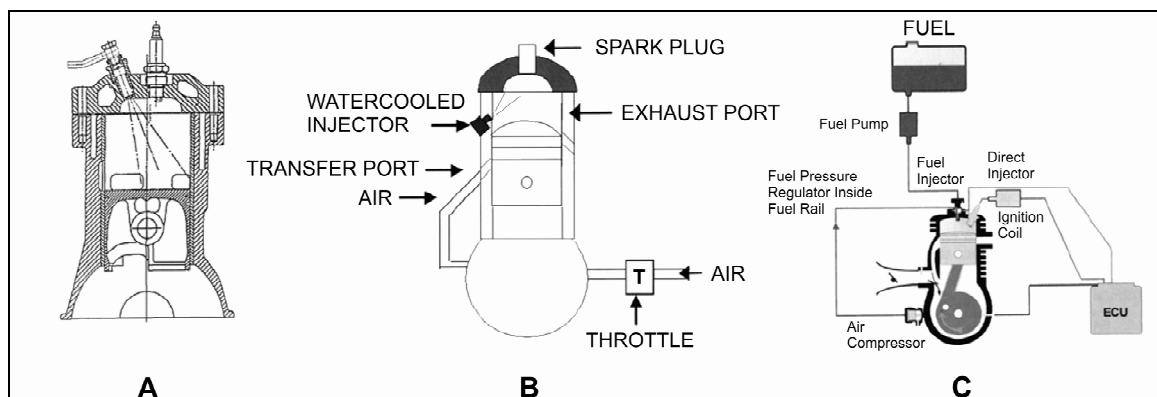


Fig. 4. Two-stroke injection systems ([3], [14] and [15])

### 1.1.2.1 High-pressure direct fuel injection

The biggest advantage of using a high-pressure direct-fuel-injection system in a two-stroke engine is that the fuel injection occurs after the complete or at least partial closing of the exhaust port(s). This leads to the prevention, or at least to the reduction of fresh-mixture short circuiting. For this reason, direct high-pressure fuel injection can dramatically reduce the hydrocarbon concentration in the engine's raw emissions and improves the engine's fuel consumption.

An additional advantage is that the engine can operate with stratified charge, meaning that an area with a rich mixture can be positioned around the spark plug, within a global lean-mixture operation. This, potentially, is a suitable way to reduce raw emissions of carbon monoxide and hydrocarbons. Furthermore, the engine can operate with a higher compression ratio, which leads to a higher break-mean-effective-pressure potential.

When considering all these advantages and potentials of high-pressure direct-fuel-injection systems, the disadvantages cannot be ignored. The injection system must generate a high fuel pressure (30-70 bar). For this reason, additional high-tech and high-cost elements have to be added to the engine. To use the full fresh-mixture short circuiting prevention potential of high-pressure fuel-injection systems, the injection timing has to be, in the ideal case, short before the closing of the exhaust port(s), but the time between the exhaust closing and the ignition is very short. This can be best illustrated by the following example: If the ignition timing is 20° before TDC and the exhaust ports close at 100° before TCD, only 80°CA can be used for the fuel injection and the mixture formation. At an engine speed of 8000 rpm, which is a recommended value for 50cc engines, the time the crankshaft needs to move 80°CA is about 2 milliseconds. These facts limit the possible field of application for high-pressure direct-fuel-injection systems in small two-stroke engines.

### 1.1.2.2 Low-pressure fuel-injection

The costs for the application of low-pressure fuel-injection systems, which work in a fuel pressure range of 3 to 6 bar are considerably lower than for a high-pressure system. For these (semi-) direct-injection systems, standard automotive fuel injectors can be used. The potential of avoiding fresh-mixture short circuiting is not as high as that of high-pressure fuel-injection systems.

Compared with a standard carburetor engine, the fuel consumption can be decreased by up to 30%, hydrocarbon raw emissions by up to 60%, and carbon monoxide emissions by up to 70%.

These improvements are the result of improved fuel atomization, lower fresh-mixture short

circuit losses and the improved possibilities to optimize the air/fuel ratio for the whole engine operating range.

### 1.1.2.3 Air-assisted fuel injection

An additional possibility of fuel injection is the use of an air-assisted fuel-injection system. These systems inject a compressed air/fuel mixture into the combustion chamber. An air compressor boosts air at a pressure of up to 6 bar into an injection chamber. Into this mixture chamber, fuel is added with a low-pressure injector. This prepared air/fuel mixture, with a good level of atomization, is injected into the combustion chamber, as far as possible after the complete closing of the exhaust port(s). In some systems, this injection is controlled by a pressure-sensitive valve. In this case the injection timing cannot be adjusted during the engine operation. An additional optimization possibility is the use of a solenoid valve; this leads to higher system complexity and costs, but enables improved engine settings, especially under part load conditions.

The advantages of air-assisted fuel-injection systems are similar to those of high-pressure direct-fuel-injection systems. Additional costs are caused by the need for an air-compressor. The fuel injectors are working in a lower pressure range and are therefore cheaper than those that are applied in high-pressure injection systems.

## 1.2 Costs

Increasing competition due to globalization reduces the benefit margins for two-wheeler manufacturers. In the compact two-wheeler sector the pressure on costs is particularly high. Fig. 5 shows a comparison of the engine-production costs for different engine configurations.

The standard two-stroke engine with a carburetor and an oxidation catalyst, and the two-stroke engine with a low-pressure-in-cylinder injection are the most common ways to fulfill the legal requirements for EUROMOPED EURO1. All the other above-mentioned two-and four-stroke engines are known as having the potential to fulfill the strict Euro 2 emission limits, but with even higher production costs. This is the motivation for a development project with the aim to achieve Euro 2 homologation by only optimizing the components of a standard two-stroke engine.

## 2 A POSSIBLE "LOW-COST" TWO-STROKE SOLUTION

This section describes the results of a "low-cost" two-stroke scooter-engine development project, which has been carried out at the Institute

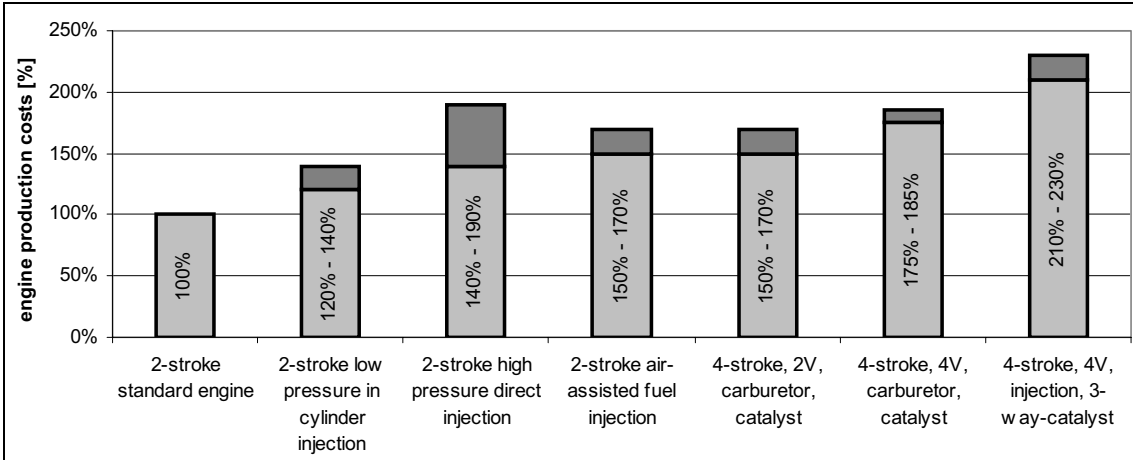


Fig. 5. Comparison of production costs for different engine configurations [3]

for Internal Combustion Engines and Thermodynamics at Graz, University of Technology. The starting point for this project was a 50cc fan-cooled scooter engine, which has already been optimized for EUROMOPED Euro 1 homologation. In the following the necessary modifications and optimizations to achieve the EUROMOPED Euro 2 exhaust-emission limits are listed.

## 2.1 Modified engine components

As the production costs of the new engine had to be kept as low as possible, as few modifications as possible should be made to the already existing engine.

### 2.1.1 Intake silencer / air-filter box

To ensure that the intake flow and pressure conditions are the same for each engine, the intake cross section of the intake silencer / air-filter box has to be exactly and reproducibly defined. For this reason, the design of the existing part had to be improved to avoid leakage and to guarantee that the only possible air-intake flow is through the calibrated cross section of the intake snorkel.

### 2.1.2 Carburetor

The aim for the carburetor setting is to achieve a lean air/fuel ( $\lambda > 1$ ) mixture in combination with a good throttle response and vehicle drivability. To reach this goal across the entire required engine-speed range, a balanced setting of the carburetor's setting parts (main jet, idle jet, slider valve, needle jet, needle) had to be worked out and tested on the engine and the vehicle test-bench.

Although the emission measurement in the ECE R-47 test-cycle does not include the cold-start phase, an auto-choke time, that is as short as possible, is required. During the auto-choke time the delivered

air/fuel mixture is rich. The fuel evaporation heat leads to a colder combustion and exhaust-gases temperature. For a short light-off time of the catalyst, high exhaust temperatures are essential, even more so for aged catalysts.

### 2.1.3 Cylinder and cylinder head

For two-stroke engines the design of the cylinder with its scavenging ports has an essential influence on the engine characteristics, achievable exhaust emissions and the leaning potential.

Due to the fact that during the two-stroke scavenging process the intake and exhaust ports are open at the same time, an optimization of the ports' geometry is essential to avoid high hydrocarbon exhaust emissions, caused by fresh-charge short-circuiting scavenging losses. At the same time, improved trapping efficiency is necessary to optimize the engine's fuel consumption. Furthermore, the scavenging must enable the engine to run on the lean side, without hesitation in the throttle response or misfiring. This can be realized by a high cylinder-charge turbulence velocity induced by a high cylinder-entrance velocity. To achieve this high cylinder-entrance velocity the entrance area of the transfer ports must be optimized.

The left-hand side of Fig. 6 shows a section view through the cylinder and cylinder head of the optimized engine. The right-hand side of Fig. 6 shows the symmetrical arrangement of the cylinder's scavenging ports. This layout of the ports is optimized for the loop scavenging process and consists of two main and two auxiliary transfer ports and one rear transfer and one exhaust port. Loop scavenging refers to the flow pattern generated by the transfer port's duct shapes and the port entry angles and area. The gases are directed to merge together and travel up the intake side of the bore into the head and loop around towards the exhaust port [10]. This scavenging process was already patented

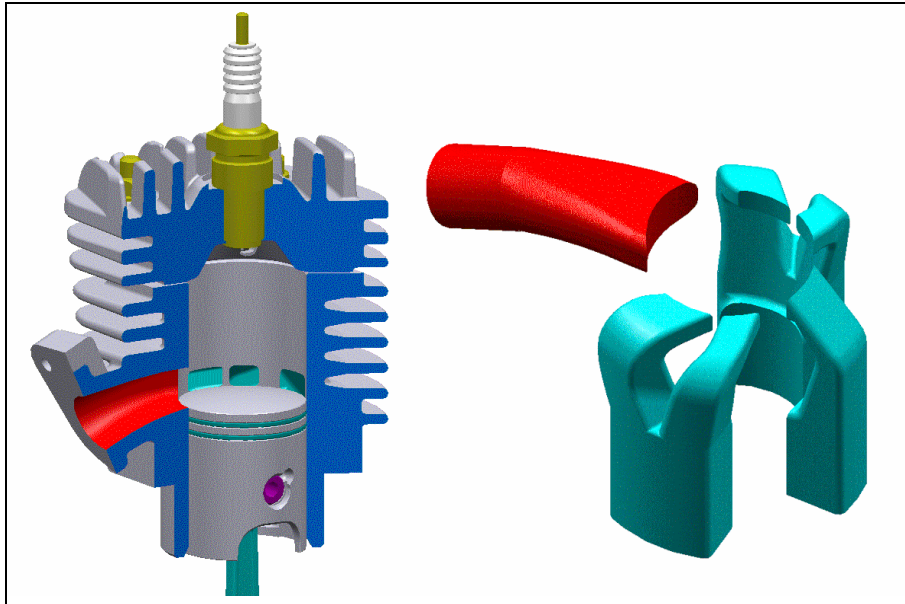


Fig. 6. Cross-section through cylinder and cylinder head and ports geometry

in 1908 [13], and is a suitable way to decrease the fresh-mixture short circuiting losses.

Because of the higher temperature of lean combustion the cylinder cooling had to be improved. For this reason, additional cooling fins were added and the fins' length on the opposite side of the fan was increased to compensate for the bad cooling situation on this cylinder side, which was caused by the lower air flow.

A well-adjusted cooling system is essential to avoid asymmetric thermal expansion of the cylinder. The cooling of the cylinder head had to be improved as well. Two additional fins, orthogonal to the cylinder axis, were added to force the air flow directly to the hot areas around the spark plug. This modification causes higher production costs, due to the additionally needed die separating direction.

The combustion-chamber volume is designed for a four-stroke combustion ratio of  $\varepsilon_{4\text{-stroke}} = 8.4$ , which leads, when combined with the port timing, to a two-stroke compression ration of  $\varepsilon_{2\text{-stroke}} = 5.9$ .

The material of the cylinder is, due to low-tech production requirements, gray-cast iron, and the cylinder head is made out of cast aluminum alloy.

#### 2.1.4 Piston

Because of the higher combustion temperature of lean combustion, the heat transfer between the piston and the cylinder must be increased. For this reason, a small the clearance between cylinder and the piston is required. To avoid piston seizure an extensive piston-shape development is essential. Additionally, this small clearance helps to avoid noise emission caused by piston slap. Because of the lower

thermal expansion coefficient of the gray-cast-iron cylinder a cast aluminum alloy with a high percentage of silicon was chosen as the piston material.

Due to the optimized cylinder cooling, an approximately round cylinder shape can be ensured during engine operation. For this reason, a round-shaped piston can be used. To assist the heat transfer and to reduce the friction, the piston surface should have  $R_{3z} < 3\mu\text{m}$ .

#### 2.1.5 Exhaust system

The main requirements for two-stroke engines exhaust systems are the support of the scavenging process with its gas dynamics, the conversion of the raw exhaust emissions with the integrated oxidation catalyst and the reduction of noise emissions.

The length of the exhaust manifold and the geometry of the diffuser are important for the engine characteristics. A well-positioned oxidation catalyst in the exhaust system is important for finding a compromise between a short light-off time, due to the small distance to the exhaust port(s), and low impact, due to the engine-boosting exhaust system's gas dynamics.

#### 2.2 Additional costs for the “Low-Cost” Two-Stroke Solution

Table 1 shows an overview of the additional mass-production costs for the required modification to the proposed “Low-Cost” Two-Stroke Solution. The basis for the cost calculation is a fan-cooled engine, already optimized to fulfill Euro 1 homologation regulations.

Table 1. Additional costs for the "Low-Cost" Two-Stroke Solution

Part	Additional costs		Part costs [% of engine]	Cost-increasing facts
	part costs	% of engine cost		
Intake Silencer	10%	0,2%	2,0%	calibrated intake snorkel, improved gasket design/material
Carburetor	0%	0,0%	5,0%	no modification
Cylinder	15%	1,0%	6,5%	higher casting quality, port positioning, additional material for improved cooling
Cylinder Head	40%	0,6%	1,5%	additional die separating direction and material
Spark Plug	10%	0,1%	0,5%	long-thread version required
Piston	10%	0,3%	2,5%	material and machining costs
Crank Mechanism	0%	0,0%	9,0%	no modification
Crank Case	0%	0,0%	16,0%	no modification
Exhaust System	20%	2,5%	12,5%	catalyst with higher cell density, heat-resistant material
Transmission	0%	0,0%	29,5%	no modification
Covers	0%	0,0%	6,5%	no modification
Electronic parts	0%	0,0%	8,5%	no modification
<b>Total</b>		<b>4,6%</b>	<b>100,0%</b>	

A cost-splitting of the engine parts indicates the estimated increase of costs caused by the conversion of the engine from the Euro 1 to the Euro 2 emission level. The cost increase is less than 5% compared to the already optimized Euro 1 serial production engine. This can be said to be the most effective way to achieve the Euro 2 emission level, if only the costs are considered.

### 2.3 Achievable results

The reduction of HC and CO emissions during the ECE 47 driving cycle is remarkable (Fig. 7).

The light-off of the catalyst in the EURO 2 engine occurs during the first seconds of the second full-load period in the test-cycle, while the EURO 1 engine needs 3 complete cycles to start the conversion of HC emissions. These effects are due to the higher exhaust-gas temperature of lean combustion and a higher oxidation level caused by an oxygen surplus [4]. After the warm-up phase, HC and CO emission levels are significantly lower than in the EURO 1 engines. This is the result of reduced scavange losses caused by the optimized scavange-port geometry.

The impact of the new scavange strategy and the new exhaust geometry can be seen in the

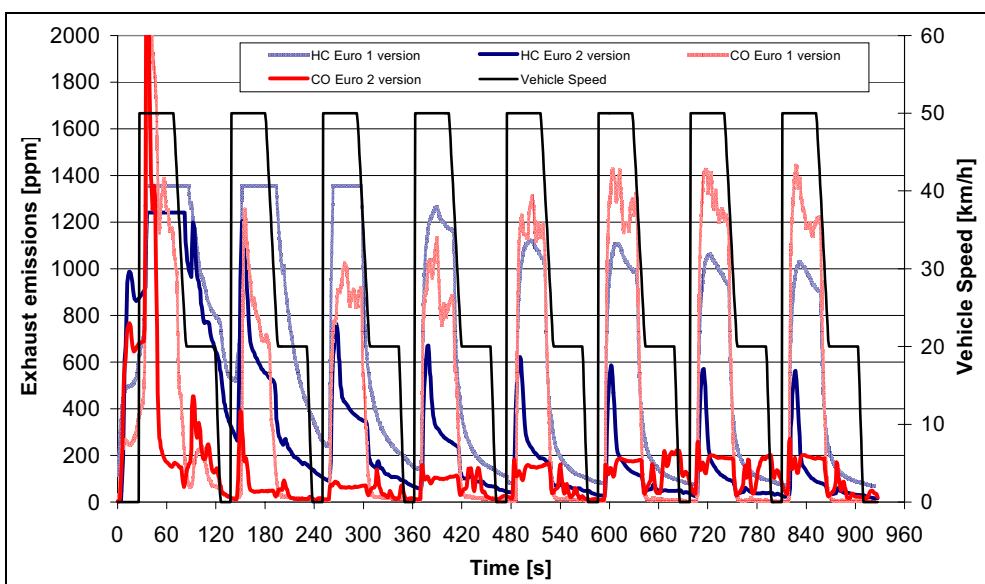


Fig. 7. Exhaust emissions during the ECE R 47 driving cycle

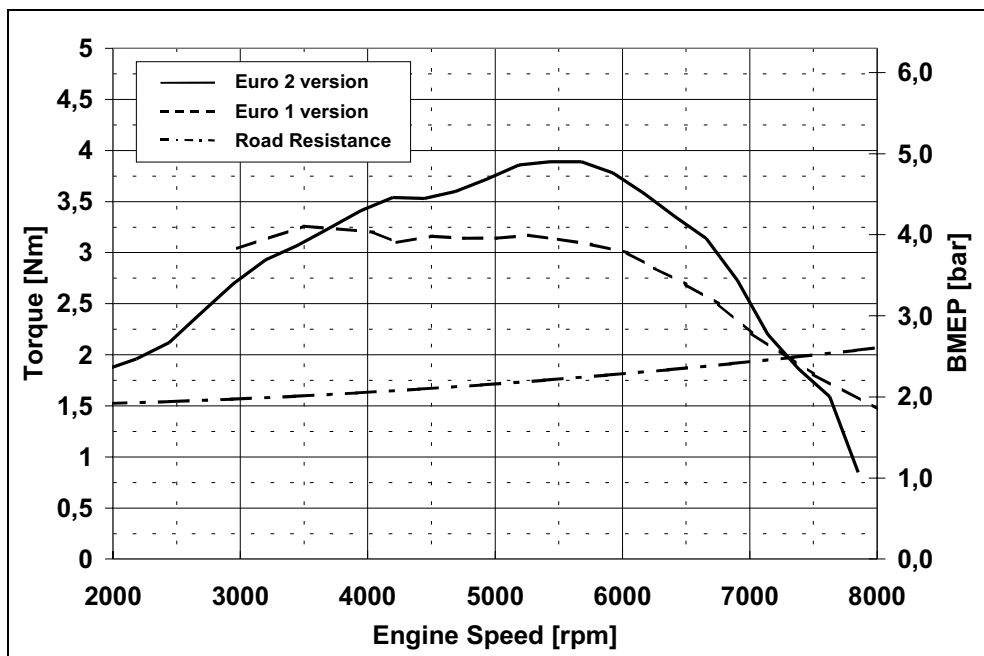


Fig. 8. BMEP comparison of the Euro 1 and the Euro 2 engine

achievable performance of the engine (Fig. 8). The rise of BMEP over the complete engine speed range gives a better drivability, especially in terms of acceleration and climbing. With the EURO 2 engine the maximum speed can be adjusted accurately, because the decrease of the BMEP curve at high engine speed gives a well-defined cross-section of engine torque and road resistance. With this defined intersection, different speed versions for different markets can be realized, simply by changing the transmission ratio.

Spot tests of vehicles currently on the market show that the development requirements to achieve the EURO 2 emission standards are comparable for four-stroke and two-stroke standard engines (Fig. 9).

Already-existing DI two-stroke engines with much higher production costs (see Fig. 5) have the same backlog demands to achieve the legal limits of EURO 2. The "Low-Emission Low-Cost" concept of Graz, University of Technology, shows excellent emission results as a prototype engine and in pre-serial production. The required modifications for the mass production of this low-cost concept are well accepted and can easily be implemented in mass-production technology.

### 3 FUTURE PERSPECTIVES

In the years from 2006 to 2010 the Euro moped EURO 3 emission legislation for two wheelers

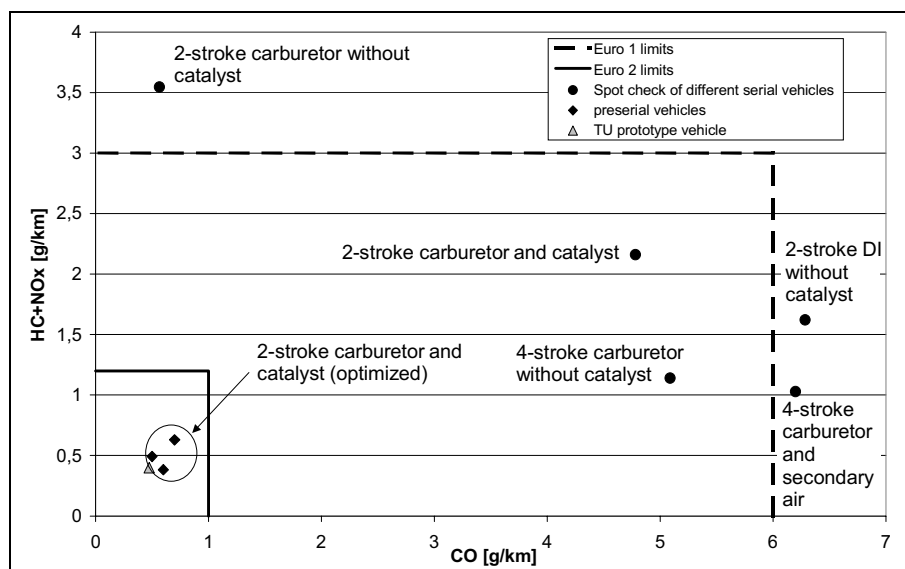


Fig. 9. Emission results in comparison

will come into force. The discussions concerning the reduction of HC, CO, and NOx levels and the cold-start behavior are still going on. In any case, the "Low-Emissions Low-Cost" concept has the potential for further optimization. To analyze the further potential of this "Low-Emissions Low-Cost" concept for EURO 3 emission legislation, the following topics need to be investigated:

- reduction of the light-off time for the catalyst by a close position to the exhaust port(s) or an additional pre-catalyst

- reduction of scavenge losses by controlled scavenge parameters
- use of secondary-air and/or improved carburetor technology
- use of new cold-start strategies

In any case, all these further improvements should take note of production costs. Rising competition due to globalization reduces benefit margins, especially in the compact two-wheeler sector. This cost pressure will increase and require lean production and use of low-cost technologies.

#### 4 REFERENCES

- [1] [www.emitec.de/de/index2.htm](http://www.emitec.de/de/index2.htm)
- [2] Richtlinie 97/24/EG des Europäischen Parlaments und des Rates vom 17. Juni 1997 über bestimmte Bauteile und Merkmale von zweirädigen oder dreirädigen Kraftfahrzeugen, Kapitel 5, Anhang I.
- [3] Nuti, M. Emissions from two-stroke engines, *Society of Automotive Engineers, Inc.* ISBN 0-7680-0215-X.
- [4] Pischinger, R., M. Klell, T. Sams, Thermodynamik der Verbrennungskraftmaschine, Zweite, überarbeitete Auflage, Der Fahrzeugantrieb, *Springer Wien New York*, ISBN 3-211-83679-9.
- [5] Meister, G. F., R. S. Kirchberger, Future prospects of two stroke engines and possible technical solutions for East/South Asian markets.
- [6] Pischinger, R., S. Hausberger (1998) Scenarios for transport demand, energy consumtion and CO2 emissions for global traffic up to the year 2100, *Commissioned by: Department of Enviroment, Yough and Family Affairs*, Report No. 8/98.
- [7] Meister, G.M. (1998) Flow and spray simulation in a loop scavenged 125cc two-stroke engine, Diploma Thesis, Graz, *University of Technology*.
- [8] Payreder, H. (2000) Analyse eines 50cc 2-Takt Rollers hinsichtlich Dauerhaltbarkeit und Performance, Diploma Thesis, Graz, *University of Technology*.
- [9] Krobath, A. (2001) Konstruktion einer 50 ccm Zweitakt Motorenfamilie, Diploma Thesis, Graz, *University of Technology*.
- [10] <http://www.eric-gorr.com/twostktech/2techterms.htm>
- [11] Koller, G. (1999) Einsatz der Methode der Finiten Elemente zur Auslegung von Kolbenmaschinen-Bauteilen unter besonderer Berücksichtigung akustischer Gesichtspunkte, Diploma Thesis, Graz, *University of Technology*.
- [12] Dabadie, J.C., J. Lavy, J. Favennec, M. Dubus (2001) DI two stroke engine catalyst development for 2 wheelers application, 2001 01 1847/4265, *Small Engine Technology Conference and Exhibition*, 7<sup>th</sup> Edition, Vol. II, 28-29-30 November 2001, Pisa – Italy.
- [13] Kind, P.A. Anordnung von Einführungsschlitten an Verbrennungskraftmaschinen, *Deutsche Kaiserliche Patentschrift*, No. 207107, 29. Jan. 1908.
- [14] Ramakrisanan, E. (2001) Improving the performance of two-stroke spark ignition engine by direct injection, *Robert Bosch India, Indian Institute of Technology (India)*, SETC 2001 01 1843-4262.
- [15] <http://www.synerject.com>

Authors' Address: Dr. Roland Kirchberger  
Gernot Koller  
Institute for Internal Combustion  
Engines and Thermodynamics  
Graz, University of Technology  
Inffeldgasse 25 / B  
A-8010 Graz, Austria  
[kirchberger@vkmc.tu-graz.ac.at](mailto:kirchberger@vkmc.tu-graz.ac.at)  
[koller@vkmc.tu-graz.ac.at](mailto:koller@vkmc.tu-graz.ac.at)

Prejeto:  
Received: 9.9.2003

Sprejeto:  
Accepted: 12.2.2004

Odprto za diskusijo: 1 leto  
Open for discussion: 1 year

## Numerične analize preoblikovanja cevi z visokim notranjim tlakom

### Numerical Analyses of Tube Hydroforming by High Internal Pressure

Tomaž Pepelnjak

Avtomobilска industriја се заради заhtev по povečevanju togosti vozil ob hkratnem zmanjševanju njihove mase srečuje s tehnološkimi problemi izdelave vse bolj zahtevnih preoblikovanih komponent. Oblikovne in mehanske lastnosti preoblikovancev pogosto ne omogočajo več izdelave z običajnimi preoblikovalnimi tehnologijami, kakor so krivljenje, izbočevanje in globoki vlek.

Zaradi zahtevnosti predvsem strukturnih delov avtomobila se vse pogosteje uporablja preoblikovanje cevi z medijem pri visokih notranjih tlakih. Postopek je zaradi velikega števila parametrov zelo zahteven. Preoblikovalni tlaki reda velikosti od nekaj sto do nekaj tisoč barov delujejo v notranjosti cevi in pomenijo omejitve, ki zahteva posebna preoblikovalna orodja in stroje.

V prispevku so predstavljeni parametri preoblikovanja cevi z medijem pri visokih notranjih tlakih, analizirani postopkovni in geometrijski parametri postopka ter izvedene numerične simulacije preoblikovanja dveh tipičnih preoblikovancev – kosa T in kosa Y.

© 2004 Strojniški vestnik. Vse pravice pridržane.

(Ključne besede: preoblikovanje cevi, tlaki visoki, analize končnih elementov, parametri postopka)

*Because of demands for increased vehicle rigidity, along with a simultaneous reduction of vehicle weight, the automotive industry is facing technological problems involving the manufacture of ever more complex formed parts. Often, the shape and mechanical properties of formed parts no longer permit their manufacture using conventional forming technologies, such as bending, stretching and deep drawing.*

*Due to the complexity of primarily structural vehicle parts, tube hydroforming is increasingly used. However, because of the large number of process parameters, this procedure is very demanding. Forming pressures inside a tube with orders of magnitude of a few hundred to a few thousand bars represent a process limitation that requires special forming tools and machines.*

*This paper presents the process parameters of tube hydroforming, the analysed process and the geometrical parameters, and the performed numerical simulations for the forming of two typical formed parts –T-parts and Y-parts.*

© 2004 Journal of Mechanical Engineering. All rights reserved.

(Keywords: tube hydroforming, finite element analysis, process parameters)

#### 0 UVOD

V sodobni industrijski proizvodnji se pojavlja vedno več razlogov, od katerih je odvisna izdelava tehnološko zelo zahtevnih komponent. Zaradi dragih energetskih virov in surovin iščemo izdelovalne postopke, ki omogočajo izdelavo čim zahtevnejših komponent ob čim manjši porabi energije in najmanjšem odpadku materiala. Zmanjševanje porabe goriva prevoznih sredstev po drugi strani, predvsem v avtomobilski industriji, sili proizvajalce k iskanju optimalnih razmerij med maso vgrajenih komponent in njihovo togostjo. Vse naštete zahteve spodbujajo iskanje novih materialov (npr.

#### 0 INTRODUCTION

In modern industrial manufacture there are ever more reasons for the need to manufacture technologically very complex components. Because of expensive energy sources and raw materials, manufacturing procedures are sought that would enable the manufacture of increasingly complex components with the lowest possible energy consumption and the minimum material waste. On the other hand, the demand to reduce the fuel consumption of transport vehicles forces manufacturers (primarily in the automotive industry) to search for optimum weight-to-rigidity ratio of

aluminija, magnezija, večfaznih in mikrolegiranih jekel, kompozitnih materialov ipd.), zasnutkov in tehnologij ([1] in [2]). Sad teh iskanj so sodobne izdelovalne tehnologije in zamisli, kakor so krojeni pritezi, panel pločevine, preoblikovanje z medijem ([3] do [6]). Vpeljevanje novih tehnologij in zamisli poteka tudi v tesni sodelavi z oblikovalci in konstrukterji. Takšna sodelava vodi k vse boljši stroškovni in tehnološki optimizaciji izdelanih proizvodov [7].

Avtomobilска industrija teži tudi k skrajševanju montažnih časov s poenostavljanjem montažnih opravil. Te se v veliki meri skrajšujejo z zmanjševanjem števila vgrajenih komponent, ki so zaradi tega geometrijsko vedno bolj zahtevne [1]. Za izdelavo geometrijsko najzahtevnejših delov, ki se jih z drugimi preoblikovalnimi postopki ne da narediti, so se razvili postopki preoblikovanja z medijem.

Sam postopek preoblikovanja z medijem je v raziskovalnem okolju poznan že dalj časa, saj segajo prve raziskave preoblikovanja tankostenskih cevi z uporabo notranjega tlaka že v šestdeseta in sedemdeseta leta prejšnjega stoletja [8]. Glavne omejitve izredno zahtevnega postopka so takrat predstavljeni razpoložljivi hidravlični stroji, preoblikovalni stroji ter pomanjkanje ustrezne računalniško opreme za napovedovanje poteka preoblikovalnega postopka. S skokovitim razvojem strojne opreme in programov za računalniško podprtje simulacije preoblikovalnih postopkov (analize MKE) se je bliskovito razširila uporaba preoblikovanja cevastih preoblikovancev z visokimi notranjimi tlaki medija – t.i. "tube hydroforming". Postopek se je najprej uporabljal pri proizvodnji geometrijsko zahtevnih izpušnih sistemov. V zadnjih desetih letih ta postopek vedno več uporablja tudi pri izdelavi nosilnih delov karoserije, nosil motorja, oseh in gredeh ter varnostnih karoserijskih komponentah kakor so nosila vetrobranskih stekel, A, B in C nosila, blažila, okrovi sedežev itn. Tudi na Fakulteti za strojništvo v Ljubljani so potekale raziskave postopkov sorodnih preoblikovanju cevi z visokimi notranjimi tlaki s ciljem izdelati kroglaste okrove iz cevastih surovcev ([9] in [10]).

Najpomembnejše prednosti postopka preoblikovanja z visokimi notranjimi tlaki lahko strnemo v naslednjih točkah:

- Preoblikovati se da zelo zahtevne geometrijske oblike cevastih izdelkov, ki se jih z drugimi preoblikovalnimi postopki ne da narediti.
- Zaradi zahtevne geometrijske oblike lahko več sestavnih delov sklopa nadomestimo z enim samim izdelkom, kar poenostavlja montažo in s tem izboljšuje izdelovalne tolerance.
- Trdnost izdelkov in porazdelitev debelin sta zaradi »mehkega« delovanja sil med preoblikovanjem enakomernejša kakor pri drugih postopkih.
- Tanjšanje materialov med preoblikovanjem je

installed components. All of these demands encourage manufacturers to search for new materials (e.g. aluminium, magnesium, multiphase and microalloyed steels, composite materials etc.), concepts and technologies ([1] and [2]). These endeavours have resulted in modern manufacturing technologies and concepts, such as tailored blanks, sandwich steel, hydroforming, etc. ([3] to [6]). New technologies and concepts are also implemented in close cooperation with designers and mechanical engineers, which leads to ever better optimisation of the manufacturing technology and product costs [7].

There is also a tendency in the automotive industry to shorten assembly times by simplifying assembly operations. This is achieved mainly by reducing the number of components, which, as a result, need to have increasingly complex geometrical shapes [1]. Hydroforming procedures have been developed specifically for the manufacture of the geometrically most demanding parts, which cannot be produced using other forming processes.

The hydroforming process has been known for a while in research circles. The first research in the forming of thin-walled tubes using inner pressure date back to the 1960s and 1970s [8]. The main limitations of this extremely complex process were hydraulic aggregates and the forming machines that were available at that time, as well as a lack of appropriate computer equipment for predicting the course of the forming process. With the rapid developments in machine equipment and software for computer-aided simulations of the forming process (FE analyses), the use of tube hydroforming has spread very quickly. This process was first used in the manufacture of geometrically demanding exhaust systems. Over the last ten years, this procedure has also been increasingly used in the manufacture of space-frame components, engine cradles, axles and shafts, and body and safety parts, such as windshield headers, A, B and C pillars, shock absorbers, seat frames, etc. Research in other processes similar to tube hydroforming has also been conducted at the Faculty of Mechanical Engineering, Ljubljana, with the goal of manufacturing spherical housings from tubular formed parts ([9] and [10]).

The most important advantages of the hydroforming process can be summarised as follows:

- Very complex geometries of tubular formed parts can be achieved, which are not attainable with other forming processes.
- Due to complex geometry, several components of an assembly can be replaced with a single formed part, thus simplifying the assembly and improving manufacturing tolerances.
- "The softer" action of the forces during forming yields more uniform strength and thickness distribution than other equivalent processes.
- The thinning of materials during forming is smaller

manjše kakor pri drugih postopkih.

- Masa komponent je zaradi enakomernejše porazdelitve debelin manjša v primerjavi z izdelki, narejenimi z drugimi tehnologijami.
- Delež elastičnega izravnavanja je manjši kakor pri drugih postopkih, zato lahko izdelujemo preoblikovance z boljšimi izdelovalnimi tolerancami.
- Površina izdelkov je zelo gladka.

Pomanjkljivost postopka preoblikovanja z visokimi notranjimi tlaki je predvsem zelo draga oprema in zahtevno krmiljenje parametrov postopka. Visoki procesni tlaci v orodjih, ki se gibljejo od nekaj sto do nekaj tisoč barov, terjajo posebno konstrukcijo orodij, veliko trdnost orodnih materialov in ustrezne varnostne ukrepe. Zaradi naštetih zahtev so orodja za preoblikovanje z medijem dražja od orodij za druge preoblikovalne postopke.

## 1 ZNAČILNOSTI POSTOPKA

Postopek preoblikovanja z medijem z visokim notranjim tlakom popišemo s sklopom vplivnih parametrov, ki jih delimo v štiri skupine:

- parametri postopka (vzdolžna sila, zapiralna sila, notranji tlak, pomiki itn.),
- omejitve postopka (gubanje, izbočenje, izbruh, trenje),
- parametri surovca (dolžina, premer, debelina, material, oblika),
- orodje (oblika, kakovost površine, trdota).

Vplivni parametri prve skupine se med preoblikovanjem spreminja, med postopkom jih moramo nadzorovati in krmiliti. Omejitve postopka, npr. gubanje, izbočenje in izbruh, so povezani z geometrijsko obliko in materialom preoblikovanca. Osnovne enačbe pojava omenjenih kritičnih napak na preoblikovancu temeljijo na izbočenju cevi, prekoračitvi natezne trdnosti materiala in čezmernem nakrčevanju, ki pripelje do pojava gubanja preoblikovanca ([11] in [12]):

*Izbruh* : prekoračitev natezne trdnosti:

*Gubanje*: prevelik vzdolžni pomik cevi:

$$p_n = \frac{2s_0 R_m}{d_0 - s_0} \quad (1)$$

*Lokalizacija*: prekoračitev izbočilne odpornosti cevi:

$$\sigma_a = \frac{2E_T s_0}{1,65 d_0} \quad (2)$$

than in other equivalent processes.

- Because of a more uniform thickness distribution, component weight is lower than with other equivalent technologies.
- Springback is also lower than in other processes, therefore formed parts can be produced using better manufacturing tolerances.
- The surfaces of these products are very smooth.

The shortcomings of tube hydroforming are mainly very expensive equipment and demanding process-parameter control. High process pressures in the die, ranging from a few hundred to a few thousand bars, require a special tool structure, a high strength of tool material and the appropriate safety elements. Because of this, hydroforming tools are more expensive than those for equivalent forming processes.

## 1 PROCESS CHARACTERISTICS

The hydroforming process is described with a set of influential parameters, which are divided into four groups:

- Process parameters (axial force, closure force, inner pressure, feedings, etc.),
- Process limitations (wrinkling, buckling, bursting, friction),
- Formed-part parameters (length, diameter, thickness, material, shape),
- Tools (shape, surface quality, hardness).

The influential parameters from the first group vary during forming and should be regulated and controlled during the process. Process limitations such as wrinkling, buckling and bursting are related to geometry and workpiece material. The basic equations for the appearance of the above-mentioned critical defects on the formed parts are the result of tube buckling, exceeding of the material's tensile strength and excessive upsetting, which leads to the appearance of wrinkling ([11] and [12]):

*Bursting*: exceeding of tensile strength:

*Wrinkling*: excessive axial tube feedings:

$$\sigma_a = \frac{2E_T s_0}{1,65 d_0} \quad (2)$$

*Localisation*: exceeding the tube-buckling resistance:

$$\varepsilon = \varepsilon_e \quad (3)$$

kjer so  $p_n$  notranji tlak,  $R_m$  natezna trdnost materiala,  $s_0$  in  $d_0$  debelina in premer cevi,  $\sigma_a$  vzdolžna napetost med preoblikovanjem,  $E_T$  tangentični modul materiala in  $\varepsilon_e$  primerjalna specifična deformacija cevi.

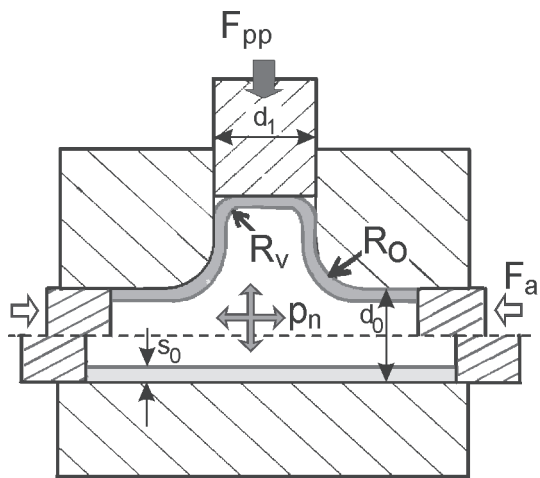
V zadnjih letih se bazične raziskave preoblikovanja z medijem usmerjajo vedno bolj v iskanje ustreznih maziv ter v analize vplivov različnih

where  $p_n$  is the inner pressure,  $R_m$  is the tensile strength of the material,  $s_0$  and  $d_0$  are the tube thickness and diameter, respectively,  $\sigma_a$  is the axial stress during forming,  $E_T$  is the tangent modulus and  $\varepsilon_e$  is the equivalent specific tube deformation.

Over the past few years, basic research in hydroforming has focused on the search for

koeficientov trenja na potek postopka preoblikovanja z visokimi notranjimi tlaki. Poseben poudarek je na oblikovanju izdelka, porazdelitvi debelin izdelka in napakah, ki se pojavljajo zaradi neustreznega trenja [13].

Geometrijski parametri surovca in preoblikovanca so pomembni pri določevanju izdelovalnih tehnoških mej postopka in v veliki meri vplivajo na kakovost izdelave s postopkom preoblikovanja z visokim notranjim tlakom. Osnovne geometrijske parametre prikazuje slika 1 na primeru tipičnega preoblikovanca – kosa T [12].



appropriate lubricants and analyses of the influence of different coefficients of friction on the course of the hydroforming process. Special emphasis is placed on product design, thickness distribution and the defects resulting from inappropriate friction [13].

The geometric parameters of the preform and the formed part are important for determining the manufacturing technological process limits and have a large effect on the quality of hydroforming-based manufacture. The basic geometric parameters are shown in Figure 1, for an example of a typical formed part – T-part [12].

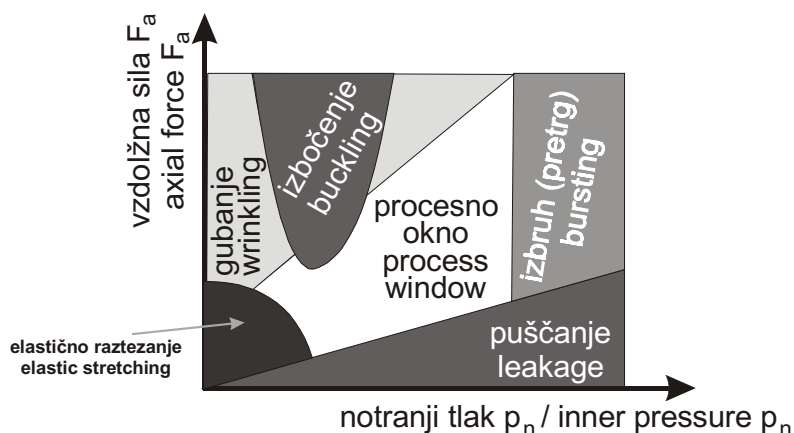
$d_0$	začetni premer cevi / initial tube diameter
$s_0$	začetna debelina cevi / initial tube thickness
$d_1$	premer oblike T / diameter of the T-feature
$R_o$	polmer orodja / die radius
$R_v$	polmer zaokrožitve izbočitve oblike T / radius of the T-feature
$p_n$	notranji tlak / inner pressure
$F_a$	vzdolžna sila pestičev / axial punch force
$F_{pp}$	sila protipestiča / counterpunch force

Sl. 1. Geometrijski parametri preoblikovanca [12]

Fig. 1. Geometric parameters of the formed part [12]

Najpomembnejša parametra postopka, ki ju med postopkom spremojamo, sta gib orodja oziroma vzdolžna sila, s katero delujemo na preoblikovanec ter notranji tlak. Oba parametra postopka moramo za optimalno preoblikovanje cevastega preoblikovanca med postopkom nadzorovano spremojati znotraj meja tehnološkega okna uspešnega preoblikovanja. Slednje je opredeljeno s kritičnimi napakami preoblikovanca in ga najlepše prikažemo v diagramu

The most important process parameters, which are varied during the process, are the punch stroke or axial force on the formed part, and the inner pressure. For optimum forming of tubular parts, both process parameters must be varied in a controlled manner during the process, within the limits of the technological window for successful forming. The latter is defined by critical defects on the formed part and is best shown by a diagram of the variation of the axial



Sl. 2. Diagram odvisnosti vzdolžne sile od notranjega tlaka [14]

Fig. 2. Diagram of the variation of axial force with inner pressure [14]

odvisnosti vzdolžne sile od notranjega tlaka med preoblikovanjem (sl. 2). V primeru prenizkih vzdolžnih sil sistem ne tesni, pri premajhnih vzdolžnih silah in tlakih pa ne presežemo meje plastičnosti preoblikovanega materiala. Preveliki notranji tlaki povzročijo izbruh, prevelike vzdolžne sile ob ustreznih notranjih tlakih pa pojave gubanja in izbočenja cevi.

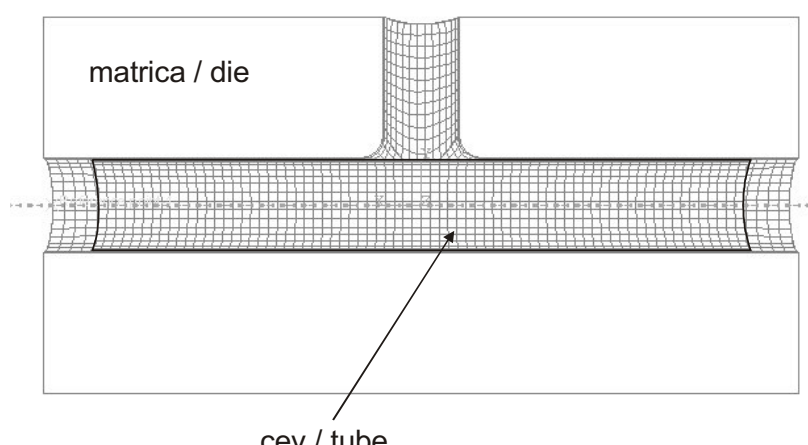
Poznavanje vseh naštetih vplivnih parametrov smo analizirali na preoblikovanju kosa T in kosa Y s poudarkom na vplivih koeficiente trenja in vzdolžnih pomikov pestičev na oblikovanje končnega izdelka.

## 2 NUMERIČNE (MKE) ANALIZE PREOBLIKOVANJA CEVI Z VISOKIM NOTRANJIM TLAKOM

### 2.1 Analiza preoblikovanja kosa T

Preoblikovanje kosa T je ena glavnih oblik preoblikovanja cevi z medijem. Na izbočenje in oblikovanje oblike T največji meri vplivajo geometrijska oblika cevi in orodja, vzdolžne sile pestičev, časovno spremenjanje notranjega tlaka ter trenje med preoblikovancem in orodjem. Na primeru preoblikovanja cevi iz jekla 1.0333.6 smo v računalniško podprttem okolju analizirali vpliv koeficientov trenja na oblikovanje kosa T. Analize so bile izvedene z numeričnim reševanjem problema z metodo končnih elementov (MKE) in izvedene z računalniškim programom Abaqus Explicit verzija 6.3 [15]. Model orodja in preoblikovanca (cevi) za analize MKE in upoštevane materialne lastnosti cevi so prikazani na sliki 3. Na sliki so zaradi boljše preglednosti izpuščeni vzdolžni pestiči ter protipestiči. Enosna simetrija omogoča uporabo polovičnega modela celotnega sistema orodje - preoblikovanec.

Pri izbiri časovnega poteka delovanja notranjega tlaka smo izbrali profil s hitrim povečevanjem tlaka do vrednosti  $p_{nl}$ , ki zagotavlja pričetek plastičnega deformiranja materiala ter



Sl. 3. Model MKE orodja in cevi za izdelavo kosa T  
Fig. 3. FE model of tool and tube for manufacturing T-parts

force with inner pressure during forming – Figure 2. If the axial forces are too low, the system is not fluid-tight, whereas at insufficient axial forces and pressures the yield strength of the formed material is not exceeded. Excessive inner pressures cause bursting, whereas excessive axial forces with appropriate inner pressures cause tube wrinkling and buckling.

All of the stated influential parameters were analysed on the forming of T-parts and Y-parts, with the emphasis on the influence of the coefficient of friction and the axial punch feedings on the forming of the final products.

## 2 NUMERICAL FINITE-ELEMENT ANALYSES OF TUBE HYDROFORMING

### 2.1 Analysis of T-part forming

The forming of a T-part is one of the basic types of tube hydroforming. The factors affecting the forming of T-parts are the tube and die geometry, the axial punch forces, the time variation of the inner pressure, and the friction between the formed part and the die. The influence of the coefficient of friction on T-part forming was analysed in a computer-aided environment for the case of tube forming made of 1.0333.6 steel. The analyses were performed numerically using the finite-element method (FEM) and the software Abaqus Explicit Ver. 6.3 [15]. The model of the tool and the formed part (tube) for FE analyses, and the material properties of the tube, are shown in Figure 3. In this figure the axial punches and the counterpunch are omitted for better clarity. Uniaxial symmetry enabled the use of a half-model for the tool/formed-part system.

For the time variation of the action of inner pressures, a curve with quick increases of pressure up to the value of  $p_{nl}$  was selected to ensure the initiation of plastic deformation of the material and

Lastnost Property	Vrednost Value
$E$	210 GPa
$\nu$	0,3
$\rho$	7800 kg/m <sup>3</sup>
$R_p$	215 MPa
$R_m$	350 MPa
$C$	537 MPa
$n$	0,227
$r$	1

linearno povečevanje tlaka do vrednosti  $p_{n_2}$  ob koncu preoblikovanja. Vrednost tlaka  $p_{n_2}$  smo izbrali tako, da še ne pride do izbruha zaradi lokalnega stanjanja preoblikovanca.

Analizo vpliva koeficiente trenja na oblikovanje izbočitve T smo izvedli najprej brez protipeščica pri dveh vrednostih vzdolžnih pomikov  $l_a$  obeh koncov cevi:  $l_a = 1,5 \cdot d_0$  (30 mm) ter  $l_a = 2 \cdot d_0$  (40 mm). Izbrane velikosti vzdolžnih pomikov so velike v primerjavi s sorodnimi raziskavami v svetu [16]. Z velikimi vzdolžnimi pomiki smo skušali doseči čim manjše tanjšanje debelin stene preoblikovanca med samim postopkom. Pri vrednotenju vpliva trenja na geometrijsko obliko kosa T sta bili vpeljani brezrazsežno razmerje izbočitve T  $TH_r$ :

$$TH_r = \frac{H}{d_1} \quad (4)$$

in relativna višina izbočitve  $izb_r$ , podana kot razmerje:

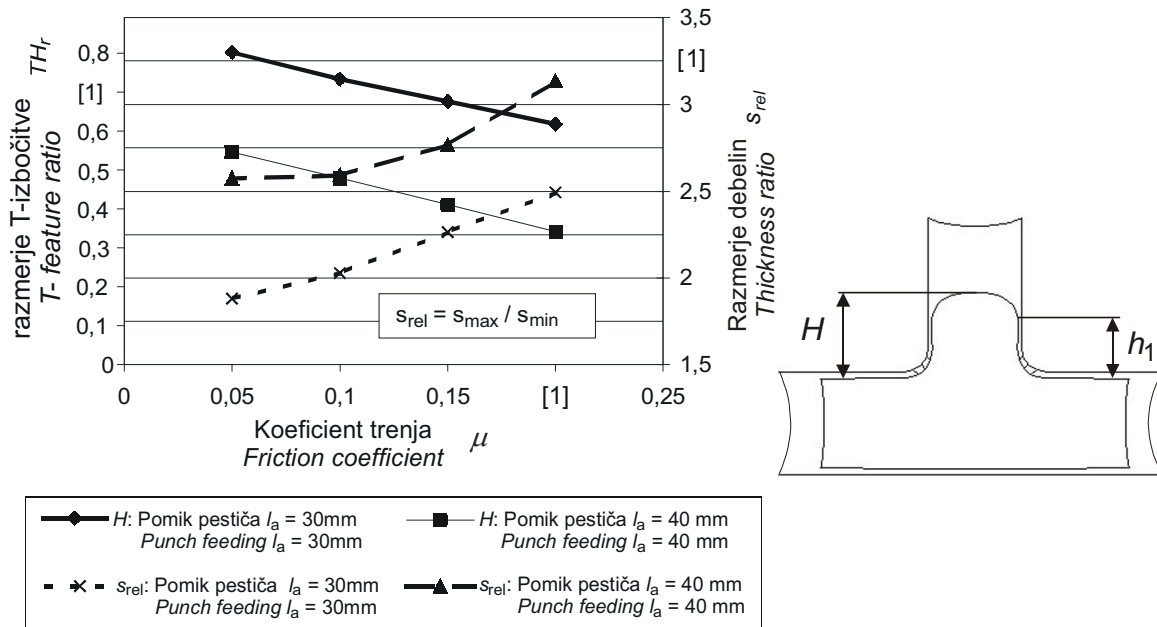
$$izb_r = \frac{H - h_1}{d_1} \quad (5),$$

kjer so  $H$  višina izbočenega dela izdelka T,  $h_1$  višina cevasto izbočenega dela izdelka T in  $d_1$  premer izbočenega dela izdelka.

Surovec ima izmere  $\phi 20 \times 160$  mm z debelino stene 1 mm. Rezultati vrednotenja izbočitve kosa T so prikazani na sliki 4. Slike je razvidno, da sta višina izbočitve, podana z razmerjem  $TH_r$ , ter koeficient trenja  $\mu$  med orodjem in preoblikovancem pri izbranih preoblikovalnih parametrih linearno odvisna. Analiza izbočitve kosa T z razmerjem  $izb_r$  je pokazala, da

linear increases of the pressure up to the value of  $p_{n_2}$  at the end of the forming. The values of pressure  $p_{n_2}$  were selected such that bursting does not take place because of the formed part's local contraction.

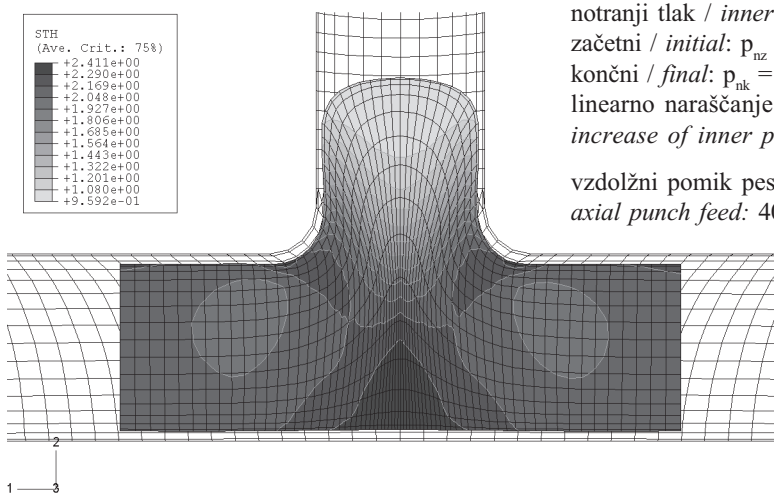
Analyses of the influence of the coefficient of friction on T-part forming were initially performed without a counterpunch for two values of the axial displacement  $l_a$  of the two tube ends:  $l_a = 1.5 \cdot d_0$  (30 mm) and  $l_a = 2 \cdot d_0$  (40 mm). The selected values of the axial displacement are high compared to similar international studies [16]. Large axial displacements were used in an attempt to achieve minimum reduction of the formed-part wall thicknesses during the forming process. When evaluating the influence of friction on T-part geometry, we introduced the dimensionless T-feature ratio,  $TH_r$ :



Sl. 4. Vpliv koeficenta trenja na izbočitev (leva lestvica) in razmerje debelin kosa T (desna lestvica)  
Fig. 4. The influence of the coefficient of friction on the T-feature's dimensions (left scale) and T part's thickness ratio (right scale)

višina ukrivljenega dela izbočitve ni odvisna niti od koeficiente trenja niti od velikosti vzdolžnega pomika pestičev. S spremenjanjem vrednosti koeficientov trenja med orodjem in preoblikovancem ob nespremenjenih preostalih parametrih postopka se spreminja le višina izbočenega dela kosa T ( $TH$ ) ter razmerje debelin najdebelejšega in najtanjšega dela izdelka (sl. 4).

Porazdelitev debelin preoblikovanega kosa T, izdelanega brez delovanja protipestiča, je prikazana na sliki 5. Izbrani parametri postopka z velikimi pomiki vzdolžnih pestičev zagotavljajo najmanjše tanjšanje kosa T. Po drugi strani se hkrati pojavlja neobičajna odebelitev koncev cevi, okolice polmera  $R_0$  in stene nasproti izbočene oblike T.



Sl. 5. Porazdelitev debelin kosa T, izdelanega brez protipestiča  
Fig. 5. Thickness distribution of a T-part produced without the use of a counterpunch

Izdelava kosov T v industriji zahteva uporabo protipestičev, ki zmanjšajo ločno izbočeni del kosa T  $H_1 = H - h_1$  (sl. 4). V ta namen med preoblikovanjem kosa T na prosto preoblikovani del cevi delujemo s silo protipestiča, ki zmanjšuje izbočenosť končnega priključka T. Slika 6 prikazuje izdelavo kosa T z uporabo protipestiča in silo njegovega delovanja. Izbrani parametri postopka zagotavljajo najmanjše tanjšanje izdelka, ki doseže le 3% na vrhu izbočene oblike T.

## 2.2 Analiza preoblikovanja kosa Y

V izpušnih sistemih, ki so eno pomembnejših področij preoblikovanja z visokimi notranjimi tlaki, se pogosto pojavljajo zahteve po izdelavi razcepov in priključkov, ki se na glavno cev ne spajajo pod pravim kotom. Tako imenovani kos Y je za izdelavo precej zahtevnejši kakor v prejšnjem poglavju obravnavani kos T. Geometrijska oblika kosa zahteva nesimetrične pomike vzdolžnih pestičev med preoblikovanjem. Vpliv velikosti pomika posameznega konca preoblikovanca se kaže v obliki priključka kosa Y. V

of the T-feature with the  $izb_r$  ratio showed that the height of the curved part of the feature does not depend on the coefficient of friction or the magnitude of the axial punch feedings. When the magnitude of the coefficient of friction is varied with other process parameters unchanged, only the T-feature's height ( $TH$ ) and the ratio of thicknesses of the thickest to the thinnest portion vary - Figure 4.

The thickness distribution of a T-part formed without the use of a counterpunch is shown in Figure 5. Selected process parameters with large displacements of axial punches have ensured minimal thinning of the T-part. On the other hand the uncommon thickening at the tube ends, around the die radius  $R_o$  and on the wall opposite the T-feature took place.

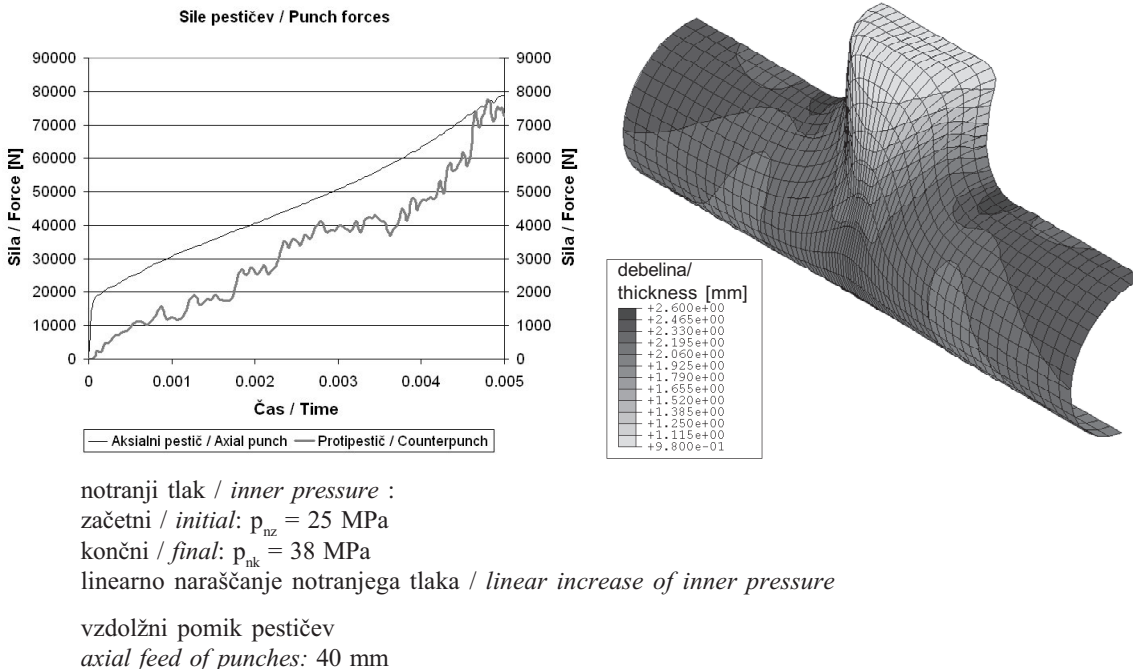
notranji tlak / inner pressure :  
začetni / initial:  $p_{nz} = 25$  MPa  
končni / final:  $p_{nk} = 38$  MPa  
linearno naraščanje notranjega tlaka / linear increase of inner pressure

vzdolžni pomik pestičev  
axial punch feed: 40 mm

The industrial manufacture of T-parts requires the use of counterpunches, which reduce the arched portion of the T-feature  $H_1 = H - h_1$  (Figure 4). For this purpose, a force is applied on the free-formed portion of the tube using a counterpunch during the T-part's forming. This force reduces the arched portion of the T-feature on the final product. Figure 6 shows the production of a T-part using a counterpunch and its force. The selected process parameters ensure minimum thinning of the part – only 3% on the top of the T-feature.

## 2.2 Analysis of Y-part forming

The manufacture of exhaust systems, one of the most important applications of hydroforming, frequently involves the production of manifolds and connectors that are not attached to the main tube at an angle of 90 degrees. The production of Y-parts is much more difficult than that of the T-parts described in the previous section. This part's geometry requires asymmetric feedings of axial punches during forming. The influence of the magnitude of displacement of the formed part's ends is reflected in the shape of the Y-part



Sl. 6. Potek preoblikovalnih sil in porazdelitev debelin modela MKE kosa T, izdelanega z uporabo protipestiča

Fig. 6. Forming forces vs. time and thickness distribution of a FE model of a T-part made using a counterpunch

delu smo analizirali vplive različnih velikosti pomikov robov cevi kosa Y. Zaradi primerljivosti dobljenih rezultatov z že znanimi [17] smo izbrali kos Y s 60 stopinjskim priključnim delom.

Podobno kakor pri analizi kosa T smo izvedli numerične simulacije preoblikovanja kosa Y z notranjim tlakom, izračunanim po enačbi 1 v poglavju 2.1. Izbrani material je imel enake materialne karakteristike kakor v poglavju 2.1. Surovec ima dimenzijs  $\phi 20 \times 160 \text{ mm}$  iz jekla 1.0333.6 z debelino stene 1 mm. Model orodja in srovca za izdelavo kosa Y je prikazan na sliki 7. Zaradi večjih pomikov desnega dela preoblikovanca je izbrani razcep Y v orodju na tretjini dolžine srovca. Enoosna simetrija preoblikovanca omogoča tudi v tem primeru analize s polovičnim modelom MKE. V primeru simulacije kosa Y se je pokazalo, da ne moremo več zadostiti pogoju najmanjšega tanjšanja stene cevi. Kot kriterij uspešnega preoblikovanja smo zato izbrali največje dovoljeno tanjšanje cevi, ki je opredeljeno z enačbo:

$$s_1 = s_0 * e^{-n} \quad (6)$$

Izbrane so bile različne kombinacije pomikov pestičev, pri čemer smo za pomik levega pestiča izbrali vrednosti  $l_{al} = d_o$  (20 mm) in  $l_{al} = 1.5 * d_o$  (30 mm). Pomike desnega pestiča smo spremenjali v razponu vrednosti od  $l_{a2} = 1.5 * l_{al}$  (30 mm) do  $l_{a2} = 3.5 * l_{al}$  (80 mm) s korakom po  $0.25 * l_{al}$ . Časovni profil notranjega tlaka med preoblikovanjem je bil pri vseh

connector. This paper analyses the influences of various displacements of the Y-part's tube ends. In order to enable comparisons of the obtained results with published results [17], a Y-part with a 60-degree connector was selected.

As with the analysis of the T-part, numerical simulations of Y-part forming were performed with an inner pressure calculated using Equation 1, section 3.1. The selected material had the same characteristics as stated in section 3.1. The preform's dimensions were  $\phi 20 \times 160 \text{ mm}$  and it was made of 1.0333.6 steel with a wall thickness of 1 mm. The model of the die and tube for the production of the Y-part is shown in Figure 7. Because of greater displacements of the right portion of the formed part, the selected Y-feature in the die is located at one third of the tube's length. In this case as well, the formed part's uniaxial symmetry enabled FE half-model-based analyses. The simulation of the Y-part showed that the condition of minimum tube wall thinning could no longer be met. As a criterion of successful forming, the maximum permissible tube thinning was therefore selected, which is defined with the equation:

Various combinations of punch feedings were used. For left punch feedings we used the values of  $l_{al} = d_o$  (20 mm) and  $l_{al} = 1.5 * d_o$  (30 mm). Right punch feedings were varied over the interval between  $l_{a2} = 1.5 * l_{al}$  (30 mm) and  $l_{a2} = 3.5 * l_{al}$  (70 mm), with an increment of  $0.25 * l_{al}$ . The variation of the fluid's inner pressure with time during forming was identical

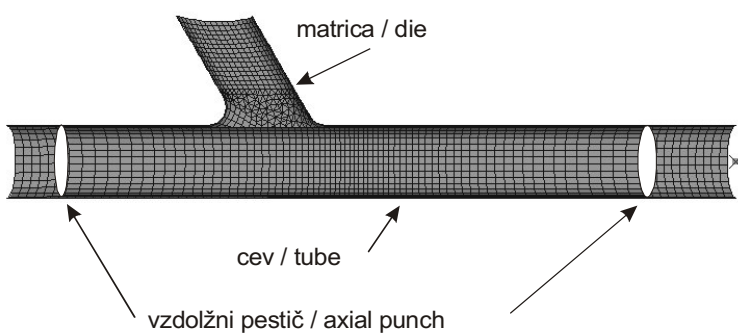
analizah preoblikovanja enak. V prvih 10% celotnega časa smo izbrali hitro naraščanje notranjega tlaka v cevi do vrednosti, ki povzroči plastifikacijo cevi. V nadaljevanju smo do konca preoblikovanja tlak linearno povečevali do mejne vrednosti, podane z enačbo [17]:

$$p_n = \frac{4s_0 R_m}{d_0 - s_0} \quad (7)$$

Koeficent trenja ima nespremenljivo vrednost  $\mu=0,05$ .

in all the analyses of forming. During the first 10% of the total time, the inner pressure was increased quickly up to the tube's yield strength. Thereafter, the pressure was increased in a linear fashion until the end of forming, up to a limit given by equation [17]:

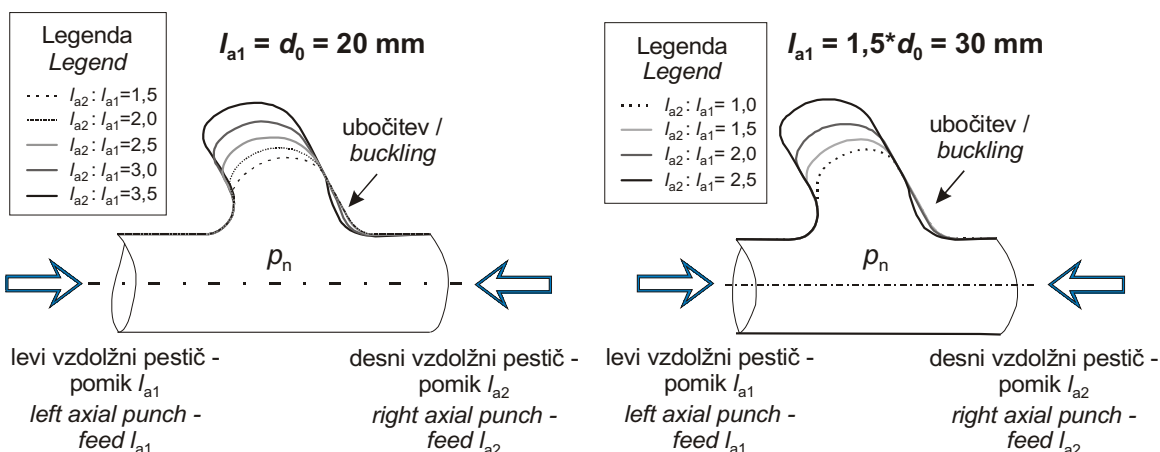
The coefficient of friction had a constant value of  $\mu=0.05$ .



Sl. 7. Model MKE orodja in cevi za izdelavo kosa Y  
Fig. 7. FE model of tool and tube for the manufacture of a Y-part

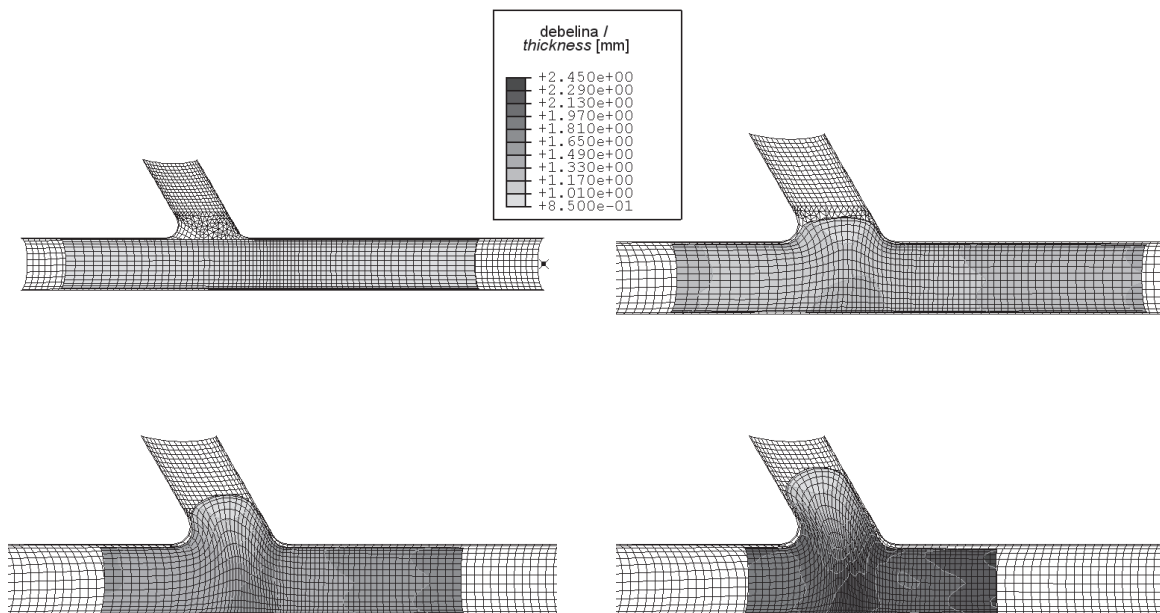
V simulacijah preoblikovanja smo analizirali višino kraka Y, njegovo obliko in debelino. Kriterija mejnega uspešnega preoblikovanja sta bila dovoljeno tanjšanje materiala (enačba 6) in pojav ubočitve preoblikovanca na prehodu cevi v krak Y. Ubočitev se pojavi ob prevelikem pomiku desnega vzdolžnega pestiša. Analize so pokazale, da se v primeru levega pomika pestiša za  $l_{a1} = d_o$  pojavi guba na kraku Y pri trikratni velikosti pomika desnega pestiša ( $l_{a2}/l_{a1} = 3$ ), medtem ko se pri večjem pomiku levega pestiša ( $l_{a1} = 1,5*d_o$ ) ta guba pojavi že pri vrednosti  $l_{a2}/l_{a1} = 2,25$ .

During simulations of forming, the Y-feature's height was analysed, along with its shape and thickness. The used limits for successful forming were the permissible material thinning (Equation 6) and the appearance of buckling on the transition from the tube to the Y-feature. Buckling appears at excessive right axial punch feedings. Analyses showed that for left punch feedings of  $l_{a1} = d_o$ , a wrinkle appears on the Y-feature at three times the value of right punch feeding ( $l_{a2}/l_{a1} = 3$ ), whereas during greater left punch feedings ( $l_{a1} = 1.5*d_o$ ) this wrinkle appears already at a value of  $l_{a2}/l_{a1} = 2.25$ .



Sl. 8. Oblika kraka Y pri različnih pomikih vzdolžnih pestičev  
Fig. 8. Y-feature at different axial punch feedings

Oblikovanje kraka Y v odvisnosti od pomikov pestičev je prikazano na sliki 8 – pomik levega pestiča  $l_{a1} = d_o$  (levo) in  $l_{a1} = 1,5 \cdot d_o$  (desno). Potek preoblikovanja in porazdelitev debel in največjega uspešno izdelanega kosa Y s pomiki vzdolžnih pestičev  $l_{a1} = 30$  mm in  $l_{a2} = 60$  mm sta prikazana na sliki 9.



Sl. 9. Porazdelitev debelin največjega uspešno preoblikovanega kosa Y  
Fig. 9. Thickness distribution of the largest successfully formed Y-part

V industrijskem okolju izdelava preoblikovanca sestoji iz več tehnoloških faz, od katerih smo simulirali le najpomembnejšo fazo – preoblikovanje z visokim notranjim tlakom. Pred to fazo se v notranjost cevi dovaja še tlačni medij in povečuje tlak do delovnega tlaka medija, po samem preoblikovanju pa sledi še faza kalibracije. Ta faza se uporablja samo pri preoblikovanju s protipestiči, v njej se preoblikovancu s povečanim kalibracijskim tlakom da končno obliko izdelka.

Analizo preoblikovanja kosa Y s protipestičem smo izvedli za kombinaciji vzdolžnih pomikov pestičev, pri katerih smo dobili največji še uspešno izdelani krak Y izdelka. To sta kombinaciji pomikov  $l_{a1} = 20$  mm :  $l_{a2} = 55$  mm in  $l_{a1} = 30$  mm :  $l_{a2} = 60$  mm. Končno obliko izdelka, ki naleže na protipestič pri 32% pomika vzdolžnih pestičev, prikazuje slika 10. Na sliki je prikazana tudi oblika izdelka po fazi kalibracije, v kateri smo povečali notranji tlak medija za 50% končne vrednosti tlaka med preoblikovanjem.

### 3 SKLEPI

Preoblikovanje z visokimi notranjimi tlaki se vedno bolj uveljavlja v avtomobilski industriji pri izdelavi izpušnih sistemov ter nosilnih in strukturnih

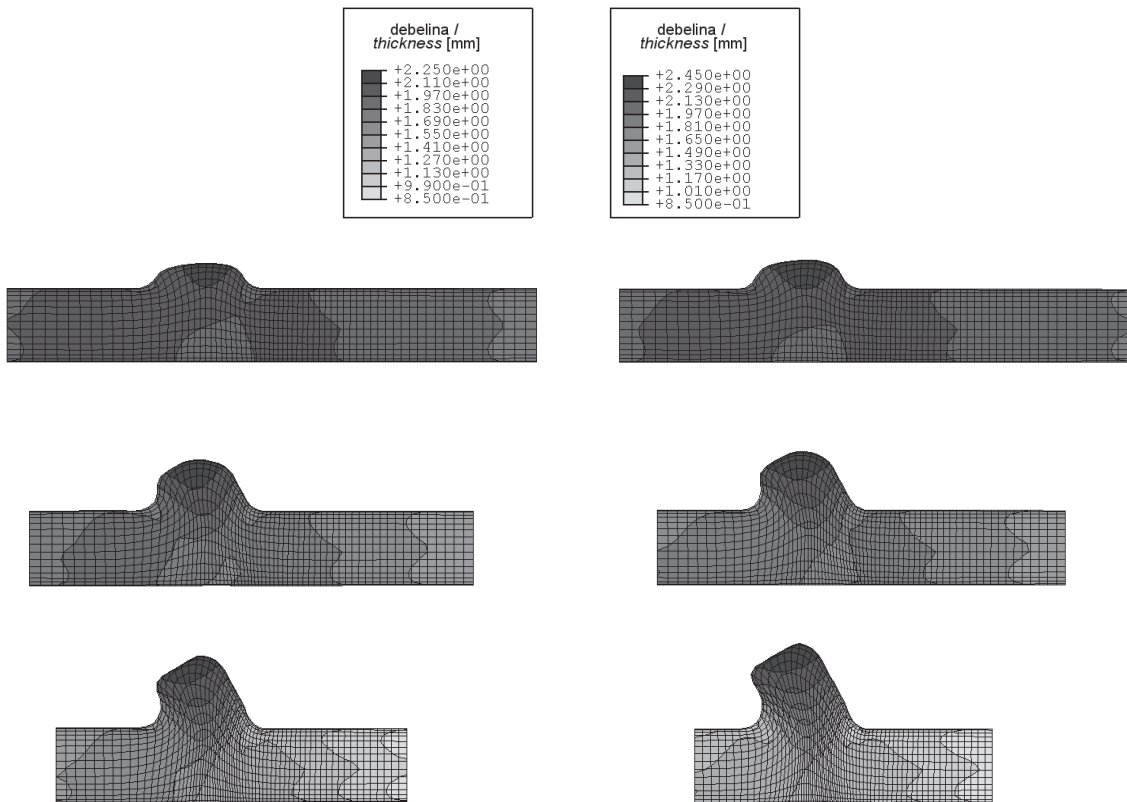
The forming of Y-feature vs. punch feedings is shown in Figure 8 – left punch feedings  $l_{a1} = d_o$  (left) and  $l_{a1} = 1,5 \cdot d_o$  (right). The course of forming and the thickness distribution for the largest successfully produced Y-part with punch feedings  $l_{a1} = 30$  mm and  $l_{a2} = 60$  mm are presented in Figure 9.

In industrial environments, the production of hydroformed parts consists of several technological phases, of which only the most important one, the forming procedure, was simulated. Prior to this phase, a pressure medium is fed to the tube's interior and it increases the pressure up to the working pressure. Forming is followed by the calibration phase, which is only used in forming with counterpunches; increased calibration pressure is applied in order to give the formed part its final shape.

The analysis of Y-part forming using a counterpunch was performed for the combinations of axial punch feedings at which the largest still successfully formed Y- feature was obtained. These were feeding combinations of  $l_{a1} = 20$  mm :  $l_{a2} = 55$  mm and  $l_{a1} = 30$  mm :  $l_{a2} = 60$  mm. The final product portion which comes into contact with the counterpunch at 32% axial punch feeding is shown in Figure 10. This figure also shows the formed part's shape after the calibration phase, in which the medium's inner pressure was increased by 50% of the final pressure value during forming.

### 3 CONCLUSIONS

Hydroforming is increasingly used in the automotive industry for the manufacture of exhaust systems, and load-bearing and structural



Sl. 10. Izdelava kosa Y z uporabo protipestiča na 1/3 (zgoraj), 2/3 (v sredini) preoblikovanja in po kalibraciji (spodaj) - pomiki  $l_{a1} = 20 \text{ mm} : l_{a2} = 55 \text{ mm}$  (levo) in  $l_{a1} = 30 \text{ mm} : l_{a2} = 60 \text{ mm}$  (desno)  
 Fig. 10. Manufacture of a Y-part using a counterpunch at 1/3 (top), 2/3 (middle) of forming time and after forming (bottom) – punch feedings  $l_{a1} = 20 \text{ mm} : l_{a2} = 55 \text{ mm}$  (left) in  $l_{a1} = 30 \text{ mm} : l_{a2} = 60 \text{ mm}$  (right)

delov avtomobila. Sama tehnologija preoblikovanja z visokimi notranjimi tlaki je zaradi velikega števila časovno spremenljivih parametrov postopka zelo zahtevna. Veliko število vplivnih parametrov je odvisno tudi od geometrijske oblike surovca in izdelka ter uporabljenega materiala.

Zaradi velikega števila vplivnih veličin postopke preoblikovanja z visokimi notranjimi tlaki načrtujemo v navideznem računalniško podprttem okolju, ki omogoča variacije posameznih parametrov postopka in iskanje optimalnih tehnoloških rešitev. Vplivnost koeficiente trenja in vzdolžnih pomikov pestičev sta analizirana na preoblikovanju kosa T in kosa Y. V obeh primerih smo notranjost cevi obremenjevali z notranjim tlakom, ki smo mu med preoblikovanjem linearno spremenjali vrednost. Velikost tlaka smo spremenjali od vrednosti, potrebne za plastično deformacijo cevi na začetku, do tlaka, ki še ne povzroči lokalizacije in izbruha na koncu preoblikovanja. Analize preoblikovanja kosa T brez protipestiča so pokazale linearno povezanost koeficiente trenja in izbočenosti preoblikovanca. Preoblikovanec se zaradi tlačnih vzdolžnih obremenitev ob večjih pomikih pestičev v največji meri odebeli pri koncih cevi, v okolini polmera orodja

components. Because of the large number of process parameters that vary with time, hydroforming technology is very demanding. A large number of influential parameters also depend on the geometry of the preform and formed part and the material used.

Because of a large number of influential parameters, hydroforming procedures are planned in a virtual environment that enables the variation of individual process parameters and searching for optimum technological solutions. The effects of the coefficient of friction and axial punch feedings are analysed on the forming of T-parts and Y-parts. In both cases, the inside of the tube was subjected to an inner pressure, the value of which was varied during forming in a linear manner. The magnitude of the pressure was varied from the value required for initial plastic tube deformation to a value just before localisation and bursting at the end of forming. An analysis of T-part forming without a counterpunch showed a linear relationship between the coefficient of friction and the formed part's feature. Because of the axial pressure loads, thickening of the formed part's wall is most pronounced at large punch feedings on tube ends, around the die radius  $R_o$  and on the

$R_o$  in na steni preoblikovanca nasproti izbočene oblike T. Do najmanjšega tanjšanja prihaja le na najbolj izbočenem delu preoblikovanca. Analize so pokazale, da se vrednosti tanjšanja v izbranih preoblikovalnih razmerah pri jeklu 1.0333.6 gibljejo vedno pod 7% začetne debeline stene.

Preoblikovanje izdelka Y, ki se uporablja v veliki meri pri izdelavi priključkov in razvodov izpušnih sistemov, smo analizirali glede na različne vzdolžne pomike cevi med postopkom. Zaradi oblike Y ne moremo uporabljati simetričnih pomikov cevi. Glede na izmere cevi, končno geometrijsko obliko kosa Y ter dovoljeno tanjšanje materiala se izbira velikost vzdolžnih pomikov. Pri izbranih velikostih pomikov levega pestiča v velikosti  $l_{a1} = d_o$  in  $l_{a1}' = 1,5 * d_o$  sta za uspešno preoblikovanje cevi največja dovoljena pomika desnega pestiča  $l_{a2} = 2,75 * l_{a1}$  v prvem in  $l_{a2}' = 2 * l_{a1}$  v drugem primeru.

Predstavljene analize preoblikovanja kosa T in kosa Y bomo v nadaljevanju raziskovalnega dela razširili z geometrijsko zahtevnejšimi uporabami ter vrednotenji vplivov različnih kombinacij pogojev vzdolžnih sil in notranjih tlakov na oblikovanje končnega izdelka.

wall opposite the T-feature. Minimum thinning takes place only on the most prominent portion of the formed part. Analyses have shown that the values of thinning during the selected forming conditions for steel 1.0333.6 always range below 7% of the initial wall thickness.

The forming of Y-parts, which is largely used in the production of manifolds and connectors for exhaust systems, was analysed in terms of the different axial tube displacements during the procedure. Because of the Y-feature, symmetric tube displacements could not be used. The magnitude of axial feedings is selected based on tube dimensions, the final Y-feature geometry and permissible material thinning. At the selected left punch feedings of  $l_{a1} = d_o$  and  $l_{a1}' = 1.5 * d_o$ , the maximum permissible right punch feedings for successful tube forming are  $l_{a2} = 2.75 * l_{a1}$  in the first case and  $l_{a2}' = 2 * l_{a1}$  in the second case.

In the continuation of our research, the presented analyses of the forming of T-parts and Y-parts will be expanded with geometrically more complex applications and evaluations of the influence of different combinations of axial forces and inner pressures on the forming of final products.

#### 4 LITERATURA 4 REFERENCES

- [1] Schmoeckel, D. et al. (1999) Metal forming of tubes and sheets with liquid and other flexible media, *Annals of CIRP*, Vol 48/2.
- [2] Kampuš, Z., J. Jiang., B. Dodd (1994) Net shape cold plastic forming of aluminium-based metal matrix composites. *J. mater. sci. lett.*, 13, 80-81.
- [3] Merklein, M., M. Geiger (2002) New materials and production technologies for innovative lightweight constructions, *Journal of material processing technology*, Vol. 125: Sp. Iss. SI SEP 9, 532-536.
- [4] Vollertsen, F., M. Kreimeyer, M. Beckmann (2003) Deep drawing of laser welded aluminium-steel/aluminium-titanium tailored blanks, *Proc. of IDDRG 2003 Conference*, 11-14.maj 2003, Bled, 273-282.
- [5] Gantar, G., M. Ljevar, K. Kuzman (2001) Uporaba numeričnih simuliranj pri razvoju orodij za izdelavo pločevinastih sestavnih delov avtomobilov (The use of numerical simulations in the development of tools for the sheet-metal parts of cars). *Stroj. vestnik*, 47, št. 10, 605-614.
- [6] Groche, P., R. Steinheimer, D. Schmoeckel (2003) Process stability in the tube hydroforming process, *Annals of the CIRP*, Vol. 52/1/2003, 229-232.
- [7] Pepelnjak, T., B. Jurkošek, K. Kuzman (1997) Sodoben tržno prilagodljiv razvoj in proizvodnja novih modulno grajenih pločevinastih izdelkov, *Strojniški vestnik*, 43, 9/10, Fakulteta za strojništvo, Ljubljana, 415-426.
- [8] Limb, M.E. et al. (1973) The forming of axisymmetric and asymmetric components from tube, *Proceedings of the 14<sup>th</sup> International MTDR Conference*, 799-805.
- [9] Pipan, J. (1993) Proces preoblikovanja cevi z notranjim tlakom in aksialnim pritiskom, disertacija, Ljubljana 1993.
- [10] Pipan, J., F. Kosel (2002) Numerical simulation of rotational symmetric tube bulging with inside pressure and axial compression. *Int. j. mech. sci.* [Print ed.], 44, no. 3, 645-664.
- [11] Vollertsen, F., T. Prange, M. Sander (1999) Hydroforming: needs, developments and perspectives, *Proceedings of the Advanced Technology of Plasticity*, Vol II, Erlangen, 1197-1209.
- [12] Koc, M., T. Altan (2001) An overall review of the tube hydroforming (THF) technology, *Journal of Materials Processing Technology*, 108, 384-393.
- [13] <http://hydroforming.mb.uni-magdeburg.de/kompend/rohre.htm> (stanje/stage 22.9.2003).
- [14] N.N.: Innehochdruck-Umformen – Grundlagen, *VDI Richtlinie 3146 Blatt 1*, VDI, 1999.

- [15] ABAQUS users manual, ver 6.3, Hibbit, Karlsson & Sorenson, Inc., 2003.
- [16] Koc, M., T. Allen, S. Juratheranat, T. Altan (2000) The use of FEA and design of experiments to establish design guidelines for simple hydroformed parts, *International Journal of Machine Tool & Manufacture*, 40(2000), 2249-2266.
- [17] [http://nsm.eng.ohio-state.edu/Final\\_TPJ\\_Y-shape\\_0904.pdf](http://nsm.eng.ohio-state.edu/Final_TPJ_Y-shape_0904.pdf) (stanje/stage 31.10.2003).

Avtorjev naslov: dr. Tomaž Pepelnjak  
Fakulteta za strojništvo  
Univerza v Ljubljani  
Aškerčeva 6  
1000 Ljubljana  
tomaz.pepelnjak@fs.uni-lj.si

Author's Address: Dr. Tomaž Pepelnjak  
Faculty of Mechanical Eng.  
University of Ljubljana  
Aškerčeva 6  
1000 Ljubljana, Slovenia  
tomaz.pepelnjak@fs.uni-lj.si

Prejeto: 11.11.2003  
Received: 11.11.2003

Sprejeto: 12.2.2004  
Accepted: 12.2.2004

Odprto za diskusijo: 1 leto  
Open for discussion: 1 year

## Obravnavanje curka plinskega olja in nadomestnih goriv

### A Spray Analysis of Petrol and Alternative Fuels

Martin Volmajer - Breda Kegl

V prispevku je obravnavana numerična analiza curkov plinskega olja in nekaterih nadomestnih goriv. Z uporabo paketa računske dinamike tekočin FIRE so bile določene karakteristike curkov (velikost kapljic in domet) plinskega olja, biodizla in odpadnega rastlinskega olja. Nekatere vrednosti karakterističnih veličin curka so bile primerjane tudi z vrednostmi, izračunanimi z uporabo znanih empiričnih modelov za določitev karakteristik curka. Analize so bile izvedene za dva tipa vbrizgalnih šob oz. vbrizgalnih sistemov (neposredni in posredni). V primeru slednjega so rezultati numerične analize primerjani še s fotografijami curka.

© 2004 Strojniški vestnik. Vse pravice pridržane.

(Ključne besede: vbrizgavanje goriva, olje plinsko olje, biodizel, olja odpadna, olja rastlinska)

This paper presents numerical analyses of sprays of diesel and some alternative fuels. The fuel spray characteristics (the droplet size and the penetration length) of diesel fuel, biodiesel and waste cooking oil were calculated using the computational fluid dynamics program FIRE. Some of the characteristics were calculated using existing empirical models. The analyses were made for two different injection systems: direct and indirect injection. In the case of indirect injection, the results were also compared with fuel-spray photographs.

© 2004 Journal of Mechanical Engineering. All rights reserved.

(Keywords: fuel injection, diesel fuels, biodiesel, waste cooking oils)

#### 0 UVOD

Z uporabo nadomestnih goriv rastlinskega porekla lahko klasičen dizelski motor z notranjim zgrevanjem obratuje brez prirastka emisij ogljikovega dioksida ( $\text{CO}_2$ ). To pomeni, da se z uporabo teh goriv ne povečuje količina  $\text{CO}_2$  v atmosferi. Kot gorivo rastlinskega porekla se običajno uporablajo estri maščobnih kislin rastlin, to so: oljna repica, sončnično olje, sojino olje ipd. Ti estri se imenujejo biodizel. Lahko pa nadomestna goriva izdelujemo tudi iz odpadnega rastlinskega olja.

Znano je, da lastnosti goriva, kakor tudi njegova sestava, odločilno vplivajo na postopek vbrizgavanja ter s tem neposredno na postopek zgrevanja in nastanek nezaželenih ostankov. Ob upoštevanju dejstva, da se sestava goriv rastlinskega porekla razlikuje od sestave mineralnih goriv, je za prilagoditev delovanja dizelskega motorja z nadomestnimi gorivi potrebno dobro poznавanje omenjenih postopkov.

Z uporabo paketov računske dinamike tekočin (CFD) računalniška oprema dandas dopušča razmeroma hitre analize postopka

#### 0 INTRODUCTION

A conventional compression ignition engine is capable of running with a zero net emission of a carbon dioxide ( $\text{CO}_2$ ) when alternative fuels based on vegetable oil are used. In this way the concentration of  $\text{CO}_2$  in the atmosphere stays the same. For the plant source it is common to use esters from rapeseed, sunflower, soya, etc. These esters are commonly referred to as biodiesel. Alternative fuels can also be made of waste cooking oils.

It is well known that the fuel characteristics and the fuel composition significantly affect the injection process, which in turn has a direct effect on the combustion and emission-formation processes. Since the composition of vegetable-source fuels differs from that of petroleum-based fuels, the conventional compression-ignition engine needs to be adapted to run on alternative fuels. This step requires a good understanding of the injection and combustion processes of alternative fuels.

Today we are able to run relatively fast analyses of the injection and spray-formation processes, as well as the combustion and emission-formation

vbrizgavanja, nastanka curka, kakor tudi zgorevanja in nastanka emisij, s čimer lahko že pred prvimi praktičnimi preizkušnjami do neke mere prilagodimo motor novim delovnim razmeram.

Z namenom spoznavanja vplivov nadomestnih goriv na postopek vbrizgavanja in nastanek curka ter možnostjo predelave sedanjih sistemov za obratovanje z nadomestnimi gorivi so bile izvedene tudi analize v tem prispevku.

## 1 TEORETIČNE OSNOVE

### 1.1 Lastnosti goriva

Rastlinska olja so zgrajena v obliki trigliceridov, ki jih sestavljajo tri verige ogljikovodikov povezane med seboj z glicerolom. Kot takšna sicer gorijo, a jih v takšni obliki v praksi zelo redko uporabljamo. Njihova največja pomanjkljivost je zelo velika viskoznost, ki povzroča težave z dovodom goriva. Tem težavam se lahko izognemo z gretjem goriva, večjim prezom cevi ali s kemičnim postopkom esterifikacije, to je s proizvodnjo biodizla. To je postopek, pri katerem esterske vezi v triglyceridih hidroliziramo, s čimer nastanejo proste maščobne kisline, ki po reakciji z metanolom ali etanolom delajo metil- ali etilestre. Njihove lastnosti se lahko razlikujejo v odvisnosti od osnovne rastline.

Kot druga nadomestila se lahko uporabi tudi odpadno rastlinsko olje. To ima podobne lastnosti kakor čisto rastlinsko olje, zato neesterificirano ni najprimernejše za uporabo. Lastnosti biodizla (BIO), plinskega olja (D2) in odpadnega rastlinskega olja (ORO-WCO) so predstavljene v preglednici 1. V predstavljenih analizah je bilo, ne glede na nekatere predhodne negativne izkušnje, uporabljeno rastlinsko olje, pri katerem ni bil izведен postopek esterifikacije.

### 1.2 Numerična analiza

Numerična analiza je narejena z uporabo programskih paketov RDT FIRE v7.2b in FIRE v.8.1 (AVL) na delovnih postajah HP 9000/782 in 9000/785 oz. osebnem računalniku P3 450 MHz.

processes, by using computational fluid dynamics (CFD) programs. By using these tools we are able to partly adjust the engine to the new conditions, even before the first experimental tests.

The objective of this paper is to learn how the alternative fuels affect the injection and spray-formation processes and to get some information about how the existing injection systems should be adapted to run with these fuels.

## 1 THEORETICAL BACKGROUND

### 1.1 Fuel characteristics

Vegetable oils exist in the form of triglycerides, which consist of three hydrocarbon chains connected together by glycerol. Vegetable oils are combustible, but they are rarely used in this form. The problem with vegetable oils is their very high viscosity, which causes problems with fuel flow from the tank to the engine. Those problems can, however, be reduced by preheating the oil and using larger fuel lines or by chemical modification, i.e. producing biodiesel. In this process the ester bonds in the triglycerides are hydrolysed. The result is free fatty acids, which form methyl or ethyl esters after a reaction with methanol or ethanol. The properties of these esters are mainly dependent on the source plant.

An alternative is to use waste cooking oil. But since it has similar properties to pure vegetable oil, in its unesterified form it is not suitable to be used as a fuel. The characteristics of diesel fuel (D2), biodiesel (BIO) and waste cooking oil (WCO) are presented in Tab. 1. The WCO used in the presented analyses was, in spite of past negative experiences, unesterified.

### 1.2 Numerical analyses

The numerical analyses were made using the CFD programs FIRE v7.2b and FIRE v.8.1 (AVL) on two workstations (HP 9000/782 and HP 9000/785) and a P3 personal computer (450 MHz), respectively.

Preglednica 1. Lastnosti goriv [1] in [2]

Table 1. Fuel characteristics [1] and [2]

	D2	BIO	ORO / WCO
$\rho$ (kg/m <sup>3</sup> )	820 do/to 845	875 do/to 900	915
$\nu$ (mm <sup>2</sup> /s)	2 do/to 4,5	3,5 do/to 5,0	36,7
$H$ (MJ/kg)	42,6	37,3	-
cetansko št./cetane no.	46	>49	-

### 1.3 Empirični modeli

Kot hiter kazalnik razvoja sprememb oblike curka in kakovosti razpršitve lahko uporabimo tudi nekatere empirične modele, s katerimi lahko ocenimo srednji Sauterjev premer ( $d_{32}$ ) in domet curka ( $L_p$ ). V predstavljenem delu sta bila uporabljena naslednja modela: Filipović [3] (1) za srednji Sauterjev premer kapljic ter Yule-Filipović [4] (2) za domet curka:

$$d_{32} \text{ v } \mu\text{m} = 324,6 \cdot \left( \frac{\rho_a \cdot u_0^2 \cdot d_h}{\sigma_f} \right)^{-0,233} \cdot \left( \frac{\rho_f \cdot d_h \cdot \sigma_f}{\mu_f^2} \right)^{-0,082} \quad (1)$$

$$L_p \text{ v } \text{mm} = 2,65 \cdot 10^3 \cdot d_h \cdot \left( \frac{\rho_a \cdot u_0^2 \cdot d_h}{\sigma} \right)^{-0,1} \cdot \left( \frac{\rho_f \cdot u_0 \cdot d_h}{\mu_f} \right)^{-0,3} \cdot \left( \frac{\rho_f}{\rho_a} \right)^{0,08} \quad (2).$$

V enačbah (1) in (2) sta  $\rho_a$  gostota zraka,  $\rho_f$  gostota goriva,  $\sigma$  pomeni površinsko napetost goriva,  $\mu_f$  dinamično viskoznost goriva,  $\mu_a$  pa dinamično viskoznost zraka. Iztočna hitrost je označena z  $u_0$ , tlačna razlika z  $\Delta p$ , medtem ko  $d_h$  pomeni premer odprtine šobe. Vse enote so v skladu s sistemom SI.

### 1.4 Vbrizgalni sistemi

V predloženem delu je bil analiziran postopek vbrizgavanja in nastanka curka za dva vbrizgalna sistema: (i) VBRIZGALNI SISTEM 1 (VS1) – klasičen vbrizgalni sistem z linjsko tlačilko in vbrizgalno šobo s štirimi izvrtinami premera 0,375 mm, pri katerem imata odprtini št. 1 in št. 4 nagibni kot kanala odprtine 95°, odprtini št. 2 in št. 3 pa kot 49°, (ii) VBRIZGALNI SISTEM 2 (VS2) – vbrizgalni sistem z rotacijsko tlačilko in šobo s čepom, s premerom odprtine 1,1 mm.

## 2 ŠTEVILČNI PRIMERI

Analize so bile izvedene pri dveh različnih obratovalnih režimih (njavečji vrtilni moment (VS1\_A) in največja moč (VS1\_B) pri VS1 in največji vrtilni moment (VS2\_C) ter 80% vrtilne frekvence največje moči (VS2\_D) pri VS2 za tri različna goriva: biodiesel (BIO), odpadno rastlinsko olje (ORO) in plinsko olje (D2).

Vrtilni frekvenci tlačilke v primeru VS1 sta 600 min<sup>-1</sup> in 1000 min<sup>-1</sup>, medtem ko vrtilni frekvenci pri VS2 znašata 1000 min<sup>-1</sup> in 2000 min<sup>-1</sup>.

Analiza z uporabo RDT je za VS1 potekala v diskretiziranem modelu v obliki kocke s stranico 300 mm, za VS2 pa v modelu oblike kvadra izmer 50x50x500 mm. Obe geometrijski oblikli predstavljata vbrizgalno komoro. Izmere so bile izbrane v skladu s pričakovanimi dometi in obliko curkov.

Za izračun karakteristik vbrizgavanja, potrebnih za določitev začetnih in robnih pogojev

### 1.3 Empirical models

The empirical model for calculating the Sauter mean diameter ( $d_{32}$ ) and the spray penetration length ( $L_p$ ) can be used as a tool for fast analyses, showing the tendency of the spray changes and the quality of the atomisation. In this paper, two empirical models were used: Filipović [3] (Eq.1) for the Sauter mean diameter of the droplets, and Yule - Filipović [4] (Eq.2) for the spray penetration length:

$$d_{32} \text{ v } \mu\text{m} = 324,6 \cdot \left( \frac{\rho_a \cdot u_0^2 \cdot d_h}{\sigma_f} \right)^{-0,233} \cdot \left( \frac{\rho_f \cdot d_h \cdot \sigma_f}{\mu_f^2} \right)^{-0,082} \quad (1)$$

$$L_p \text{ v } \text{mm} = 2,65 \cdot 10^3 \cdot d_h \cdot \left( \frac{\rho_a \cdot u_0^2 \cdot d_h}{\sigma} \right)^{-0,1} \cdot \left( \frac{\rho_f \cdot u_0 \cdot d_h}{\mu_f} \right)^{-0,3} \cdot \left( \frac{\rho_f}{\rho_a} \right)^{0,08} \quad (2).$$

In Eq.1 and 2,  $\rho_a$  is the air density,  $\rho_f$  is the fuel density,  $\sigma_f$  represents the surface tension,  $\mu_f$  is the viscosity of the fuel, and  $\mu_a$  is the air viscosity. The outflow velocity is denoted by  $u_0$ ,  $\Delta p$  is the pressure difference, and  $d_h$  is the nozzle hole diameter. The units of all the input values are according to the SI system.

### 1.4 Injection system

The injection characteristics and the spray formation process were analysed for two injection systems: (i) INJECTION SYSTEM 1 (VS1) – a conventional fuel-injection system with an in-line pump and a four-hole injection nozzle (hole diameter 0.375 mm, holes #1 and #4 have an inclination angle of 95°, whereas holes #2 and #3 have an inclination angle of 49°), (ii) INJECTION SYSTEM 2 (VS2) – an injection system with a rotational pump and a pintle nozzle (hole diameter 1.1mm).

## 2 NUMERICAL EXAMPLES

The analyses were made for two different operating conditions: maximum torque (VS1\_A) and rated (VS1\_B) for injection system 1 (VS1), and maximum torque (VS2\_C) and 80% of the rotational speed at maximum power (VS2\_D) for injection system 2 (VS2)). Three different fuels were used: biodiesel (BIO), waste cooking oil (WCO) and diesel fuel (D2).

The pump rotational speeds for VS1 were 600 min<sup>-1</sup> and 1000 min<sup>-1</sup>, and for VS2 the rotational speeds were 1000 and 2000 min<sup>-1</sup>.

The CFD analyses were made on the cube model with a side of 300 mm for VS1 and on the block model with sides 50x50x500 mm for VS2. Both geometries represent the injection chamber. The dimensions were set according to the expected spray shapes and the penetration lengths.

The injection characteristics needed for the setting of the initial and boundary conditions were

numeričnih analiz, je bil uporabljen enorazsežni matematični model [6] oz. meritve. V primeru VS1 so karakteristike vbrizgavanja za posamezno gorivo dobljene iz rezultatov analize, predstavljeni v [7], medtem ko so bile pri VS2 le-te dobljene na podlagi meritv. Tlak v komori je 1 bar, temperatura 313 K. Začetna velikost kapljic in verjetnostna porazdelitev (začetni pogoji) sta določeni v skladu z ugotovitvami predhodne analize [8]. Pri verjetnostnih porazdelitvah v primeru analize nadomestnih goriv je določena velikost kapljic z največjo verjetnostjo za okrog 15% večja od tiste pri plinskem olju.

### 3 REZULTATI

V nadaljevanju so predstavljeni rezultati numeričnih in empiričnih analiz za vbrizgalni sistem 1 (VS1) in 2 (VS2) ter fotografije curka VS2.

#### 3.1 Vbrizgalni sistem 1

##### 3.1.1 Numerična analiza

Na slikah 1 do 4 so prikazane oblike curka in lega kapljic ob koncu vbrizgavanja, izračunane srednje vrednosti srednjega Sauterovega premera v komori ter največji domet curka pri posameznem gorivu. Na slikah 1 do 3 je velikost kapljic predstavljena z velikostjo krožcev. S slik je razvidno, da je domet curka odpadnega rastlinskega olja večji od dometov biodizla in plinskega olja. Prav tako je jasno vidna razlika med dometi curka v posameznem obratovalnem režimu.

Zanimivo je, da so v primerjavi izračunanih največjih dometov (sl.4) razlike nekoliko manjše, kakor bi lahko sklepali iz grafičnega prikaza curkov. Razlike med grafičnim prikazom in absolutnimi vrednostmi so verjetno posledica tega, da največji domet pomeni pot

obtained by using the one-dimensional mathematical model [6] and the experimental results, respectively. In the case of VS1 the injection characteristics for all three fuels were obtained from the results presented in [7], whereas the characteristics in the case of VS2 were measured. The pressure in the chamber was 1 bar, while the temperature was 313 K. The initial size of the bubble and the probability distributions were defined according to the findings of previous analyses [8]. The bubble-size distribution in the case of the alternative fuels was set 15% higher than in the case of diesel fuel.

### 3 RESULTS

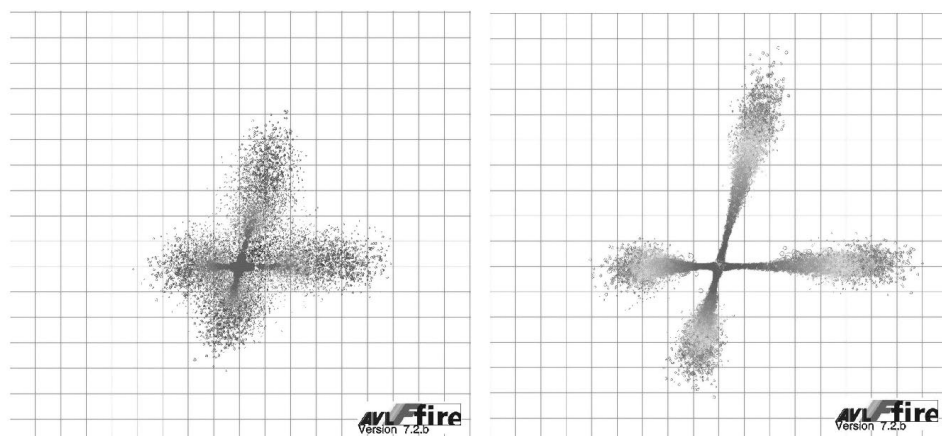
The results of the numerical and empirical analyses for the injection system 1 (VS1) and 2 (VS2) and the fuel-spray photographs for VS2 are presented below.

#### 3.1 Injection system 1

##### 3.1.1 Numerical analysis

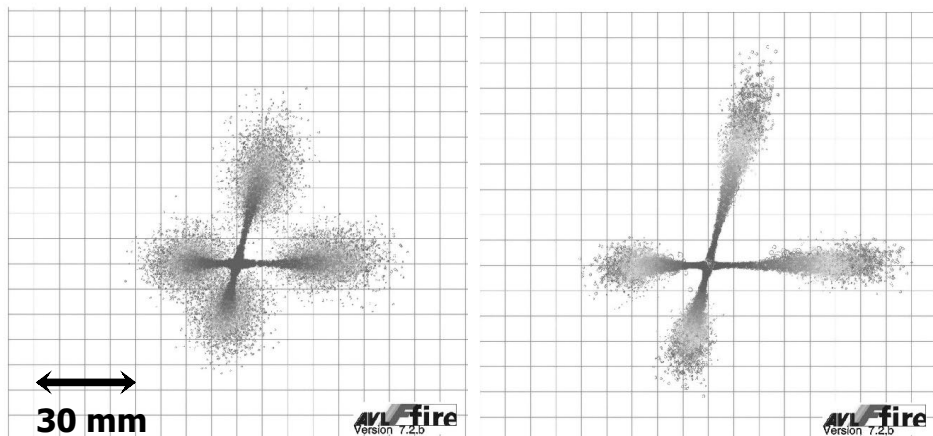
Fig. 1-4 show the spray shapes and the positions of the droplets at the end of the injection process, the calculated mean values of the Sauter mean diameter in the chamber, and the maximum spray penetration length for all three fuels. In Fig. 1-3 the size of the droplets is represented by the size of the circles. From the figures presented below it is clear that the penetration length when using the waste cooking oil is larger than in the case of the biodiesel and the diesel fuel. An obvious difference in the penetration lengths under different operating conditions can also be seen.

It is interesting that the differences between the calculated values of the penetration length are smaller than the differences between the penetration lengths shown in the figures. These differences are probably the result of the definition of the maximum penetration length, which is equal to the path of the droplet that travelled the

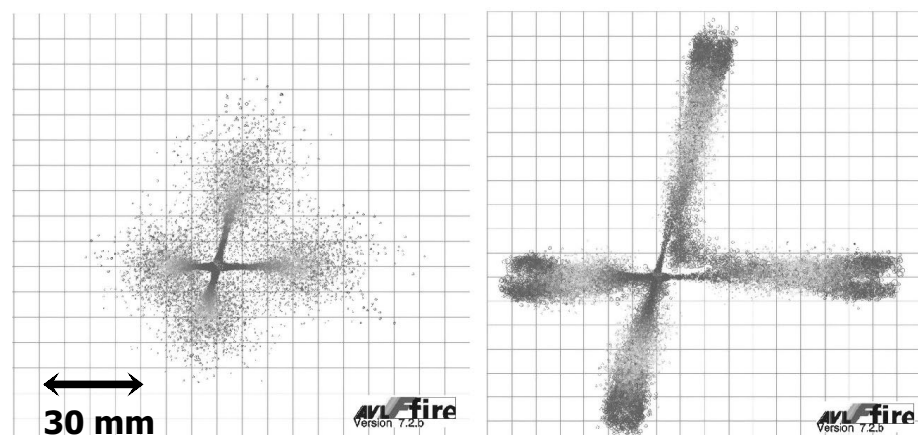


Sl. 1. Curek plinskega olja (levo: največji vrtilni moment (VS1\_A), desno: največja moč (VS1\_B))

Fig. 1. Diesel fuel spray (left: maximum torque (VS1\_A), right: rated (VS1\_B))

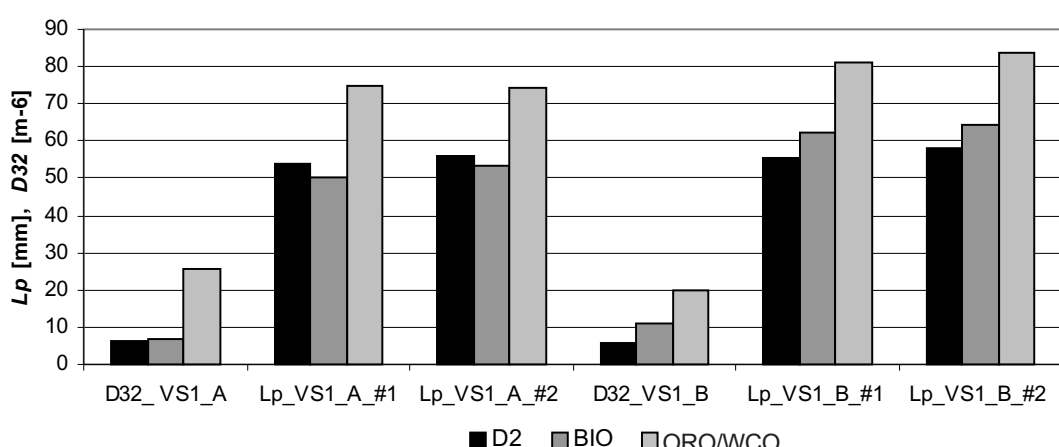


Sl. 2. Curek biodizla (levo: največji vrtljni moment (VS1\_A), desno: največja moč (VS1\_B))  
Fig. 2. Biodiesel spray (left: maximum torque (VS1\_A), right: rated (VS1\_B))



Sl. 3. Curek odpadnega rastlinskega olja (levo: največji vrtljni moment (VS1\_A), desno: največja moč (VS1\_B))

Fig. 3. Waste cooking-oil spray (left: maximum torque (VS1\_A), right: rated (VS1\_B))



Sl. 4. NUMERIČNA ANALIZA - primerjava karakteristik curka obravnavanih goriv pri najv. vrt. momentu (D32\_VS1\_A, LP\_vrtlni moment\_VS1\_A) in največji moči (D32\_VS1\_B, Lp\_VS1\_B), D32 je Sauterjev srednji premer, Lp je domet curka, #1 pomeni odprtini 1 in 4, #2 pomeni odprtini 2 in 3

Fig. 4. NUMERICAL ANALYSIS – Comparison of spray characteristics at max. torque (VS1\_A) and rated (VS1\_B): D32 is the Sauter mean diameter; Lp is the penetration length, #1 represent holes 1 and 4, #2 represent holes 2 and 3

najbolj oddaljene kapljice iz posamezne odprtine. Te pa so zaradi majhne ločljivosti slabše vidne. Pri izračunih srednjih vrednosti srednjih Sauterjevih premerov (sl. 4) v komori je dobro viden trend večanja kapljic z uporabo goriv z večjo viskoznostjo.

Velikost kapljic in domet curka sta glavna kazalnika razpada curka goriva. Boljši razpad curka pomeni, da so kapljice majhne, domet pa čim krajši. Boljši razpad curka vpliva pozitivno na postopek zgorevanja, manjše pa so tudi emisije saj oz. trdnih delcev. Iz predstavljenih rezultatov je razvidno, da je razpad curka najboljši v primeru uporabe plinskega olja, sledi biodizel, medtem ko je razpad curka pri odpadnem rastlinskem olju najslabši.

### 3.1.2 Empirična analiza

Rezultati empirične analize karakteristik curka so prikazani na sliki 5, od koder je ponovno jasno razviden najboljši razpad curka v primeru uporabe plinskega olja (D2).

## 3.2 Vbrizgalni sistem 2

### 3.2.1 Numerična analiza

V primeru VS2 je bila numerična analiza izdelana le za dizelsko gorivo. Rezultati za obravnavana obratovalna režima (VS2\_C in VS2\_D) so prikazani na slikah 6 in 7. Izračunan največji domet v primeru VS2\_C je okrog 240 mm, pri VS2\_D pa okrog 210 mm. Srednji Sauterjev premer kapljic znaša v prvem primeru okrog 65 µm, v drugem pa okrog 62 µm. Na slikah 6 in 7 velikost krogel pomeni velikost kapljic.

longest distance. Because of the low resolution figures these are not easily seen. It is mainly the core of the spray that can be observed from the figures. The calculated values of the Sauter mean diameter (Fig. 4) show that the values are larger for fuels with a higher viscosity.

The droplet size and the penetration length are the most important parameters, showing the quality of the spray atomisation. By the term ‘better atomisation’, we understand that the droplets are smaller and the penetration length is shorter. The quality of the atomisation positively effects the injection and combustion process and the soot emission. From the above-presented results it is clear that the atomisation is the best in the case of the diesel fuel, followed by the biodiesel and the waste cooking oil.

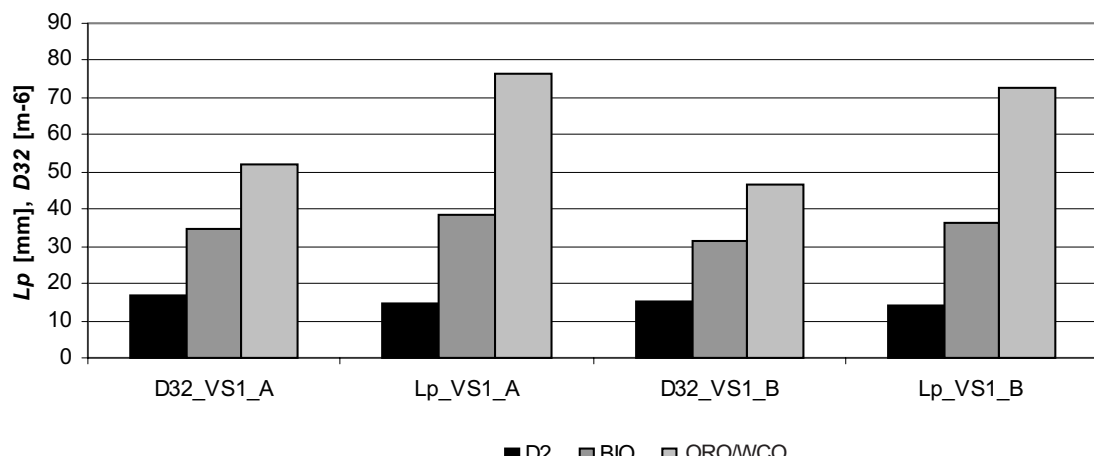
### 3.1.2 Empirical analysis

The empirical analysis results of the spray characteristics are presented in Fig. 5, where it can be seen that the best atomisation is calculated for the diesel fuel (D2).

## 3.2 Injection system 2

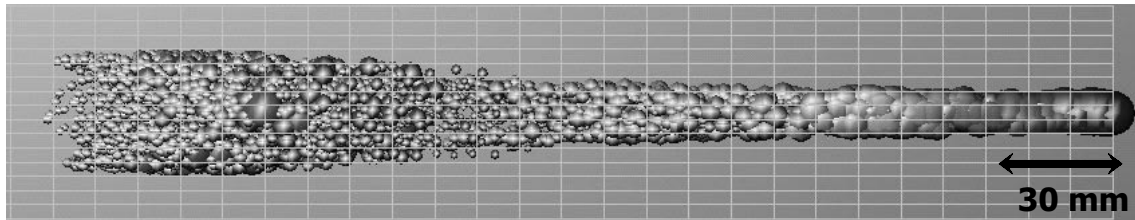
### 3.2.1 Numerical analyses

For VS2 the numerical analyses were made only for the diesel fuel. The results for both operating conditions – VS2\_C and VS2\_D – are presented in Fig. 6 and 7. The calculated maximum penetration length for VS2\_C is about 240 mm, whereas for VS2\_D it is 210 mm. The Sauter mean diameter is 65 µm for the first case and 63 µm for the second case. The size of the spheres in Fig. 6 and 7 represents the size of the droplets.

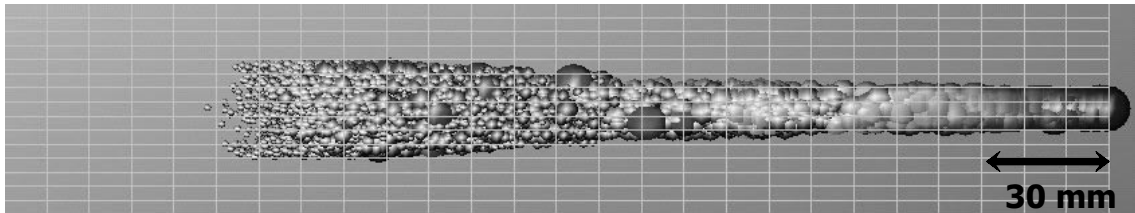


Sl. 5. EMPIRIČNA ANALIZA - primerjava karakteristik curka obravnavanih goriv pri največjem vrtljnem momentu (D32\_VS1\_A, LP\_VS1\_A) in največji moči (D32\_VS1\_A, Lp\_VS1\_B) , D32 je Sauterjev srednji premer , Lp je domet curka

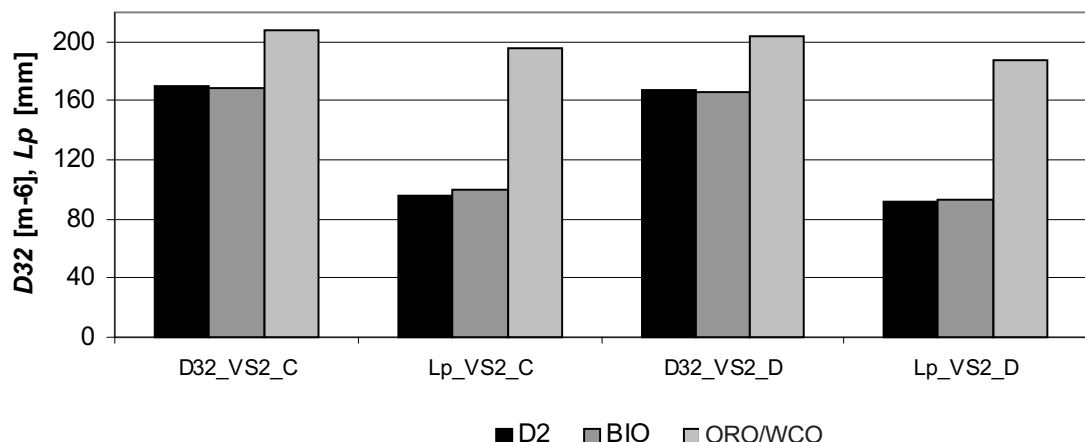
Fig. 5. EMPIRICAL ANALYSIS - Comparison of the spray characteristics at max. torque (VS1\_A) and rated (VS1\_B): D32 is the Sauter mean diameter, Lp is the penetration length



Sl. 6. Curek plinskega olja pri največjem vrtilnem momentu (VS2\_C)  
Fig. 6. Diesel fuel spray at maximum torque (VS2\_C)



Sl. 7. Curek plinskega olja pri 80% vrtilne frekvence največje moči (VS2\_D)  
Fig. 7. Diesel fuel spray at the 80 % of maximum power rotational speed (VS2\_D)



Sl. 8. EMPIRIČNA ANALIZA - primerjava karakteristik curka obravnavanih goriv pri najv. vrt. momentu (D32\_VS2\_C, LP\_VS2\_C) in 80% vrt. frekvenci najv. moč (D32\_VS2\_D, Lp\_VS2\_D) , D32 je Sauterjev srednji premer , Lp je domet curka

Fig. 8. EMPIRICAL ANALYSIS - Comparison of spray characteristics at the max. torque (VS2\_C) and at the 80% of rotational speed of the maximum power (VS2\_D): D32 is the Sauter mean diameter; Lp is the penetration length

### 3.2.2 Empirična analiza

Rezultati empirične analize za VS2 so prikazani na sliki 8. Na prvi pogled je razvidno, da uporabljeni modeli napovesta razmeroma kratke curke z velikimi vrednostmi srednjih Sauterjevih premerov, kar ni v skladu s predhodnimi numeričnimi ugotovitvami (sl. 7 in 8) ter v nadaljevanju predstavljenimi fotografijami curka (sl. 9 in 10).

### 3.2.3 Fotografiranje curka

Za primer VS2 je bilo v okviru Laboratorija za motorje z notranjim zgorevanjem Fakultete za strojništvo Maribor izvedeno fotografiranje curka (sl. 9 in 10).

Zaradi razmeroma preprostega postopka in izvedbe je kakovost slik sorazmerno slaba, vidni pa

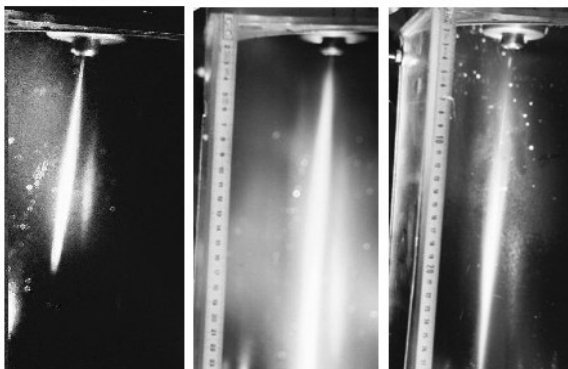
### 3.2.2 Empirical analysis

The empirical analysis results for VS2 are presented in Fig. 8. It can be clearly seen that the empirical models gave rather short sprays with relatively high values of the Sauter mean diameter, which is not in accordance with the numerical results (Fig. 7 and 8) and the photographs (Fig. 9 and 10) for this case.

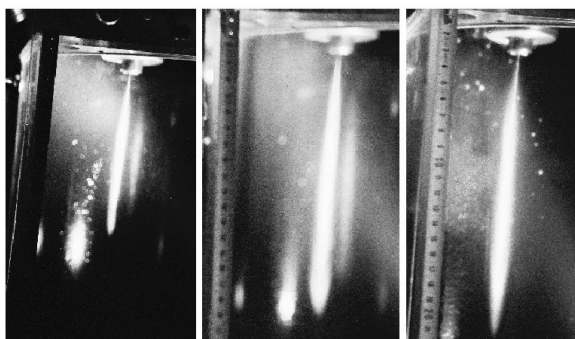
### 3.2.3 Spray photography

For VS2 the spray photographs were taken at the Engine Research Laboratory of the Faculty of Mechanical Engineering, Maribor (Fig. 9 and 10).

The quality of presented photographs is relatively low, due to the low resolution and the back



Sl. 9. Fotografije curkov pri VC2\_C (od leve: plinsko olje, biodizel, odpadno rastlinsko olje)  
Fig. 9. Spray photographs for VS2\_C (from left: diesel fuel, biodiesel, waste cooking oil)



Sl. 10. Fotografije curkov pri VC2\_D (od leve: plinsko olje, biodizel, odpadno rastlinsko olje)  
Fig. 10. Spray photographs for VS2\_D (from left: diesel fuel, biodiesel, waste cooking oil)

Preglednica 2. Domet curka, dobljen s fotografij

Table 2. Spray penetration length acquired from the spray photographs

	VC2_C	VC2_D
D2	150 mm	120 mm
BIO	230 mm	185 mm
WCO	280 mm	215 mm

so tudi številni odsevi. Kljub temu je bilo mogoče do neke mere določiti največji domet pri posameznem obratovalnem režimu.

S fotografij je razvidno, da je domet v obeh primerih najkrajši v primeru uporabe plinskega olja, najdaljši pa v primeru odpadnega rastlinskega olja. Izmerjene vrednosti so predstavljene v pregl. 2. Vidno je tudi, da je kot curka v bližini odprtine največji pri plinskem olju, kar kaže na boljši razpad goriva. Pri nadomestnih gorivih, posebej pri odpadnem rastlinskem olju, je vidna nit goriva na izstopu iz odprtine, ki se začne trgati komaj na razdalji okrog 70 mm v primeru VS2\_C (sl. 9) oz. 50 mm v primeru VS2\_D (sl. 10). Šele od tukaj dalje lahko govorimo o razpadu curka.

### 3.3 Razprava

Kljub temu, da se rezultati numerične in empirične analize, kakor tudi vrednosti določene s

scattering of the stroboscope lamp. Both are the result of a relatively simple procedure. Nevertheless, we were able to measure the spray penetration length under certain operating conditions.

From the photographs it is clear that the penetration length is always the shortest when using diesel fuel, and the longest when using waste cooking oil. The measured values are presented in Tab. 2. The spray-cone angle is the largest for the diesel fuel, which also indicates better atomisation of the spray. For the alternative fuels, especially the waste cooking oil, a filament of the fuel at the nozzle outlet can be observed. This starts to decay at a distance of about 70 mm from the nozzle outlet, for VC2\_C (Fig. 9), and at about 50 mm for VC2\_D (Fig. 10). From this point on we can talk about the spray atomisation.

### 3.3 Discussion

Even though the results of the numerical and empirical analyses as well as the results obtained

fotografijami, medsebojno v celoti ne ujemajo, lahko ugotovimo, da je v vseh analizah zaznan podoben trend spremenjanja karakterističnih veličin curka. Na podlagi podobnih gibanj lahko analiziramo ter do neke mere določimo, kakšen vpliv ima posamezno gorivo na postopek vbrizgavanja, zgorevanja in tvorbe nezaželenih produktov zgorevanja.

Tako je v vseh primerih, pri vseh analizah, najslabši razpad curka zaznan pri uporabi odpadnega rastlinskega olja, najboljši pa v primeru plinskega olja. Vrednosti za biodiesel so v skoraj vseh primerih med obema omenjenima gorivoma. V odvisnosti od uporabljenih analize so te enkrat bližje vrednostim plinskega olja, drugič pa bližje tistim pri odpadnem rastlinskem olju.

Glede na to, da je biodiesel danes praktično že v uporabi; dovoljenje za uporabo le-tega pa je tudi na svojih najsodobnejših dizelskih motorjih odobrilo precejšnje število proizvajalcev [9], je na vprašanje smiselnosti in ustreznosti uporabe tega goriva že bolj ali manj odgovorjeno. Vsekakor pa velja pri starejših vbrizgalnih sistemih, ki so bili razviti zlasti za klasično gorivo in dosegajo manjše tlake vbrizgavanja, pred uporabo nadomestnih goriv razmisiliti o morebitni predelavi vbrizgalnega sistema in zgorevalnega prostora.

Na tem mestu se vprašanje ustreznosti oz. vpliva na postopke vbrizgavanja, zgorevanja in tvorbe nezaželenih produktov zgorevanja postavlja bolj za odpadno rastlinsko olje, ki bi lahko ob predstavljenih rezultatih povzročalo nepopolno zgorevanje ter s tem povezan nastanek nezaželenih ostankov zgorevanja. Težave se lahko pričakujejo predvsem s predolgom dometom in s tem povezanim zadevanjem goriva ob steno zgorevalne komore, zato je pametno poiskati možnost spremembe geometrijske oblike zgorevalne komore v primeru delovanja motorja z odpadnim rastlinskim oljem. Na podlagi tega lahko po predstavljenih analizah do neke mere že zanesljivo trdimo, da nepredelano odpadno rastlinsko olje ni primerno gorivo za dizelske motorje.

Če na temelju dobljenih karakteristik curka odpadnega rastlinskega olja vseeno do neke mere poskusimo določiti, kako je z emisijami, lahko zapišemo naslednje. V splošnem pri dizelskem motorju, ki obratuje s plinskim oljem, velja, da v primeru slabšega razpada curka prihaja do povečanja emisij saj oz. trdnih delcev. Ne glede na to, da rezultati pri odpadnem rastlinskem olju kažejo najslabši rezultat, teh sklepov zaradi drugačne sestave goriva ne moremo neposredno prenesti na odpadno rastlinsko olje. Rastlinska olja imajo namreč v molekulah vezanega več kisika, kar bi lahko ugodno vplivalo na postopek zgorevanja tudi v primeru slabšega razpada oz. v primeru, ko ni velikega presežka zraka. Težava je tudi v tem, da so trdni delci, ki nastajajo pri postopku zgorevanja nadomestnih goriv, svetlejše barve od tistih pri plinskem olju, zato jih z optičnimi merilnimi tehnikami ne moremo zaznati.

Glede drugih emisij lahko do neke mere sklepamo, da bi lahko bile emisije  $\text{NO}_x$ , zaradi slabšega

from the photographs differ significantly, we were able to determine that the trend in the changes of the characteristic values is the same for all the analyses. On this basis we are able to discuss the results and to define how a specific fuel is affecting the injection, combustion and emission-formation processes, at least to some extent.

The worst spray atomisation was always obtained when waste cooking oil was used as a fuel; the best results were obtained for the diesel fuel. The values for the biodiesel were always in between. Depending on the analyses used, the results for the biodiesel were closer to one or other fuel.

As biodiesel is already available on several markets and since many engine producers allow it to be used in their diesel engines [9], the questions concerning its suitability are more or less answered. However, conventional injection systems, which were primarily designed for use with diesel fuel and for which injection pressures are lower, need to be redesigned before using alternative fuels. In particular, the combustion chamber should be redesigned.

The suitability and the influence on the processes of injection, combustion and emission formation, should be discussed for the waste cooking oil, since these factors could cause incomplete combustion followed by emission formation. The problems could occur due to a high penetration length and possible collision with the combustion-chamber walls. For this reason possible ways of changing the combustion-chamber geometries when waste cooking oil is used as a fuel should be discussed. According to these discussions we can already confirm the statement that unmodified waste cooking oil is not suitable for use as a fuel in compression-ignition engines.

Based on the presented waste cooking-oil spray characteristics we can try to predict the emissions, to some extent. In general, the soot emissions of a compression-ignition engine operating on diesel fuel are bigger when the fuel atomisation is worse. However, despite the fact that the spray atomisation in the case of waste cooking oil was the worst, we cannot directly transfer these statements to the case of waste cooking oil, since the structure of the fuel is different. Vegetable oils have more oxygen bonded in the molecule, which positively affects the combustion process, even if the spray atomisation is bad and there is no large excess of air. The other problem is that the particulate matter during the alternative-fuel combustion process is brighter than in case of diesel fuel. This means it cannot be measured with conventional optical methods.

Regarding the other emissions, the emission of  $\text{NO}_x$  could be smaller since the combustion temperatures could be lower due to worse atomisation.

razpada curka, nekoliko manjše, česar pa zaradi razlik v sestavi goriva ponovno ne moremo zanesljivo trditi.

#### 4 SKLEP

Na podlagi predstavljenih rezultatov so mogoči naslednji sklepi v zvezi z uporabo plinskega olja, biodizla in odpadnega rastlinskega olja v dizelskem motorju:

Vse analize kažejo podobne usmeritve vplivov goriva na značilnosti curka.

Biodizel in odpadno rastlinsko olje pri postopku vbrizgavanja obeh vbrizgalnih sistemov dajeta večje kapljice in imata daljši domet, kar je posebej očitno v primeru odpadnega rastlinskega olja.

Prve analize kažejo, da bi lahko uporaba nadomestnih goriv na klasičnih vbrizgalnih sistemih oz. motorjih, zasnovanih za uporabo plinskega olja, povzročala težave z zadevanjem curka goriva ob stene zgorevalnega prostora oz. vdolbine na batu.

Predstavljeni rezultati kažejo, da bodo za boljše poznavanje vpliva nadomestnih goriv na postopek vbrizgavanja potrebne še podrobnejše analize. Tako bo treba opraviti še številne meritve obratovalnih značilnosti motorja ter pred tem po možnosti tudi curka vbrizganega goriva. Prav tako je smiseln izboljšati sistem za vidno opazovanje curka (fotografiranje), kakor tudi vpeljati sodobnejše tehnike merjenja značilnosti curka. Nenazadnje pa bo treba razmišljati tudi o modelih vbrizgavanja (RDT), ki bodo dovolj natančno popisali pogoje pri nadomestnih gorivih.

#### 5 ZAHVALA

Za rezultate meritev karakteristik vbrizgavanja VS2 in sodelovanje pri fotografirjanju curka se avtorja najlepše zahvaljujeta sodelavcem Fakultete za strojništvo Maribor, mag. Gorazdu Bombeku, Avgustu Polaniču in Andreju Pagonu ter študentu Borutu Peklarju.

#### 6 LITERATURA 6 REFERENCES

- [1] DIN V 51606, Ausgabe:1994-06 Flüssige Kraftstoffe; Dieselkraftstoff aus Pflanzenölmethylester
- [2] Koerbitz, W. (1999) Biodiesel production in Europe and North America, *an Encouraging Prospect, Renewable Energy* 16, 1078-1083
- [3] Filipović I. (1983) Analiza motornih parametra ubrizgavanja alternativnih goriva, PhD Thesis, *Mašinski fakultet Univerze u Sarajevu*, Sarajevo.
- [4] Yule, A.J., I. Filipović (1992) On the break-up times and lengths of diesel sprays, *Int. J. Heat and Fluid Flow*, 13, 197-206.
- [5] Hiruyasu, H. et al. (1980) Fuel spray characterization in diesel engines, combustion modelling in reciprocating engines, 369-408, Plenum Press.
- [6] Kegl, B., An improved mathematical model of conventional FIE processes, SAE 950079.
- [7] Volmajer, M., B.Kegl, P.Pogorevc (2002) Injection characteristics of an in-line fuel injection system using the nadomestne fuels, *Journal of KONES*, vol.9, no.1-2, 259-267.
- [8] Volmajer, M., B. Kegl (2001) Obravnavanje curka plinskega olja, Diesel-spray analysis. *Strojniški vestnik.*, letnik 47, št. 10, 627-636.
- [9] BIODIESEL: Aussagen der Fahrzeughersteller, UFOP, Berlin, 2002 (<http://www.ufop.de/Freigaben.pdf>)

But there is again the question how the fuel structure influences these processes.

#### 4 CONCLUSION

The following conclusions can be made regarding the use of diesel, Biodiesel and waste cooking oil in a compression-ignition engine:

All the analyses gave similar trends concerning how the fuel affects the spray characteristics.

The penetration length is higher and the droplets are bigger when the Biodiesel and the waste cooking oil are used. The results vary, particularly in the case of waste cooking oil.

The first analyses show that the use of alternative fuels in conventional injection systems, i.e. engines designed for diesel fuel, could cause problems related to the collision of the spray with the chamber wall or the piston.

The presented results show that for a better understanding of the alternative fuel's influence on the injection process some further analyses need to be made. In future, many additional measurements of the engine characteristics should be made. The system for optical spray observation should be modified. And last, but not least, the CFD models should be modified in order to run the analyses with alternative fuels more accurately.

#### 5 ACKNOWLEDGMENT

The authors' special thanks go to their co-workers at the Faculty of Mechanical Engineering, Maribor (mag. Gorazd Bombek, Andrej Pagon, Avgust Polanič), and to student Borut Peklar for providing the experimental results of the injection characteristics for VS2 and for helping with the spray photography.

Naslov avtorjev: mag. Martin Volmajer  
doc.dr. Breda Kegl  
Univerza v Mariboru  
Fakulteta za strojništvo  
Smetanova ulica 17  
2000 Maribor  
[martin.volmajer@uni-mb.si](mailto:martin.volmajer@uni-mb.si)  
[breda.kegl@uni-mb.si](mailto:breda.kegl@uni-mb.si)

Authors' Address: Mag. Martin Volmajer  
Doc.Dr. Breda Kegl  
University of Maribor  
Faculty of mechanical eng.  
Smetanova ulica 17  
2000 Maribor, Slovenia  
[martin.volmajer@uni-mb.si](mailto:martin.volmajer@uni-mb.si)  
[breda.kegl@uni-mb.si](mailto:breda.kegl@uni-mb.si)

Prejeto: 13.10.2003  
Received: 13.10.2003

Sprejeto: 12.2.2004  
Accepted: 12.2.2004

Odprto za diskusijo: 1 leto  
Open for discussion: 1 year

# Metode za oblikovanje elementov sesalnega zbiralnika batnega motorja z notranjim zgorevanjem

Design Methods for the Intake-Manifold Elements of Reciprocating Internal Combustion Engines

Darko Kozarac - Ivan Mahalec - Zoran Lulić

V uvodu prispevka so prikazane metode oblikovanja sesalnih zbiralnikov, ki omogočajo povečanje prostorninskega izkoristka zaradi dinamičnih sprememb tlaka. Predstavljene so analitične metode za optimiranje premera in dolžine sesalnih cevi glede na vrtilno frekvenco motorja ter metode, ki upoštevajo resonanco v sesalnem zbiralniku. V osrednjem delu prispevka je predstavljena analiza učinkovitosti posameznih metod, ki je bila izvedena s simulacijo na modelu štirivaljnega motorja z notranjim zgorevanjem. Pri simulaciji so bili upoštevani fizikalni in kemični učinki od trenutka, ko pride zrak v sesalni zbiralnik, do trenutka, ko izpušni plini zapustijo izpušni zbiralnik. V prispevku je prikazan tudi način uporabe enorazsežnega modela za analizo vpliva izbranega elementa sesalnega sistema na prostorninski izkoristek motorja ter za izbiro optimalne rešitve pri danih zahtevah.

© 2004 Strojniški vestnik. Vse pravice pridržane.

(Ključne besede: motorji z notranjim zgorevanjem, zbiralniki sesalni, optimiranje, simuliranje, metode analitične)

Methods for intake-manifold design that will lead to an increase in volumetric efficiency by using dynamic changes of pressure, are presented in the introductory part of this paper. Analytical methods for tuning the intake-pipe length and diameter to a specific engine speed, and methods dealing with the resonance in the intake manifold are considered. The main part of the paper comprises an analysis of these methods that was conducted on a simulation model of a four-cylinder spark-ignition engine. Physical and chemical processes are considered in the model, from the moment the air enters the intake system until the combustion gases leave the exhaust pipe. It is also shown how one-dimensional simulation calculations can be used for the analysis of a single intake-system element's influence on the volumetric efficiency of the engine, and for the selection of the optimal solution for given demands.

© 2004 Journal of Mechanical Engineering. All rights reserved.

(Keywords: internal combustion engines, intake manifold, optimization, simulation, analytical methods)

## 0 UVOD

Na tok plina skozi motor z notranjim zgorevanjem v glavnem vplivajo sesalni in izpušni sistem ter konstrukcija in krmiljenje ventilov. Lahko torej rečemo, da je sesalni sistem zelo pomemben del motorja, katerega oblika in izmere vplivajo na prostorninski izkoristek motorja, porabo goriva in hrup. Med delovanjem motorja prihaja v sesalnem sistemu do dinamičnih sprememb, kar vodi do sprememb njegove učinkovitosti v odvisnosti od vrtilne frekvence motorja. S spremembijo geometrijske oblike sesalnega sistema je pri dani vrtilni frekvenci motorja mogoče povečati njegov prostorninski izkoristek. Sesalni sistemi tekmovalnih motorjev so prilagojeni doseganju največjega prostorninskega

## 0 INTRODUCTION

Fluid flow through an internal combustion engine is mainly influenced by the intake system, the exhaust system and by the valve mechanism. Therefore, the intake system is an important engine element whose shape and dimensions influence the volumetric efficiency, fuel consumption, and noise pollution. During the engine's operation, dynamic changes occur in the intake manifold, which leads to a change in its efficiency with the change of the engine's speed. With a change to the geometry of the intake system, it is possible to increase the engine's volumetric efficiency at a specific engine speed. The intake systems of racing engines are tuned to produce maximum volumetric efficiency at a high engine

izkoristka pri visokih vrtilnih frekvencah motorja, pri večini preostalih motorjev pa doseže sesalni sistem največji prostorninski izkoristek pri nižjih vrtilnih frekvencah motorja. Za zmanjanje vpliva geometrijske oblike sesalnega zbiralnika na obnašanje motorja so bili razviti sesalni zbiralniki s spremenljivko geometrijsko obliko. S spremjanjem dolžine sesalnih cevi dosežemo povečanje prostorninskega izkoristka motorja v širokem območju vrtilnih frekvenc. Za določitev izmer takšnega sesalnega sistema pa moramo poznati vpliv geometrijske oblike na prostorninski izkoristek in seveda tudi same metode za izračun izmer sesalnega sistema.

## 1 IZRAČUN GEOMETRIJSKE OBLIKE SESALNEGA ZBIRALNIKA

Za izračun geometrijske oblike sesalnih zbiralnikov je bilo razvitih več metod, ki jih lahko razdelimo tri razdelimo v tri skupine:

- Analitične metode** za izračun optimalne vrtilne frekvence pri danih izmerah sesalnega zbiralnika.
- Enorazsežne numerične simulacije** za izračun izmenjane količine plina med delovanjem motorja.
- Trirazsežne numerične simulacije** za izračun izmenjane količine plina med delovanjem motorja.

Metode, ki spadajo v tretjo skupino, so časovno zelo potratne, zato niso primerne za analizo celotnega sesalnega zbiralnika, temveč le za posamezne manjše dele, npr. za simulacijo toka plina skozi sesalni ventil. Zaradi tega metode v tretji skupini ne bodo opisane bolj podrobno.

### 1.1 Analitične metode

Sesalne zbiralnike, ki vodijo do povečanja prostorninskega izkoristka motorja, lahko razdelimo v dve skupini: v *optimirane* in *resonančne* sesalne zbiralnike.

**Optimirani sesalni zbiralniki** dosežejo tlačno konico pri določeni vrtilni frekvenci motorja kar vodi do največjega prostorninskega izkoristka. Raziskave so pokazale, da je prostorninski izkoristek največji v primeru, če doseže tlak v sesalnem zbiralniku največjo vrednost v območju zasuka glavne gredi 20 do 50 stopinj pred zaprtjem sesalnega ventila. Vrtilna frekvanca motorja, pri kateri pride do največje vrednosti, imenujemo optimalna vrtilna frekvenca.

Po [1] lahko na podlagi predpostavke o poteku tlakov v sesalnem zbiralniku pred sesalnim ventilom določimo nihajni čas, ko so sesalni ventili odprtji  $t_1$ , oziroma teče plin v valj, in čas, ko so ventili zaprta  $t_2$ , oziroma ni pretoka. Na podlagi teh dveh nihajnih časov izračunano dolžino  $l_p$  in prerez  $A_p$

speed, whereas with most other engines, the intake systems produce maximum volumetric efficiency at a lower engine speed. To overcome different intake-manifold geometry effects on the engine behaviour, variable intake manifolds are being developed. The increase in the volumetric efficiency over a broad range of engine speeds is achieved by varying the intake runner. In order to determine the dimensions of such a manifold, it is necessary to be familiar with the influence of the intake-manifold geometry on the volumetric efficiency, as well as with some methods for calculating the manifold dimensions.

## 1 INTAKE-MANIFOLD GEOMETRY CALCULATIONS

In the past a large number of expressions and methods for calculating the dimensions of intake manifolds have been developed. They can be divided into three main groups:

- Analytical expressions** that calculate the tuning engine speed using manifold dimensions.
- One-dimensional simulation calculations**, which calculate the amount of fluid that is exchanged during the engine's operation.
- Three-dimensional simulation calculations**, which calculate the amount of fluid that is exchanged during the engine's operation.

This third group of methods is not suitable for the entire intake manifold because these methods consume a considerable amount of time for the model design and calculation. But they are useful for the simulation of individual small parts, such as the flow through the intake valve. Therefore, this group of methods will not be described in more detail.

### 1.1 Analytical expressions

The intake manifolds that result in an increase of engine's volumetric efficiency can be divided into *tuned intake manifolds* and *resonant intake manifolds*.

At some engine speed a **tuned intake manifold** causes a pressure trace in the manifold that leads to the maximum volumetric efficiency. Research has shown that if the pressure in the intake manifold is a maximum in the period of 20–50 crank angle degrees (CA deg) before the intake valve closes, then the maximum volumetric efficiency is obtained. The engine speed at which this maximum occurs is called the tuned engine speed.

According to [1], from the assumed pressure trace in the intake manifold in front of the intake valve, the oscillation time period when the valves are open  $t_1$ , and when the valves are closed  $t_2$  are determined. With these time periods, the length  $l_p$ , and a cross-sectional area  $A_p$  of the primary intake pipe are

glavne sesalne cevi po enačbah (1) in (2):

$$l_p = c \cdot \frac{720^\circ - \alpha_{ivo}}{24 \cdot \kappa_c \cdot n}, \text{ m} \quad (1)$$

$$A_p = \frac{12 \cdot \pi \cdot \kappa_o \cdot V_c \cdot n}{c \cdot \alpha_{ivo}} \cdot \tan \left[ 90 \cdot \kappa_o \cdot \frac{720^\circ - \alpha_{ivo}}{\kappa_c \cdot \alpha_{ivo}} \right], \text{ m}^2 \quad (2),$$

kjer so:  $c$  v m/s – hitrost zvoka;  $n$  v  $\text{min}^{-1}$  – vrtilna frekvenca motorja;  $t_{ivo} = \alpha_{ivo}/(6n)$  in  $t_{ivc} = \alpha_{ivc}/(6n)$ , s – čas ko je sesalni ventil odprt oz. zaprt.;  $V_c$  v  $\text{m}^3$  – prostornina valja;  $\alpha_{ivo}$  in  $\alpha_{ivc}$ ,  $^\circ$  – zasuk glavne gredi, ko je sesalni ventil odprt oz. zaprt;  $\kappa_o = t_{ivo}/t_1$  in  $\kappa_c = t_{ivc}/t_2$  – razmerje med časom odprtja/zaprtja sesalnega ventila in pripadajočim nihajnim časom.

Posledica spreminjanja tlaka v sesalni cevi v času, ko so sesalni ventili odprti, so tlačna nihanja, ki se ohranijo tudi po trenutku, ko se sesalni ventil zapre. Po [2] lahko ta preostala tlačna nihanja v sesalni cevi še dodatno povečajo prostorninski izkoristek, če se največji tlačni vrh preostalega nihanja ujame z zgornjo mrtvo lego (ZML) pri sesalnem taktu. Enačba za popis omenjenega stanja je naslednja:

$$(2 \cdot k - 1) \cdot \theta_t + \theta_d = 720 \quad (3),$$

kjer je:  $\theta_t = (12nl_p)/c$  v stopinjah – zasuk glavne gredi za čas potovanja tlačnega vala od valja do sesalne cevi in nazaj;  $\theta_d$  v stopinjah – zasuk glavne gredi za čas sesalnega pulza v sesalni cevi.

Po [4] izračunamo optimalno vrtilno frekvenco motorja kot:

$$n = \frac{1}{q_s} \cdot \frac{\theta^*}{24} \cdot \frac{c}{l_p}, \text{ min}^{-1}/\text{rpm} \quad (4),$$

kjer so:  $q_s$  - število celih tlačnih valov v preostalem tlačnem nihanju;  $\theta^* = 540 + \theta_{ivo}$  v stopinjah – zasuk glavne gredi, v katerem ta preostala tlačna nihanja obstajajo;  $\theta_{ivo}$  v stopinjah – zasuk glavne gredi pri zaprtjem sesalnem ventilu po spodnji mrtvi legi (SML).

Pri resonančnem sesalnem zbiralniku vpliva na povečanje prostorninskega izkoristka motorja ujemanje tlačnih nihanj z resonančno frekvenco sesalnega zbiralnika ali enega izmed njegovih delov. Največji prostorninski izkoristek ponovno dosežemo le pri določeni vrtilni frekvenci motorja.

V viru [4] so tlačna nihanja v sesalnem zbiralniku razdeljena na dva osnovna tlačna vala. Prvi tlačni val je posledica oblike glavne sesalne cevi in ima kratko periodo, medtem ko na drugi tlačni val z daljšo periodo vpliva oblika celotnega sesalnega zbiralnika. Tam so bili izpeljani tudi izrazi za izračun resonančne frekvence  $\omega$  (rad/s) sesalnega zbiralnika s širimi posamičnimi glavnimi sesalnimi cevmi (sl. 1):

$$\cos \frac{\omega \cdot l_p}{c} = 0 \quad (5)$$

$$\frac{A_s}{A_p} \cos \frac{\omega \cdot l_s}{c} = \frac{\omega \cdot V_{sb}}{A_p \cdot c} + 4 \tan \frac{\omega \cdot l_p}{c} \quad (6),$$

calculated using Eq. (1) and (2):

where:  $c$ , m/s – speed of sound;  $n$ , rpm – engine speed;  $t_{ivo} = \alpha_{ivo}/(6n)$  i  $t_{ivc} = \alpha_{ivc}/(6n)$ , s – time during which the intake valve is open or closed;  $V_c$ ,  $\text{m}^3$  – cylinder volume;  $\alpha_{ivo}$  i  $\alpha_{ivc}$ , deg – crankshaft angle during which the intake valve is open or closed;  $\kappa_o = t_{ivo}/t_1$  i  $\kappa_c = t_{ivc}/t_2$  – ratio of the valve timings with oscillation time periods.

As a result of pressure changes in the intake pipe during the time the intake valves are open, the pressure in the pipe continues to oscillate after the intake valve closes, and these oscillations are called residual waves. According to [2], if a peak pressure of the residual wave from the previous cycle occurs at the top dead centre (TDC) of the intake stroke, an additional improvement in the volumetric efficiency is obtained. From this approach, the following equation is derived:

where:  $\theta_t = (12nl_p)/c$ , CA deg – time period of wave travel from the engine cylinder to the pipe end and back;  $\theta_d$ , CA deg – time period of a suction pulse in the intake pipe.

Ref. [4] proposed a slightly modified, simpler expression for calculating the tuned engine speed:

where:  $q_s$  - the number of complete residual wave oscillations;  $\theta^* = 540 + \theta_{ivo}$ , CA deg – period in which residual waves exist;  $\theta_{ivo}$ , CA deg – angle of intake valve closure after BDC.

At a defined engine speed the resonant intake manifold causes an increase in the volumetric efficiency due to the correspondence of the pressure disturbance frequency with the intake manifold resonant frequency, or one of its parts.

Ref. [4] concluded that pressure oscillations in the intake manifold are comprised of two basic waves. One wave, which is influenced by the shape of the primary intake pipe, has a short oscillation period, and the other, which has a longer oscillation period, is influenced by the whole intake manifold. It also derived expressions for calculating the resonant frequency  $\omega$  (rad/s) of the intake manifold with four individual primary intake pipes (Fig.1):

kjer so:  $A_s$  v  $\text{m}^2$  – prerez vstopne sesalne cevi;  $l_s$  v m – dolžina vstopne sesalne cevi (to je cev, ki je pred zbirnim prostorom sesalnega zbiralnika);  $V_{sb}$  v  $\text{m}^3$  – prostornina zbirnega prostora sesalnega zbiralnika.

Vir [5] pa je dopolnil zgornja izraza še z upoštevanjem vpliva prostornine valja. Enačba (7) podaja resonančno frekvenco za glavno sesalno cev, enačba (8) pa resonančno frekvenco za celoten sesalni zbiralnik:

$$\frac{A_c}{A_p} \tan \frac{\omega \cdot l_c}{c} \tan \frac{\omega \cdot l_p}{c} = 1 \quad (7)$$

$$\frac{A_s}{A_p} \cot \frac{\omega \cdot l_s}{c} = \frac{\omega \cdot V_{sb}}{A_p \cdot c} + \frac{A_p \tan \frac{\omega \cdot l_p}{c} + A_c \tan \frac{\omega \cdot l_c}{c}}{A_p - A_c \tan \frac{\omega \cdot l_p}{c} \tan \frac{\omega \cdot l_c}{c}} + 3 \cdot \tan \frac{\omega \cdot l_p}{c} \quad (8),$$

kjer sta:  $A_c$  v  $\text{m}^2$  – prerez valja,  $l_c$  v m – dolžina valja (definirana kot polovica delovnega giba bata).

Z uporabo zapisanih enačb je mogoče izračunati izmere optimalnega resonančnega sesalnega zbiralnika v zelo kratkem času. Žal pa te enačbe ne upoštevajo vseh vplivnih dejavnikov, npr: *spremembo prostornine valja, vpliv krmiljenja ventilov, sprememb v prerezu sesalnih cevi, vpliva hitrosti in tlaka plina na tlačnem valu, vpliva tlačnih nihanj od preostalih valjev pri motorju z več valji, vpliv izpušnega zbiralnika, vpliv segrevanja plina zaradi segrevanja samega sesalnega zbiralnika, vpliv tlačnih uporov v sesalnih ceveh itn.* Poleg tega pa omenjeni avtorji ne podajajo enačb za izračun prostorninskega izkoristka motorja.

## 1.2 Enorazsežne numerične simulacije

Z enorazsežnimi numeričnimi simulacijami lahko izračunamo časovni potek tlaka, temperature, masnega pretoka, hitrosti plina itn. v sesalnih cevih, ki so nadalje namenjeni za izračun prostorninskega izkoristka motorja za izbrane robne pogoje oz. razpored. Optimizacijo sesalnega zbiralnika izvedemo s ponavljanjem izračunov pri različnih robnih pogojih. Osnova za izračune so enačbe enorazsežnega toka neviskoznega plina:

Kontinuitetna enačba:

gibalna enačba:

$$\frac{\partial \rho}{\partial t} + \frac{\partial(\rho \cdot v)}{\partial x} + \frac{\rho \cdot v}{A} \cdot \frac{dA}{dx} = 0 \quad (9)$$

momentum equation:

$$\frac{\partial(\rho \cdot v)}{\partial t} + \frac{\partial(\rho \cdot v^2 + p)}{\partial x} + \frac{\rho \cdot v^2}{A} \cdot \frac{dA}{dx} + \rho \cdot v \cdot |v| \cdot f \frac{2}{D} = 0 \quad (10)$$

energy equation:

$$\frac{\partial(\rho \cdot e_0)}{\partial t} + \frac{\partial[\rho \cdot v \cdot h_0]}{\partial x} + \frac{\rho \cdot v \cdot h_0}{A} \frac{dA}{dx} + \rho \cdot q = 0 \quad (11).$$

where:  $A_s$ ,  $\text{m}^2$  – cross-sectional area of the secondary intake pipe;  $l_s$ , m – length of the secondary intake pipe (the pipe that is located before the manifold plenum);  $V_{sb}$ ,  $\text{m}^3$  – intake manifold plenum volume.

Ref. [5] considered the influence of the cylinder volume. With Eq.(7), the resonant frequency  $\omega$  that is related to the primary intake pipe is calculated, whereas by Eq.(8) the resonant frequency related to whole intake manifold is calculated:

where:  $A_c$ ,  $\text{m}^2$  – cross-sectional area of the cylinder;  $l_c$ , m – length of the cylinder (set to be equal to half of the piston stroke).

With all these equations it is possible to calculate the dimensions of a tuned or resonant intake manifold, for the defined engine speed, in a short period of time. These equations, however, do not take into account all the relevant factors, such as: *cylinder volume change, influence of valve timing, influence of valve lift, change in pipe cross-sectional area, influence of gas velocity and gas pressure on the wave speed, the influence of waves from other intake pipes in a multi-cylinder engine, the influence of the exhaust manifold, the influence of gas heating, the influence of the friction resistance in the pipes, etc.* Moreover, these equations do not give the value of the volumetric efficiency.

## 1.2 One-dimensional simulation calculations

One-dimensional simulation calculations calculate the time trace of pressure, temperature, mass flow, gas velocity, etc. in the intake pipe, and with these results they calculate the volumetric efficiency for a predetermined intake-manifold configuration. The optimisation of the intake manifold can be conducted by analysing these results for several different manifold configurations. The bases for these calculations are the equations of one-dimensional inviscid flow:

Continuity equation:

in zakon o ohranitvi energije:

$$\frac{\partial(\rho \cdot e_0)}{\partial t} + \frac{\partial[\rho \cdot v \cdot h_0]}{\partial x} + \frac{\rho \cdot v \cdot h_0}{A} \frac{dA}{dx} + \rho \cdot q = 0 \quad (11).$$

Pri reševanju sistema enačb enačimo stanje plina s stanjem idealnega plina, kar je za potrebe izračunov pri sesalnih zbiralnikih v večini primerov zadovoljivo [6]:

$$\frac{P}{\rho} = R \cdot T \quad (12)$$

Enačbe (9), (10) in (11) predstavljajo sistem parcialnih diferencialnih enačb v času  $t$  in legi  $x$ , ki analitično niso rešljive. Za reševanje se zato uporabljo numerične metode, ki z napredkom računalništva dajejo vedno natančnejše rešitve.

## 2 RAČUNSKI MODEL

Računski model temelji na štirivaljnem štitrakttnem vrstnem motorju z vžigalno svečko, katerega osnovne izmere so podane v preglednici 1. V analizi je uporabljen sesalni zbiralnik s štirimi glavnimi sesalnimi cevmi in štiritočkovnim vbrizgom goriva (sl. 1).

Optimalna vrtilna frekvenca motorja je bila izračunana z enačbami (1) do (8), za nekaj različnih razporedov sesalnega zbiralnika. Za identične razporede so bile izvedene tudi enorazsežne numerične simulacije, na podlagi katerih so bili dobljeni nekateri sklepi. Da bi bili rezultati numeričnih simulacij čim bolj natančni, so bili poleg uporabe predpostavke o idealnem plinu upoštevani naslednji vplivi: *izračun dogajanja v valju, vžig, pretok plina mimo ventilov, pretok plina skozi omejilnike pretoka, izračun dogodkov v zbiralnem prostoru in povezave le tega s sesalnimi cevmi*.

Preglednica 1. Osnovne izmere motorja

Table 1. Basic engine dimensions

tlačno razmerje $\epsilon$ compression ratio	8,8
premer valja $D$ bore D	80 mm
delovni gib bata $H$ stroke H	55,5 mm
dolžina ojnice con. rod length L	0,12 m
odprtje sesalnega ventila intake valve opens	40 stopinj pred ZML 40 deg CA before TDC
zaprtje sesalnega ventila intake valve closes	82 stopinj po SML 82 deg CA after BDC
odprtje izpušnega ventila exhaust valve opens	79 stopinj pred SML 79 deg CA before BDC
zaprtje izpušnega ventila exhaust valve closes	30 stopinj po ZML 30 deg CA after TDC

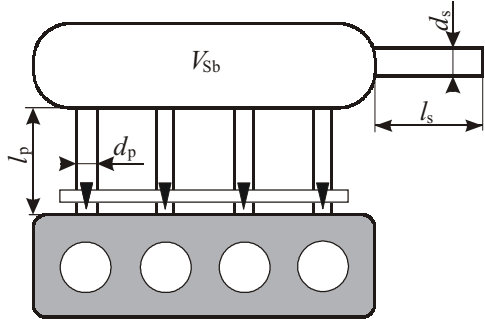
For concluding the equation set, the gas properties are related by an ideal-gas state equation, which is usually sufficiently accurate for engine manifolds [6]:

Equations (9), (10) and (11) represent a system of partial differential equations relating to the time  $t$  and the longitudinal coordinate  $x$ , and they cannot be solved analytically. For solving these equations, a numerical method must be employed. With the development of computers, more complex methods have been derived, so today it is possible to find very complex and very accurate numerical methods for solving these equations.

## 2 CALCULATION MODEL

The calculation model is based on a four-cylinder, four stroke, in-line, spark-ignition engine, whose basic dimensions are shown in Table 1. The intake manifold with four individual primary intake pipes and multi-point injection shown in Fig. 1 is used in the analysis.

The resonant or tuned engine speeds are calculated for several different intake-manifold arrangements, with Eqs.(1) to (8), and the results are shown in the next section (Table 2). For the same intake-manifold arrangements, the one-dimensional simulation calculations are conducted, and with the results from these calculations some conclusions are obtained. In order for the simulation calculations to be as accurate as possible, the calculation model, besides a one-dimensional inviscid flow calculation, comprises the following: *in-cylinder process calculation, combustion, valve flow calculation, calculation of flow through flow restrictions, calculation of processes in plenums and at plenum with pipe connections*. In this manner, a large number of influences is taken into account.



Sl. 1. Sesalni zbiralnik računskega modela ( $d_p$  – premer glavne sesalne cevi,  $l_p$  – dolžina glavne sesalne cevi,  $d_s$  – premer vstopne sesalne cevi,  $l_s$  – dolžina vstopne sesalne cevi,  $V_{sb}$  – prostornina zbirnega prostora zbiralnika)

Fig. 1. Intake manifold of calculation model ( $d_p$  – primary pipe diameter,  $l_p$  – primary pipe length,  $d_s$  – secondary pipe diameter,  $l_s$  – secondary pipe length,  $V_{sb}$  – plenum volume)

Znano je, da ima oblika izpušnega zbiralnika velik vpliv na prostorninski izkoristek motorja in da dinamične spremembe tlaka v izpušnem zbiralniku neposredno vplivajo tudi na dinamične spremembe tlaka v sesalnem zbiralniku v času, ko se odprtje sesalnega in izpušnega ventila prekrije. Omenjeni vpliv pri izračunu ni bil upoštevan, kar je bilo zagotovljeno z izbiro robnega pogoja nespremenljivega tlaka takoj za izpušnim ventilom. Na koncu prispevka so za primerjavo podani še rezultati izračuna brez zanemaritve vpliva izpušnega zbiralnika.

### 3 REZULTATI ANALIZ

Enačbe (1) do (4) neposredno povezujejo optimalno vrtilno frekvenco z izmerimi sesalnega zbiralnika  $n$  v  $\text{min}^{-1}$ , medtem ko enačbe (5) do (8) podajajo resonančno frekvenco sesalnega zbiralnika  $\omega_{\text{res}}$  v  $\text{rad/s}$  in z njim povezano resonančno vrtilno frekvenco motorja  $n_{\text{res}}$  v  $\text{min}^{-1}$ :

$$n_{\text{res}} = \frac{15 \cdot \omega_{\text{res}}}{\pi} \quad (13).$$

Slika 1 prikazuje najpomembnejše izmere sesalnega zbiralnika. Za vsako od teh izmer so bile izbrane tri različne vrednosti in izračunani optimalna in resonančna vrtilna frekvencia motorja. Pri spremenjanju ene izmere so bile preostale izmere določene kot srednja vrednost izbranih treh vrednosti. Primer: za analizo vpliva dolžine glavnih sesalnih cevi je bila optimalna in resonančna vrtilna frekvanca izračunana za tri različne dolžine glavnih sesalnih cevi  $l_p = 250, 500$  in  $750$  mm, medtem ko so bile preostale izmere nespremenljive:  $d_p = 35$  mm,  $l_s = 200$  mm,  $d_s = 50$  mm in  $V_{sb} = 8,5 \text{ dm}^3$ . Rezultati izračunov so prikazani v preglednici 2. Razvidno je, da različne enačbe dajo zelo različne rezultate. Na podlagi velikega števila enačb, ki so bile dokazane kot pravilne, velja, da se s povečevanjem dolžine glavnih sesalnih cevi resonančna vrtilna frekvanca motorja zmanjšuje, kar pa ne velja za

It is well known that the exhaust manifold configuration has a significant influence on the volumetric efficiency, and that dynamic changes of pressure in the exhaust pipe affect the dynamic changes of pressure in the intake manifold when there is valve overlapping. The exhaust manifold has not been included in the calculation model in order to neglect its influence. Instead, a boundary condition with constant pressure has been set just behind the exhaust valve. At the end of the paper, for the purpose of comparison, the calculation of the whole model is made.

### 3 ANALYSIS OF THE RESULTS

Eqs.(1) to (4) directly link the dimensions of the intake manifold with the tuned engine speed  $n$  (rpm), while with Eqs.(5) to (8) it is possible to calculate the intake manifold's resonant frequency  $\omega_{\text{rez}}$  (rad/s), and with it, it is possible to calculate the resonant engine speed  $n_{\text{res}}$ :

$$n_{\text{res}} = \frac{15 \cdot \omega_{\text{res}}}{\pi} \quad (13).$$

Fig.1 shows the most significant dimensions of the model intake manifold. For each dimension three different values were used for calculating the tuned or resonant engine speeds. While changing the value of one dimension, other dimensions are set to the middle of three values. For example, in order to analyse the influence of the length of the primary intake pipe, the tuned and resonant engine speeds are calculated for three different primary pipe lengths  $l_p = 250, 500$  and  $750$  mm, while the other dimensions were as follows:  $d_p = 35$  mm,  $l_s = 200$  mm,  $d_s = 50$  mm and  $V_{sb} = 8,5 \text{ dm}^3$ . The results of these calculations are shown in Tab.2. From the results it is clear that different equations give significantly different results. According to a large number of equations that have proven to be accurate, by increasing the length of the primary-intake pipe, the resonant engine speed decreases. An exception to this is Eq. 2. The influence of the primary pipe's diameter

enačbo (2). Vpliv premera glavne sesalne cevi se tudi razlikuje, saj se po enačbah (2) do (4) in (7) s povečevanjem premera povečuje tudi resonančna vrtilna frekvence motorja, medtem ko se po enačbah (6) in (8) le ta zmanjšuje. Enačbe (1) in (5) ne upoštevajo premera glavne sesalne cevi. Nadaljnji izračuni kažejo, da veliko enačb ne upošteva premera vstopne sesalne cevi, njene dolžine in prostornine zbirnega prostora pri izračunu resonančne vrtilne frekvence motorja.

Enorazsežne numerične simulacije so bile izvedene s programom AVL Boost. Rezultati izračuna prostorninskega izkoristka motorja pri vseh vrtilnih frekvencah motorja za vse analizirane modele (pregl. 2) so prikazani na sliki 2. Kakor je razvidno iz preglednice 2, imamo sedem različnih razporedov sesalnega zbiralnika, ki so razdeljene s ponavljanjem v pet skupin, vsaka s tremi različnimi razporedi.

Na sliki 2(a) so prikazane krivulje prostorninskega izkoristka za tri različne dolžine glavnih sesalnih cevi. S povečevanjem njihove dolžine se prostorninski izkoristek motorja pri majhnih in srednjih vrtilnih frekvencah poveča, pri višjih vrtilnih frekvencah pa se zmanjša. Pri razporedu sesalnega zbiralnika z najdaljšo cevjo ima prostorninski izkoristek pri vrtilni frekvenci  $3600 \text{ min}^{-1}$  izrazit vrh, kar lahko razložimo s pojavom resonančnega polnjenja. Primerjava teh rezultatov s tistimi iz preglednice 1 kaže največje ujemanje z enačbo (7).

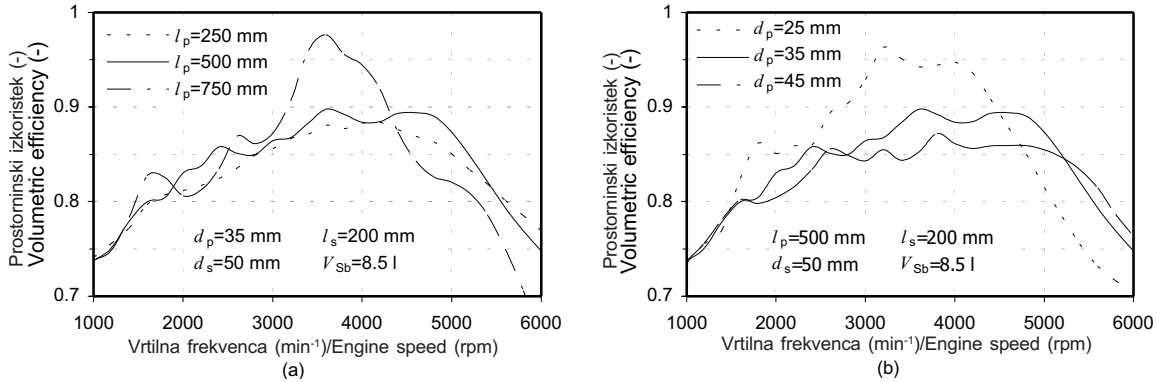
Preglednica 2. Optimalne in resonančne vrtilne frekvence motorja, izračunane z uporabo analitičnih metod  
Table 2. Tuned and resonant engine speed calculated with analytical expressions

		Vrtilne frekvence motorja ( $\text{v min}^{-1}$ ), izračunane po enačbi								
		Engine speed (rpm) calculated with equation								
		(1)	(2)	(3)	(4)	(5)	(6)	(7)	(8)	
$l_p$ mm	250	5120	7210	5890	4180	8220	1670	5600	1650	$d_p = 35 \text{ mm}$ $l_s = 200 \text{ mm}$ $d_s = 50 \text{ mm}$ $V_{Sb} = 8,5 \text{ dm}^3$
	500	2870	7580	3300	2340	4600	1580	3650	1560	
	700	1990	7720	2290	1630	3200	1490	2710	1470	
$d_p$ mm	25	2870	4110	3300	2340	4600	1660	3150	1640	$l_p = 500 \text{ mm}$ $l_s = 200 \text{ mm}$ $d_s = 50 \text{ mm}$ $V_{Sb} = 8,5 \text{ dm}^3$
	35	2870	7580	3300	2340	4600	1580	3650	1560	
	45	2870	12200	3300	2340	4600	1490	3950	1480	
$l_s$ mm	100	2870	7580	3300	2340	4600	2210	3650	2180	$d_p = 35 \text{ mm}$ $l_p = 500 \text{ mm}$ $d_s = 50 \text{ mm}$ $V_{Sb} = 8,5 \text{ dm}^3$
	200	2870	7580	3300	2340	4600	1580	3650	1560	
	500	2870	7580	3300	2340	4600	996	3650	988	
$d_s$ mm	30	2870	7580	3300	2340	4600	957	3650	950	$d_p = 35 \text{ mm}$ $l_p = 500 \text{ mm}$ $l_s = 200 \text{ mm}$ $V_{Sb} = 8,5 \text{ dm}^3$
	50	2870	7580	3300	2340	4600	1580	3650	1560	
	70	2870	7580	3300	2340	4600	2170	3650	2140	
$V_{Sb}$ mm	250	2870	7580	3300	2340	4600	1790	3650	1770	$d_p = 35 \text{ mm}$ $l_s = 200 \text{ mm}$ $d_s = 50 \text{ mm}$ $l_p = 500 \text{ mm}$
	500	2870	7580	3300	2340	4600	1580	3650	1560	
	700	2870	7580	3300	2340	4600	1430	3650	1420	

differs according to different equations. Eqs. (2) to (4) and (7) show that when the pipe diameter increases the resonant engine speed also increases, whereas Eqs.(6) and (8) show that when the diameter is increased, the resonant engine speed decreases. Eqs.(1) and (3) to (5) do not take the primary intake pipe's diameter into account. Further calculations show that a large number of the equations shown do not take into account the secondary pipe diameter, the secondary pipe length and the plenum volume when calculating tuned or resonant engine speeds.

One-dimensional simulation calculations were conducted with the AVL Boost program, and for each intake manifold configuration (shown in Table 2), the volumetric efficiency across the whole speed range is calculated. It is clear from Table 2 that there are eleven different intake manifold configurations, which are, with repetition, collected in five groups, each with three different combinations.

Fig.2(a) shows the volumetric efficiency curves for three different lengths of the primary intake pipe. With an increase in the length of the primary intake pipe, the volumetric efficiency at low and mid engine speed is improved, whereas at high engine speeds the volumetric efficiency is deteriorated. The model with the longest intake pipe has a considerable volumetric efficiency peak at 3600 rpm, which can be considered as resonant charging. The comparison of these results with the results from Tab.1 shows that the best correspondence is obtained with Eq.(7).



Sl. 2. Vpliv dolžine glavne sesalne cevi (a) in premera (b) na prostorninski izkoristek štirivaljnega motorja  
Fig. 2. Influence of the primary pipe length (a) and diameter (b) on the volumetric efficiency of a four-cylinder engine

Na sliki 2(b) so prikazane krivulje prostorninskega izkoristka za tri različne premere glavnih sesalnih cevi. Z zmanjševanjem premere se prostorninski izkoristek motorja pri nižjih vrtilnih frekvencah motorja povečuje, pri višjih vrtilnih frekvencah pa se zmanjšuje. Razvidno je tudi, da se lokalni vrh prostorninskega izkoristka z manjšanjem premere glavnih sesalnih cevi pomika v smeri manjših vrtilnih frekvenc. Primerjava rezultatov z rezultati iz preglednice 1 ponovno kaže najboljše ujemanje z enačbo (7).

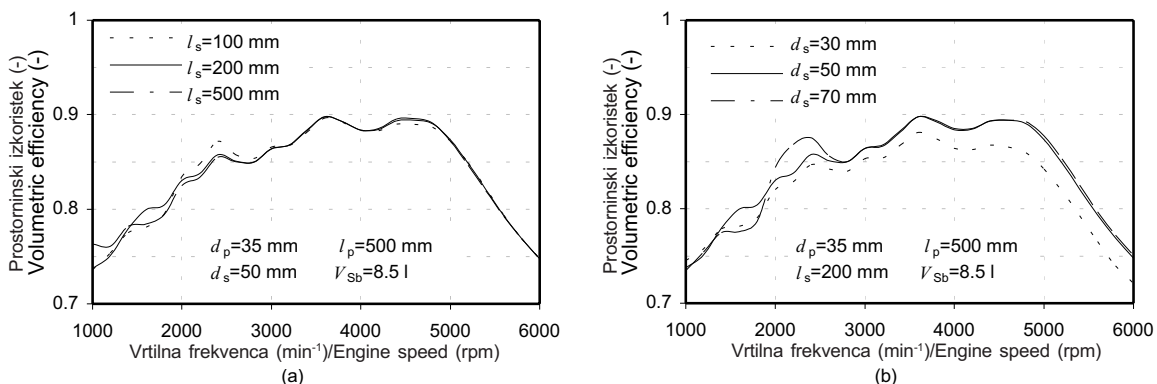
Vpliv dolžine vstopne sesalne cevi na prostorninski izkoristek je razviden iz diagramov na sliki 3a. Pri visokih vrtilnih frekvencah spremembu dolžine vstopne sesalne cevi nima vpliva na vrednost prostorninskega izkoristka, pri nizkih vrtilnih frekvencah pa se kaže v majhnih spremembah strmine krivulje prostorninskega izkoristka motorja. Vpliv dolžine vstopne sesalne cevi je bolj izrazit, če je prostornina zbirnega prostora kolektorja manjša, kar je razvidno slike 4.

Vpliv premera vstopne sesalne cevi je razviden iz diagramov na sliki 3b. Spreminjanje premera

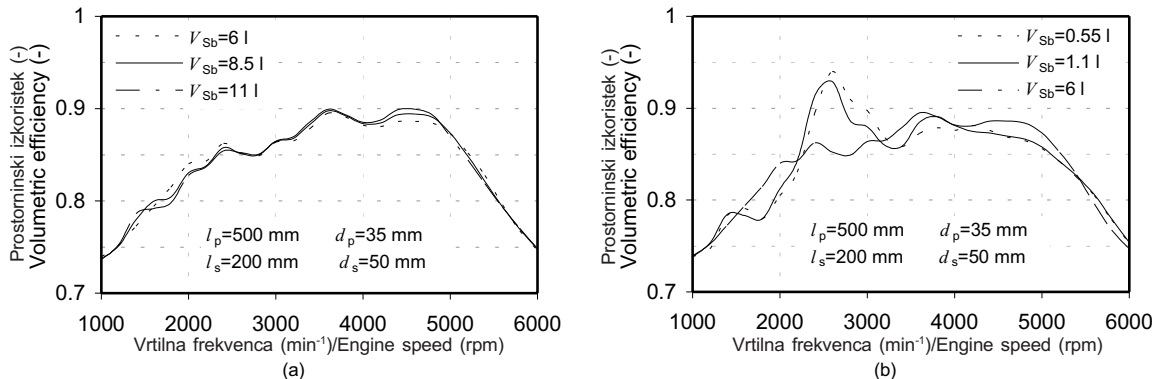
Fig. 2(b) shows the volumetric efficiency for three different primary-pipe diameters. With a decrease in the diameter of the primary pipe, the volumetric efficiency at lower engine speeds increases, while at the same time at high engine speeds it decreases. In addition, the local maxima of the volumetric efficiency curve shift to lower engine speeds with a decrease in the diameter of the primary pipe. The comparison of these results with the results from Table 1 also shows that the best correspondence is obtained with Eq.(7).

The influence of the length of the secondary intake pipe on the volumetric efficiency is shown in Fig. 3(a). The change in the length of the secondary intake pipe does not cause a change in the volumetric efficiency at high engine speeds, while at low engine speeds it causes very small changes to the shape of the curve. The influence of the secondary intake pipe on the volumetric efficiency would be greater if the plenum volume were smaller (shown in Fig. 4).

The influence of the diameter of the secondary intake pipe can be seen in Fig. 3(b). The change



Sl. 3. Vpliv dolžine vstopne sesalne cevi (a) in premera (b) na prostorninski izkoristek štirivaljnega motorja  
Fig. 3. Influence of the secondary pipe's length (a) and diameter (b) on the volumetric efficiency of a four-cylinder engine



Sl. 4. Vpliv prostornine zbiralnega prostora sesalnega zbiralnika na prostorninski izkoristek motorja  
((a) – razmeroma velika prostornina; (b) – majhna prostornina)

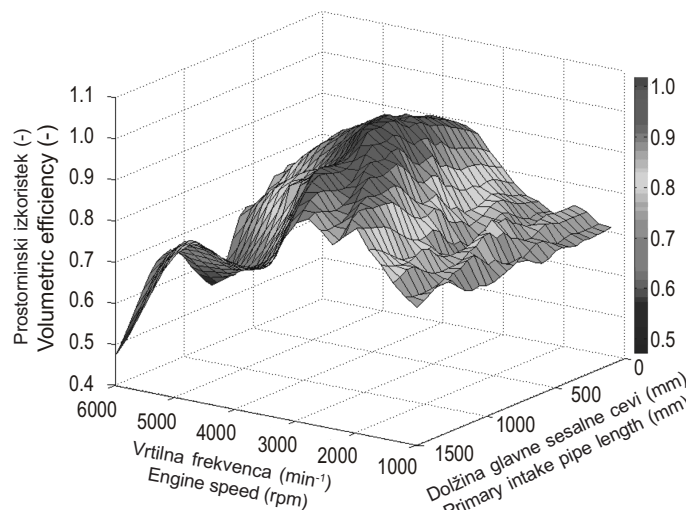
Fig. 4. Influence of the intake manifold's plenum volume on the volumetric efficiency ((a) – relatively large plenum volume; (b) – lowered plenum volumes)

vstopne sesalne cevi ne vpliva na prostorninski izkoristek motorja pri visokih vrtilnih frekvencah motorja, pri nižjih vrtilnih frekvencah pa se kaže v spremembji oblike krivulje prostorninskega izkoristka. Če zmanjšamo premer vstopne sesalne cevi preveč, deluje le ta kot dušilo, kar zmanjša prostorninski izkoristek v celotnem območju vrtilnih frekvenc. Zmanjšanje je bolj izrazito z večanjem vrtilnih frekvenc motorja.

Na sliki 4 so prikazani rezultati izračunov za nekaj različnih prostornin zbiralnega prostora sesalnega zbiralnika. Če je prostornina zbiralnega prostora razmeroma velika proti delovni prostornini motorja, majhne spremembe prostornine zbiralnega prostora nimajo vpliva na prostorninski izkoristek motorja (Sl. 4b), toda če prostornino zbiralnega prostora zmanjšamo približno na vrednost delovne prostornine motorja se pojavijo razlike v krivuljah prostorninskega izkoristka motorja. Te razlike so razmeroma majhne, toda v primerjavi z razlikami pri

of the secondary intake pipe's diameter does not change the volumetric efficiency at high engine speeds, but at low engine speeds it changes the shape of the curve. If the secondary intake pipe's diameter is decreased too much, then this pipe becomes the place of choking, and the volumetric efficiency is lowered throughout the whole speed range. At higher engine speeds, the lowering of the volumetric efficiency is greater than at lower engine speeds.

Fig.4 shows the results of simulation calculations for several different intake-manifold plenum volumes. When the plenum volume is relatively big in comparison with the displacement volume of the engine, a small change in the plenum volume will not change the volumetric efficiency curves. (Fig.4(a)). But if the plenum volume is reduced to a value around the displacement volume or smaller, then changes in the volumetric efficiency curve occur. It should be noted that small changes to the small plenum volumes do not result in significant changes in the volumetric efficiency, but in comparison with the results ob-



Sl. 5. Prostorninski izkoristek štirivaljnega motorja  
Fig. 5. Volumetric efficiency of four-cylinder engine model

večji prostornini zbiralnega prostora sesalnega zbiralnika mnogo izrazitejše (sl. 4b). Z manjšanjem prostornine zbiralnega prostora se vpliv elementov pred tem prostorom na prostorninski izkoristek motorja (npr. vhodna sesalna cev) povečuje.

Prikazani diagrami so pridobljeni z numeričnimi simulacijami brez upoštevanja izpušnega zbiralnika. Če bi želeli določiti izmere sesalnega zbiralnika na predstavljeni način, bi bilo treba tudi izpušni zbiralnik vključiti v izračun ter izvesti izračun za celoten motor. Spreminjanje prostorninskega izkoristka v odvisnosti od vrtilne frekvence motorja in dolžine glavne sesalne cevi je razvidno iz dijagrama na sliki 5, na podlagi katere lahko dolžino glavne sesalne cevi točno določimo.

#### 4 SKLEPI

Če želimo določiti izmere sesalnega zbiralnika s spremenljivo geometrijsko obliko, je treba natančno določiti izbrane izmere za vsako obratovalno točko. Predstavljene analitične enačbe sicer dajo rezultate hitro, vprašljiva pa je prav njihova točnost. Nobenega dvoma ni, da ne bi trirazsežne numerične simulacije dale mnogo boljši pogled na dogajanje v valju, toda za njihovo uporabo je treba mnogo več vhodnih podatkov. Poleg tega pa je zmogljivost današnjih namiznih računalnikov oz. delovnih postaj še premajhna, da bi bili izračuni opravljeni v sprejemljivem času.

Poiskati je torej treba poravnavo med točnostjo in potrebnim časom izračuna oz. poiskati način, kako optimalno uporabiti vse omenjene metode. V prvi fazi uporabimo za okvirno določitev izmer sesalnega zbiralnika analitične enačbe. Nadaljnjo optimizacijo dosežemo z uporabo enorazsežnih numeričnih simulacij, kar je bilo tudi prikazano in ki v večini primerov dajo dovolj natančne rezultate. Z uporabo trirazsežnih numeričnih simulacij je mogoče pridobiti nekatere stalinice, ki jih nadalje uporabimo v hitrejših enorazsežnih numeričnih simulacijah za doseganje še bolj točnih rezultatov. Na začetku so lahko ti modeli zelo preprosti - z le nekaj elementi motorja, na koncu postopka pa morajo zagotovo vsebovati vse elemente motorja. Na podlagi rezultatov takih analiz je že mogoče točno določiti izmere sesalnega zbiralnika, ki bi dale največjo zmogljivost motorja v dani točki delovanja.

tained with large plenum volumes, the change is considerable (Fig. 4(b)). When lowering the intake-manifold plenum volume, the influence of elements that are located before the plenum on the volumetric efficiency (for instance, the secondary intake pipe) is increasing.

The charts shown are obtained from the simulation calculations of a model without an exhaust manifold. If the dimensions of the intake manifold are to be determined with this kind of simulation calculation, it is necessary to include the exhaust manifold in the model and to conduct the calculations for the whole engine model. The change in the volumetric efficiency caused by a change of one intake-manifold dimension over the whole engine speed range can be shown with a three-dimensional chart (Fig.5), from which this dimension can be precisely selected.

#### 4 CONCLUSION

If an intake manifold with variable geometry is to be designed, then its dimensions must be very precisely determined for every engine working point. The presented analytical equations give results very quickly, but they may not be sufficiently accurate. There is no doubt that three-dimensional simulation calculations would give a much better insight into the charging of the cylinder, but they would require a large amount of input data, and with currently available computers the calculations would last too long.

Therefore, it is necessary to find a compromise between accuracy and the time necessary to obtain the result in the design process, and to find a way how to optimally use all the mentioned methods. In the first phase, the analytical equations will be useful for determining the approximate intake-manifold dimensions. Further optimisation can then be achieved, as has been shown, using one-dimensional simulation calculations, which in most cases give very accurate results. One-dimensional calculations have problems with the flow through sharp bends, pipe junctions and poppet valves. Using three-dimensional calculations on these elements, it is possible to obtain more accurate constants that will be used in simpler and faster one-dimensional models, for even more accurate results. In the beginning these models can be simple, with only a few engine elements, but at the end of the process they must be complete, i.e. they must contain all the engine elements. From the results of these calculations it is possible to select the dimensions of the intake-manifold elements that would give the best engine performance at a defined working point.

#### 5 LITERATURA 5 REFERENCES

- [1] Fiala, E., H.P. Willumeit (1967) Schwingungen in Gaswechselleitungen von Kolbenmaschinen. *MTZ* 4(1967) Stuttgart, 144-151.
- [2] Broome, D. (1969) Induction ram, part 1, 2 &3. *Automobile Engineer* (1969) London, April issue, 130 – 133, May issue, 180 – 184, June issue, 262-267.

- [3] Yagi, S., A. Ishizuya, and I. Fujii (1970) Research and development of high speed high performance, small displacement Honda engines. *SAE paper 700122*.
- [4] Ohata, A., Y. Ishida (1982) Dynamic inlet pressure and volumetric efficiency of four cylinder engine. *SAE paper 820407*.
- [5] Ohata, A., H. Saruhashi, I. Matsumoto, Y. Imamura (1985) Acoustic control induction system six cylinder engines. *JSAE rev.* August issue, 8-15.
- [6] Winterbone, D.E., R.J. Pearson (2000) Theory of engine manifold design. *Professional Engineering Publishing*, London , ISBN 1 86058 209 5.
- [7] Winterbone, D.E., R.J. Pearson (1999) Design techniques for engine manifolds. *Professional Engineering Publishing*, London , ISBN 1 86058 179 X.

Naslov avtorjev: Darko Kozarac  
prof.dr.Ivan Mahalec  
dr. Lulić Zoran  
Univerza v Zagrebu  
Fakulteta za strojništvo in  
ladjedelništvo  
Ivana Lučića 5  
10000 Zagreb, Croatia  
darko.kozarac @ fsb.hr  
ivan.mahalec @ fsb.hr  
zoran.lulic @ fsb.h

Autors' Address: Darko Kozarac  
Prof.Dr.Ivan Mahalec  
Dr. Lulić Zoran  
University of Zagreb  
Faculty of Mechanical Eng. and  
Naval Architecture  
Ivana Lučića 5  
10000 Zagreb, Croatia  
darko.kozarac @ fsb.hr  
ivan.mahalec @ fsb.hr  
zoran.lulic @ fsb.h

Prejeto: 16.9.2003  
Received:

Sprejeto: 12.2.2004  
Accepted:

Odperto za diskusijo: 1 leto  
Open for discussion: 1 year

## Strokovna literatura Professional Literature

### Iz revij

#### DOMAČE REVIJE

##### **EGES, Energetika, gospodarstvo in ekologija skupaj, Ljubljana**

**2003, 4**

- Visočnik Petelin, B.: Pogodbeno znižanje stroškov za energijo - kaj je to?  
Sperber, C.: Obračun stroškov za ogrevanje v Evropi - pomemben prispevek k varčevanju z energijo in varovanju okolja  
Grobovšek, B.: Načrtovanje toplotne črpalke za sisteme ogrevanja  
Peručko, D.: Hladilni stolpi - učinkovit način hlajenja  
Volovšek, S.: Hrup hišnih inštalacij, ki se prenaša iz strojnice v stanovanja

##### **Materiali in tehnologije, Ljubljana**

**2003, 5**

- Ćurčija, D.: Tribological aspects of the use of lubricants for the plastic forming of metals  
Milanič, M., Jezeršek, M., Babnik, A., Možina, J.: Optodinamsko spremljanje procesa odstranjevanja barve v realnem času

##### **Obzornik za matematiko in fiziko, Ljubljana**

**2003, 4**

- Zgonik, M.: Mikroresonatorji v integrirani optiki  
Vidav, I.: O konveksnih krivuljah

**2003, 5**

- Strnad, J.: Kako sem pisal učbenik za fiziko

##### **Organizacija, Maribor, Kranj**

**2003, 8**

- Razpet, N.: Glejte, leti!  
Pograjc Debevec M., Kljajić, M., Rajkovič, V.: Simulacija procesa učenja ob uporabi baze znanja ekspertnega sistema  
Potokar, F., Jereb, E.: Učna motivacija in ostali dejavniki uspeha na izpitih

**2003, 9**

- Šimek, D.: Zasvojenost z delom  
Močilnikar, V.: Priložnosti in pasti elektronskih arhivov

##### **Vakuumist, Ljubljana**

**2003, 2-3**

- Žitko, R.: Priprava atomsko čistih površin

#### **Varilna tehnika, Ljubljana,**

**2003, 2**

- Diaci, J., Gorkič, A., Polajnar, I.: Tvorba zvarne leče pri uporovnem točkovnem varjenju raznorodnih jekel  
Puklavec, A.: Sodobne rešitve produktivnosti in ekonomičnosti na elektroobločnih varilnih izvorih

#### **TUJE REVIJE**

##### **CDA, Condizionamento dell'aria Riscaldamento Refrigerazione, Milano**

**2003, 8**

- Bo, M.: La climatizzazione delle degenze ospedaliere  
De Marco, A.: I parametri del comfort totale

**2003, 9**

- D'Ambrosio, F.R., Raffellini, G.: I "vizi" dell'aria

##### **IDR, Industrial Diamond Review, Ascot**

**2003, 3**

- Schicker, K.-D., Thamke, D.: Machining control housings at Renault  
Pickenhahn, R., Trick, D.: New machining concept minimises manufacturing time  
Young, J.: Dealing with laser generated waste

##### **IDR, Industrie Diamanten Rundschau, Willich**

- Barthelmä, F., Lahmann, H.-W., Stöckmann, M.: Qualitätsbewertung von galvanisch gebundenen Diamant-Schleifwerkzeugen mittels Bildverarbeitung  
Engels, J.A., Fish, M.L., Morrison, G., Wright, D.N.: Einfluss der Eigenschaften von Diamant-Sägekörnungen auf das Verschleißverhalten in der Anwendung

##### **Scientific Bulletin, Bucharest**

**2002, 1 A**

- Moraru, L.: Thermal effects of 99,7 % Al melts in ultrasonic field

**2002, 2 A**

- Pred, A.M., Scarlat, E.I., Pred, L., Mihailescu, M.: Determination of a small change in the refractive index of liquids

**2002, 1 C**

- Tudose, M., Scutariu, M., Surdu, C.: Influence of the amortisseurs on a multimachine system transient phenomena  
Necula, H.: Modèle de compresseurs hermétiques à piston de machines frigorifiques

**2002, 2 C**

- Darie, G.: Technical options for reducing the atmospheric pollutants generated by the 50 MWe romanian TPPs running on lignite  
Vuza, D.T., Mocanu, M.: Relations between AC and transient simulations of synchronous detection circuits used in optical sensors  
Dumitache, C.: Practical aspects related to the digital I-PD controller for the thermomicroscopy cell

**2002, 1 D**

- Doicin, C.V., Gheorghe, M.: A method for computer aided design of the representative pieces by coupling of parts  
Baran, Gh., Baran, N.: Erosive abrasion of some types of steel and of pumps for hydro-transport  
Ghinea, F., Rosca, E.: Optimum number of vehicles in a group used in public transport program  
Sebesan, I., Oprea, R.: The amplitude of the hunting oscillations

**2002, 2 D**

- Murgulescu, S., Craifaleanu, A.: Analysis of the frequency-modulated signal spectrum  
Stanciu, V., Stentel, L.: A numerical simulation method of flow characteristic for a subsonic single rotor axial compressor  
Rotaru, E.: The modeling of the jet engines universal characteristic

**Forum - Technische Mitteilungen Thyssen Krupp, Düsseldorf**

**2003, 7**

- Graën, G., Overath, J.: Laser welded external tube for passenger car shock absorber  
Weimann, C., Götz, O.: DampMatic - automatically adjustable shock absorbers for passenger cars  
Bechtloff, A.: NovoPort® - the innovative garage door system with integrated drive unit

**Magdeburger, Magdeburg**

**2003, 1-2**

- Weismantel, R.: Diskrete Optimierung  
Tsotsas, E.: Moderne Prozess- und Produktgestaltung am Beispiel der Trocknung  
Hauptmann, P., Lucklum, R.: Sensoren - Aktueller Stand und Herausforderungen

## Osebne vesti Personal Events

### Prešernova nagrada Fakultete za strojništvo Ljubljana za leto 2003

#### ANALIZA LAMINARNEGA TOKA FLUIDA SKOZI ŠPRANJO

Avtor: Miha Brojan

Mentor in somentor: prof.dr. Franc Kosel  
i.prof.dr. Mihaela Perman

Nagrajenec Miha Brojan, univ.dipl.inž., je bil rojen 8. maja 1979 v Ljubljani. Otroštvo je preživiljal v Domžalah, kjer je obiskoval in leta 1994 tudi končal Osnovno šolo Venclja Perka. Istega leta se je vpisal na Gimnazijo Bežigrad v Ljubljani in tam 1998 maturiral. V šolskem letu 1998/99 se je vpisal v prvi letnik univerzitetnega študija na Fakulteti za strojništvo v Ljubljani.

V lanskem septembru je diplomiral na univerzitetnem študiju Fakultete za strojništvo, Univerze v Ljubljani. Diplomska naloga je bila

vsebinsko tudi s področja mehanike tekočin z naslovom "Analiza laminarnega toka fluida skozi špranjo". Izdelal jo je pod mentorstvom prof.dr. Franca Kosela in somentorstvom izr.prof.dr. Mihaela Permana.

V nalogi je kandidat obdelal primer reševanja teoretičnega problema s področja mehanike tekočin. Način reševanja vključuje uporabo matematičnega in numeričnega modela obravnavanega problema. Matematični model je popisan z Navier-Stokesovimi enačbami za laminarno, stacionarno, nestisljivo in viskozno tekočino. Pri izdelavi numeričnega modela je kandidat uporabil metodo končnih prostornin in izvedel diskretizacijo omenjenih enačb. Reševanje problema je tudi računalniško podprt z uporabo namensko izdelanega uporabniškega programa. V sklepih se je kandidat ukvarjal z vizualizacijo rezultatov in primerjavo med numerično in analitično določenimi ter z referenčnimi rezultati iz literature.

### Magisteriji, diplome

#### MAGISTERIJI

Na Fakulteti za strojništvo Univerze v Ljubljani je z uspehom zagovarjal svoje magistrsko delo:

dne 26. januarja 2004: **Jurij Prezelj**, z naslovom: "Aktivno dušenje hrupa prezračevalnih sistemov".

Na Fakulteti za strojništvo Univerze v Mariboru sta z uspehom zagovarjala svoji magistrski deli:

dne 7. januarja 2004: **Dragan Mikša**, z naslovom: "Možnosti snovne in energijske izrabe katodnega odpada iz elektroliznih celic pri pridobivanju aluminija" in **Bernardka Jurič**, z naslovom: "Uporaba recikliranega agregata in trdnih ostankov po sežigu komunalnih odpadkov v betonu".

S tem so navedeni kandidati dosegli akademsko stopnjo magistra znanosti.

#### DIPLOMIRALISO

Na Fakulteti za strojništvo Univerze v Ljubljani so pridobili naziv diplomirani inženir strojništva:

dne 15. januarja 2004: Mitja KOZOLE, Tomaž MOČNIK, Vinko ROTAR, Darja SEMOLIČ HORVAT, Jožef VRHOVEC;

dne 16. januarja 2004: Bogdan BOŠNJAK, Matic BROJAN, Janez NOVLJAN, Boštjan PEČJAK, Jasimir POLJAK, Drago TOMŠIČ;

dne 19. januarja 2004: Marko BIJOL, Tomaž FLORJANČIČ; Marko KOVAČ, Damjan VUČKO.

\*

Na Fakulteti za strojništvo Univerze v Mariboru so pridobili naziv diplomirani inženir strojništva:

dne 29. januarja 2004: Stanislav BENSA, Boštjan ČREŠNAR, Janez FRIDRIH, Aleš MEGLIČ, Gorazd VAJNGERL.

## Navodila avtorjem

### Instructions for Authors

Članki morajo vsebovati:

- naslov, povzetek, besedilo članka in podnaslove slik v slovenskem in angleškem jeziku,
- dvojezične preglednice in slike (diagrami, risbe ali fotografije),
- seznam literature in
- podatke o avtorjih.

Strojniški vestnik izhaja od leta 1992 v dveh jezikih, tj. v slovenščini in angleščini, zato je obvezen prevod v angleščino. Obe besedili morata biti strokovno in jezikovno med seboj usklajeni. Članki naj bodo kratki in naj obsegajo približno 8 tipkanih strani. Izjemoma so strokovni članki, na željo avtorja, lahko tudi samo v slovenščini, vsebovati pa morajo angleški povzetek.

#### Vsebina članka

Članek naj bo napisan v naslednji obliki:

- Naslov, ki primerno opisuje vsebino članka.
- Povzetek, ki naj bo skrajšana oblika članka in naj ne presega 250 besed. Povzetek mora vsebovati osnove, jedro in cilje raziskave, uporabljeno metodologijo dela, povzetek rezultatov in osnovne sklepe.
- Uvod, v katerem naj bo pregled novejšega stanja in zadostne informacije za razumevanje ter pregled rezultatov dela, predstavljenih v članku.
- Teorija.
- Eksperimentalni del, ki naj vsebuje podatke o postavitev preskusa in metode, uporabljene pri pridobitvi rezultatov.
- Rezultati, ki naj bodo jasno prikazani, po potrebi v obliki slik in preglednic.
- Razprava, v kateri naj bodo prikazane povezave in pospološtive, uporabljeni za pridobitev rezultatov. Prikazana naj bo tudi pomembnost rezultatov in primerjava s poprej objavljenimi deli. (Zaradi narave posameznih raziskav so lahko rezultati in razprava, za jasnost in preprostejše bralčevu razumevanje, združeni v eno poglavje.)
- Sklepi, v katerih naj bo prikazan en ali več sklepov, ki izhajajo iz rezultatov in razprave.
- Literatura, ki mora biti v besedilu oštevilčena zaporedno in označena z oglatimi oklepaji [1] ter na koncu članka zbrana v seznamu literature. Vse opombe naj bodo označene z uporabo dvignjene številke<sup>1</sup>.

#### Oblika članka

Besedilo naj bo pisano na listih formata A4, z dvojnim presledkom med vrstami in s 3 cm širokim robom, da je dovolj prostora za popravke lektorjev. Najbolje je, da pripravite besedilo v urejevalniku Microsoft Word. Hkrati dostavite odtis članka na papirju, vključno z vsemi slikami in preglednicami ter identično kopijo v elektronski obliki.

Prosimo, da ne uporabljate urejevalnika LaTeX, saj program, s katerim pripravljamo Strojniški vestnik, ne uporablja njegovega formata. V urejevalniku LaTeX oblikujte grafe, preglednice in enačbe in jih stiskajte na kakovosten laserskem tiskalniku, da jih bomo lahko presneli.

Enačbe naj bodo v besedilu postavljene v ločene vrstice in na desnem robu označene s tekočo številko v okroglih oklepajih.

#### Enote in okrajšave

V besedilu, preglednicah in slikah uporabljajte le standardne označbe in okrajšave SI. Simbole fizikalnih veličin v besedilu pišite poševno (kurzivno), (npr. *v*, *T*, *n* itn.). Simbole enot, ki sestojijo iz črk, pa pokončno (npr.  $ms^{-1}$ , K, min, mm itn.).

Vse okrajšave naj bodo, ko se prvič pojavijo, napisane v celoti v slovenskem jeziku, npr. časovno spremenljiva geometrija (CSG).

Papers submitted for publication should comprise:

- Title, Abstract, Main Body of Text and Figure Captions in Slovene and English,
- Bilingual Tables and Figures (graphs, drawings or photographs),
- List of references and
- Information about the authors.

Since 1992, the Journal of Mechanical Engineering has been published bilingually, in Slovenian and English. The two texts must be compatible both in terms of technical content and language. Papers should be as short as possible and should on average comprise 8 typed pages. In exceptional cases, at the request of the authors, speciality papers may be written only in Slovene, but must include an English abstract.

#### The format of the paper

The paper should be written in the following format:

- A Title, which adequately describes the content of the paper.
- An Abstract, which should be viewed as a miniversion of the paper and should not exceed 250 words. The Abstract should state the principal objectives and the scope of the investigation, the methodology employed, summarize the results and state the principal conclusions.
- An Introduction, which should provide a review of recent literature and sufficient background information to allow the results of the paper to be understood and evaluated.
- A Theory
- An Experimental section, which should provide details of the experimental set-up and the methods used for obtaining the results.
- A Results section, which should clearly and concisely present the data using figures and tables where appropriate.
- A Discussion section, which should describe the relationships and generalisations shown by the results and discuss the significance of the results making comparisons with previously published work. (Because of the nature of some studies it may be appropriate to combine the Results and Discussion sections into a single section to improve the clarity and make it easier for the reader.)
- Conclusions, which should present one or more conclusions that have been drawn from the results and subsequent discussion.
- References, which must be numbered consecutively in the text using square brackets [1] and collected together in a reference list at the end of the paper. Any footnotes should be indicated by the use of a superscript<sup>1</sup>.

#### The layout of the text

Texts should be written in A4 format, with double spacing and margins of 3 cm to provide editors with space to write in their corrections. Microsoft Word for Windows is the preferred format for submission. One hard copy, including all figures, tables and illustrations and an identical electronic version of the manuscript must be submitted simultaneously.

Please do not use a LaTeX text editor, since this is not compatible with the publishing procedure of the Journal of Mechanical Engineering. Graphs, tables and equations in LaTeX may be supplied in good quality hard-copy format, so that they can be copied for inclusion in the Journal.

Equations should be on a separate line in the main body of the text and marked on the right-hand side of the page with numbers in round brackets.

#### Units and abbreviations

Only standard SI symbols and abbreviations should be used in the text, tables and figures. Symbols for physical quantities in the text should be written in Italics (e.g. *v*, *T*, *n*, etc.). Symbols for units that consist of letters should be in plain text (e.g.  $ms^{-1}$ , K, min, mm, etc.).

All abbreviations should be spelt out in full on first appearance, e.g., variable time geometry (VTG).

### Slike

Slike morajo biti zaporedno oštevilčene in označene, v besedilu in podnaslovu, kot sl. 1, sl. 2 itn. Posnete naj bodo v kateremkoli od razširjenih formatov, npr. BMP, JPG, GIF. Za pripravo diagramov in risb priporočamo CDR format (CorelDraw), saj so slike v njem vektorske in jih lahko pri končni obdelavi preprosto povečujemo ali pomanjšujemo.

Pri označevanju osi v diagramih, kadar je le mogoče, uporabite označbe veličin (npr.  $t$ ,  $v$ ,  $m$  itn.), da ni potrebno dvojezično označevanje. V diagramih z več krivuljami, mora biti vsaka krivulja označena. Pomen oznake mora biti pojasnjен v podnapisu slike.

Vse označbe na slikah morajo biti dvojezične.

Za vse slike po fotografiskih posnetkih je treba priložiti izvirne fotografije ali kakovostno narejen posnetek. V izjemnih primerih so lahko slike tudi barvne.

### Preglednice

Preglednice morajo biti zaporedno oštevilčene in označene, v besedilu in podnaslovu, kot preglednica 1, preglednica 2 itn. V preglednicah ne uporabljajte izpisanih imen veličin, ampak samo ustrezne simbole, da se izognemo dvojezični podvojitvi imen. K fizikalnim veličinam, npr.  $t$  (pisano poševno), pripisite enote (pisano pokončno) v novo vrsto brez oklepajev.

Vsi podnaslovi preglednic morajo biti dvojezični.

### Seznam literature

Vsa literatura mora biti navedena v seznamu na koncu članka v prikazani obliki po vrsti za revije, zbornike in knjige:

- [1] Targ, Y.S., Y.S. Wang (1994) A new adaptive controller for constant turning force. *Int J Adv Manuf Technol* 9(1994) London, pp. 211-216.
- [2] Čuš, F., J. Balić (1996) Rationale Gestaltung der organisatorischen Abläufe im Werkzeugwesen. *Proceedings of International Conference on Computer Integration Manufacturing*, Zakopane, 14.-17. maj 1996.
- [3] Oertli, P.C. (1977) Praktische Wirtschaftskybernetik. *Carl Hanser Verlag*, München.

### Podatki o avtorjih

Članku priložite tudi podatke o avtorjih: imena, nazive, popolne poštne naslove, številke telefona in faks ter naslove elektronske pošte.

### Sprejem člankov in avtorske pravice

Uredništvo Strojniškega vestnika si pridržuje pravico do odločanja o sprejemu članka za objavo, strokovno oceno recenzentov in morebitnem predlogu za krajšanje ali izpopolnitve ter terminološke in jezikovne korekturje.

Avtor mora predložiti pisno izjavo, da je besedilo njegovo izvirno delo in ni bilo v dani obliki še nikjer objavljeno. Z objavo preidejo avtorske pravice na Strojniški vestnik. Pri morebitnih kasnejših objavah mora biti SV naveden kot vir.

Rokopisi člankov ostanejo v arhivu SV.

Vsa nadaljnja pojasnila daje:

Uredništvo  
STROJNISKEGA VESTNIKA  
p.p. 197  
1001 Ljubljana  
Telefon: (01) 4771-757  
Telefaks: (01) 2518-567  
E-mail: strojniski.vestnik@fs.uni-lj.si

### Figures

Figures must be cited in consecutive numerical order in the text and referred to in both the text and the caption as Fig. 1, Fig. 2, etc. Figures may be saved in any common format, e.g. BMP, GIF, JPG. However, the use of CDR format (CorelDraw) is recommended for graphs and line drawings, since vector images can be easily reduced or enlarged during final processing of the paper.

When labelling axes, physical quantities, e.g.  $t$ ,  $v$ ,  $m$ , etc. should be used whenever possible to minimise the need to label the axes in two languages. Multi-curve graphs should have individual curves marked with a symbol, the meaning of the symbol should be explained in the figure caption.

All figure captions must be bilingual.

Good quality black-and-white photographs or scanned images should be supplied for illustrations. In certain circumstances, colour figures may be considered.

### Tables

Tables must be cited in consecutive numerical order in the text and referred to in both the text and the caption as Table 1, Table 2, etc. The use of names for quantities in tables should be avoided if possible: corresponding symbols are preferred to minimise the need to use both Slovenian and English names. In addition to the physical quantity, e.g.  $t$  (in Italic), units (normal text), should be added in new line without brackets.

All table captions must be bilingual.

### The list of references

References should be collected at the end of the paper in the following styles for journals, proceedings and books, respectively:

- [1] Targ, Y.S., Y.S. Wang (1994) A new adaptive controller for constant turning force. *Int J Adv Manuf Technol* 9(1994) London, pp. 211-216.
- [2] Čuš, F., J. Balić (1996) Rationale Gestaltung der organisatorischen Abläufe im Werkzeugwesen. *Proceedings of International Conference on Computer Integration Manufacturing*, Zakopane, 14.-17. maj 1996.
- [3] Oertli, P.C. (1977) Praktische Wirtschaftskybernetik. *Carl Hanser Verlag*, München.

### Author information

The following information about the authors should be enclosed with the paper: names, complete postal addresses, telephone and fax numbers and E-mail addresses.

### Acceptance of papers and copyright

The Editorial Committee of the Journal of Mechanical Engineering reserves the right to decide whether a paper is acceptable for publication, obtain professional reviews for submitted papers, and if necessary, require changes to the content, length or language.

Authors must also enclose a written statement that the paper is original unpublished work, and not under consideration for publication elsewhere. On publication, copyright for the paper shall pass to the Journal of Mechanical Engineering. The JME must be stated as a source in all later publications.

Papers will be kept in the archives of the JME.

You can obtain further information from:

Editorial Board of the  
JOURNAL OF MECHANICAL ENGINEERING  
P.O.Box 197  
1001 Ljubljana, Slovenia  
Telephone: +386 (0)1 4771-757  
Fax: +386 (0)1 2518-567  
E-mail: strojniski.vestnik@fs.uni-lj.si